An Innovative Energy Dissipation System for Resisting Soft Story Behavior of Buildings

Mohammad Azimi Vaziri

Submitted to the
Institute of Graduate Studies and Research
in partial fulfillment of the requirements for the degree of

Master of Science
in
Civil Engineering

Eastern Mediterranean University
September 2020
Gazimağusa, North Cyprus

Approval of the Institute of Graduate Studies and Research

Prof. Dr. Ali Hakan Ulusoy
Director

I certify that this thesis satisfies all the requirements as a thesis for the degree of Master of Science in Civil Engineering.

Prof. Dr. Umut Türker
Acting Chair, Department of Civil Engineering

We certify that we have read this thesis and that in our opinion it is fully adequate in scope and quality as a thesis for the degree of Master of Science in Civil Engineering.

Assoc. Prof. Dr. Mahmood Hosseini
Co-Supervisor

Assoc. Prof. Dr. Mehmet Cemal Geneş
Supervisor

Examining Committee

1. Assoc. Prof. Dr. Mehmet Cemal Geneş
2. Assoc. Prof. Dr. Mahmood Hosseini
3. Assoc. Prof. Dr. Giray Özay
4. Asst. Prof. Dr. İsmail Safkan
5. Asst. Prof. Dr. Umut Yıldırım

ABSTRACT

In recent decades, several methods have been proposed by earthquake engineering specialists for seismic multi-story building response reduction. However, many of these techniques have not been acknowledged by the engineering community due to either high costs, or high technology required for their manufacturing, installation and maintenance. Among the proposed methods, using controlled soft story seems to be more desired from cost and technology points of view. This idea can specifically useful for the buildings which have open spans in their lowest story because of the architectural requirements.

In this thesis, a method is presented for employing the controlled soft story concept in multi-story RC buildings by using multi-linear hardening springs with multi-phase yielding process at the lowest story of the building, only in the central bays in each main direction, not to disturb the responsiveness of the building to the architectural needs. To show the efficiency of the proposed technique, the multi-linear hardening springs have been inserted in the computer model of some multi-story RC buildings, and by considering various values for the initial, secondary and third stiffness of the system, as well as their yielding displacements. By using a set of selected earthquakes, a number of nonlinear time history (NLTHA) analyzes have attempted to decrease buildings' seismic response to keep their performance at Immediate Occupancy (IO). Results of the conducted NLTHA show that by assigning appropriate stiffness and yielding displacement values of the multi-linear plastic springs, it is possible to control the response of the buildings and keep them basically in the desired IO performance level.

Keywords: Nonlinear Time History Analyses (NLTHA), Soft Story, Multi-linear Plastic Springs

ÖZ

Son yıllarda, deprem mühendisliği uzmanları tarafından çok katlı binaların sismik tepkisinin azaltılması için birçok yöntem önerilmiştir. Ancak, önerilen bu yöntemlerin çoğu, üretimleri, montajları ve bakımları için gerekli olan yüksek maliyet veya teknoloji açısından değerlendirildiğinde mühendiser camiası tarafından ilgi görmemiştir. Önerilen bu metotlardan biri olan Yumuşak Katın Kontrol Altında Tutulması, maliyet ve teknoloji açışından daha tercih edilebilir bir yöntem olarak görünmektedir. Bu fikir, özellikle mimari gereksinimler nedeniyle zemin katları duvarsız inşa edilmiş binalar için yararlı olabilmektedir.

Bu çalışmada, Yumuşak Katın Kontrol Altında Tutulması konseptini çok katlı betonarme binalarda uygulamak amacıyla, ve yapının mimari ihtiyaçlara duyarlılığını bozmayacak şekilde ana akslar üzerindeki merkezi açıklıklara, çok fazlı akma işlevine sahip çok fazlı lineer sertleştirme yaylarının yapının zemin katına konulmasını öneren bir yöntem sunulmaktadır. Önerilen tekniğin verimliliğini göstermek için, çok fazlı akma işlevine sahip çok fazlı lineer sertleştirme yaylarının birincil, ikincil ve üçüncül rijitlikleri ve akma deplasmanları dikkatte alacak şekilde bazı çok katlı betonarme binalarının bilgisayar modeline eklenmiş ve analizler yapılmıştır. Bir dizi seçilmiş depremler kullanılarak, doğrusal olmayan zaman-tanım alanında analizler (NLTHA) aracılığıyla deplasmanların sınırlandırılmasına ve binaların sismik tepkilerinin azaltılmasına çalışılmıştır. Böylece performansları Hemek Kullanım (HK) düzeyinde tutulmuştur. Yapılan NLTHA sonuçları, çok fazlı akma işlevine sahip çok fazlı lineer sertleştirme yaylarında uygun rijitlik ve yer değiştirme değerlerinin atanması ile

binaların tepkisini kontrol etmenin ve istenen HK performans seviyesinde tutmanın mümkün olduğunu göstermektedir.

Anahtar Kelimeler: Doğrusal Olmayan Zaman Tanım Tlanında Analiz, Yumuşak Kat, Çok Fazlı Linear Plastic Yay

DEDICATION

I dedicate this study to my lovely family. A special feeling of gratitude to my loving parents, Farnoosh Abdolmajid and Arman Azimi Vaziri whose words of encouragement and push for tenacity ring in my ears. My sister Nazanin has never left my side which was an incredible feeling for me.

ACKNOWLEDGMENT

I would first like to thank my thesis supervisor Assoc. Prof. Dr. Mehmet Camel Genes of the civil engineering at Eastern Mediterranean University. He consistently allowed this thesis to be my own work, but steered me in the right direction whenever he thought I needed it, and encouraged me to make my best for solving the problems and getting the final results.

I would also like to thank my co-supervisor Assoc. Prof. Dr. Mahmood Hosseini. The door to Prof. Hosseini office was always open during the thesis process whenever I ran into a trouble spot or had a question about my research or writing, and I am greatly indebted to him for his very valuable advices and guidance on this thesis.

I would like to acknowledge the members of my graduate committee for their constructive comments, most especially my advisor Prof. Dr. Eren Ozgur for all his advices. Special thanks go to the head of civil engineering department, Prof. Dr. Umut Turker, for his crucial support of this study.

Finally, I must express my very profound gratitude to my parents and to my sister for providing me with unfailing support and continuous encouragement throughout my years of study and through the process of researching and writing this thesis. This accomplishment would not have been possible without them. Thank you.

TABLE OF CONTENTS

ABSTRACT iii

ÖZ v

DEDICATION vii

ACKNOWLEDGMENT viii

LIST OF TABLES xii

LIST OF FIGURES xiv

LIST OF SYMBOLS AND ABBREVIATIONS xix

1 INTRODUCTION 1

1.1 Overview 1

1.1.1 Seismic Risk 1

1.2 Building Behavior during Earthquakes 3

1.3 Statement of the Problem 8

1.4 Thesis Objectives 12

1.5 Content of Thesis 13

2 LITRATURE REVIEW 15

2.1 Introduction 15

2.2 Previous Studies on Soft Story 16

2.2.1 The Effect of Floors' Stiffness in Creating a Soft Story 17

2.2.2 The Effect of Lateral Displacement of Floors on Soft Floor Creation 20

2.2.3The Effect of Resistance of Floors in Creating a Soft Story 21

2.3 Seismic Design Procedures 21

2.3.1 Force-Based Seismic Design 21

2.3.2 Performance Based Seismic Design (PBSD) 24

2.4 Seismic Evaluation Methodologies 25
2.4.1 Empirical Evaluation Methodologies 26
2.4.2 Analytical Evaluation Methods 27
2.5 Collapse Mechanism 27
2.5.1 Drift Values at Failure Due to Lateral Load 28
2.5.2 Drift Values at Failure Due to Axial Load 31
2.6 Seismic Performance Assessment 34
2.6.1 Linear Static Procedure (LSP) 34
2.6.2 Linear Dynamic Procedure (LDP) 37
2.6.3 Non-Linear Static Procedure (NSP) 37
2.6.4 Non-Linear Dynamic Procedure 41
2.6.5 Comparison of Seismic Performance Evaluation Procedures 43
2.7 Brief Review on Retrofitting Measures and Seismic Control Methods 44
3 METHODOLOGY 48
3.1 Introduction 48
3.2 Research Methodology 48
3.3 Design Specifications 48
3.3.1 Design for Earthquake Loading: 50
3.4 Mechanical Properties of the Considered Materials 53
3.4.1 Process of Model Analysis for Initial Design 54
3.4.2 Loading Compounds Applied to the Structure 54
3.5 Design with Soft Story 55
3.6 Introducing the Control Device and Its Modeling in ABAQUS 60
3.6.1 Introducing the Proposed Energy Dissipater 60
3.6.2 Introducing ABAQUS Software 65

3.6.3 Yield Criterion 66
3.6.4 Modeling of the Proposed Energy Dissipater in ABAQUS Software ... 68
3.7 Finding Initial Values of HAMSYED Parameters 71
3.8 Evaluating the Efficiency of the Soft Story HAMSEYD 75
3.8.1 ETABS and Modeling the Building and Required Links 75
3.8.2 Earthquake Record Selection 76
4 ANALYSIS RESULTS AND DISCUSSION 79
4.1 Introduction 79
4.2 Details of Modelling and Seismic Responses 79
4.3 Comparison of Time history Analysis Outputs 80
4.3.1 Comparing of Time History Response of 5 Stories Models: 81
4.3.2 Comparing of Time History Response of 7 Stories Models: 84
4.3.3 Comparing of Time History Response of 9 Stories Buildings: 87
4.4 Comparing of Plastic Hinges Formation in Buildings 90
4.5 Maximum Response of Buildings in Both Direction 92
5 CONCLUSION AND RECOMMENDATION FOR FUTURE STUDIES 96
5.1 Summary and Conclusions 96
5.2 Recommendations for Future Studies 98
REFERENCES 100

LIST OF TABLES

Table 1: Classification of Failure Mechanism (ASCE/SEI 41-06)..... 28

Table 2: Natural periods of designed buildings 52

Table 3: Drift control of five story design building example 57

Table 4: Drift control of seven story design building example..... 57

Table 5: Drift control of nine story design building example..... 58

Table 6: Stiffness control of five story design building..... 58

Table 7: Stiffness control of seven story design building..... 59

Table 8: Stiffness control of nine story design building 60

Table 9: Values of the HAMSYED device geometric parameters 65

Table 10: Details of materials used..... 69

Table 11: Damping coefficients found based on equation (26) and applied for different controlled buildings in their seismic response calculations 76

Table 12: Specification of selected earthquakes 77

Table 13: Maximum responses of the 5-story buildings, in X direction, subjected to all seven considered earthquakes 93

Table 14: Maximum responses of the 5-story buildings, in Y direction, subjected to all seven considered earthquakes 93

Table 15: Maximum responses of the 7-story buildings, in X direction, subjected to all seven considered earthquakes 93

Table 16: Maximum responses of the 7-story buildings, in Y direction, subjected to all seven considered earthquakes 94

Table 17: Maximum responses of the 9-story buildings, in X direction, subjected to all seven considered earthquakes 94

Table 18: Maximum responses of the 9-story buildings, in Y direction, subjected to all seven considered earthquakes 94

LIST OF FIGURES

Figure 1: Global seismic hazard map [4] 2

Figure 2: Seismic risk of the Mediterranean basin [5] 3

Figure 3: Earthquake effects on structures 3

Figure 4: Olive View Hospital, Psychiatric Unit, 1971 San Fernando Earthquake [10] 6

Figure 5: Collapse mechanism of a building structure having a soft 7

Figure 6: Collapse and deformation of structures in the Loma Prieta earthquake [18] 9

Figure 7: Collapse by soft story in the Northridge earthquake 1994 [20] 9

Figure 8: Soft story destruction Izmit earthquake in Turkey 1999[18] 10

Figure 9: Soft story collapse 2008 Wenchuan earthquake in China[22] 11

Figure 10: Occurrence of soft story in 2011 Van Turkey earthquake[18] 11

Figure 11: Buildings with open ground floor 18

Figure 12: Create soft story in floors[39] 19

Figure 13: Creating a soft story due to the high height of the floor[39] 19

Figure 14: Model of plastic hinges at the junction of soft story and other floors[39] 20

Figure 15*:* Design Sequence of Force-Based Design 22

Figure 16: Performance-Based Design Flow Chart 24

Figure 17: Shear strength degradation and displacement ductility 28

Figure 18: Evaluation of drift at lateral load failure 30

Figure 19: Free-body diagram of column after lateral load failure 32

Figure 20: The equilibrium forces for shear model 33

Figure 21: Concepts of equal displacement, energy and acceleration 36

Figure 22: Inelastic response spectrum 36

Figure 23: Conversion of capacity push-over curve to capacity curve 40
Figure 24: Conversion of elastic response spectrum from standard format to ADRS format 41
Figure 25: Seismic performance point determination 41
Figure 26: Rayleigh damping model 43
Figure 27: Ground floor plan of designed structure 49
Figure 28: Three-dimensional view of designed structures 50
Figure 29: Colorful presentation of D/C for the designed buildings 53
Figure 30: Beam design sample 53
Figure 31: Column design sample 54
Figure 32: Soft story control regulations [71] 56
Figure 33: The installed location of the fuse in frame 61
Figure 34: Details of the yielding plates, teeth-form elements and stopper (dark areas) of the HAMSYED device 62
Figure 35: Schematic force – displacement curves of the HAMSYED and its yielding plates series 63
Figure 36: The boundary conditions and loading of the element in HAMSYED 64
Figure 37: Installation auxiliary part of the HAMSYED device 65
Figure 38: Hardening rule 67
Figure 39: schematic unloading curve under reverse loading to illustrate the Bauschinger effect, transient behavior and permanent softening. 68
Figure 40: Check out the Von Mises stress model in ABAQUS 69
Figure 41: The close-up of the used stoppers in HAMSYED 70
Figure 42: Back-bone curves of HAMSYED 70
Figure 43: Hysteretic curves of HAMSYED 71

Figure 44: Spectral acceleration 78
Figure 45: Spectral pseudo velocity curves 78
Figure 46: A sample of the multi-linear hardening behavior of the HAMSYED device 80
Figure 47: Shear force time histories of 5-story buildings subjected to CHY025 earthquake 81
Figure 48: Shear force time histories of 5-story buildings subjected to CHY025 earthquake 81
Figure 49: Absolute acceleration response history of 5-story buildings at roof level subjected to CHY025 earthquake 82
Figure 50: Absolute acceleration response history of 5-story buildings at roof level subjected to CHY025 earthquake 82
Figure 51: Displacement of 5-story buildings at roof level 82
Figure 52: Displacement of 5-story buildings at roof level 83
Figure 53: The peak inter-story drift of the CHY025 earthquake in 5-story buildings 83
Figure 54: The peak inter-story drift of the CHY025 earthquake in 5-story buildings 83
Figure 55: Shear force time histories of 7-story buildings subjected to CHY025 earthquake 84
Figure 56: Shear force time histories of 7-story buildings subjected to CHY025 earthquake 85
Figure 57: Absolute acceleration response history of 7-story buildings at roof level subjected to CHY025 earthquake 85

Figure 58: Absolute acceleration response history of 7-story buildings at roof level subjected to CHY025 earthquake 85
Figure 59: Displacement of 7-story buildings at roof level 86
Figure 60: Displacement of 7-story buildings at roof level 86
Figure 61: The peak inter-story drift of the CHY025 earthquake in 7-story buildings 86
Figure 62: The peak inter-story drift of the CHY025 earthquake in 7-story buildings 87
Figure 63: Shear force time histories of 9-story buildings subjected to CHY025 earthquake 87
Figure 64: Shear force time histories of 9-story buildings subjected to CHY025 earthquake 87
Figure 65: Absolute acceleration response history of 9-story buildings at roof level subjected to CHY025 earthquake 88
Figure 66: Absolute acceleration response history of 9-story buildings at roof level subjected to CHY025 earthquake 88
Figure 67: Displacement of 9-story buildings at roof level 88
Figure 68: Displacement of 9-story buildings at roof level 89
Figure 69: The peak inter-story drift of the CHY025 earthquake in 9-story buildings 89
Figure 70: The peak inter-story drift of the CHY025 earthquake in 9-story buildings 89
Figure 71: PHs formed in the 5-story original (up) and controlled (down) buildings subjected to TCU063 earthquake 90

Figure 72: PHs formed in the 7-story original (up) and controlled (down) buildings subjected to TCU063 earthquake 901
Figure 73: PHs formed in the 9-story original (left) and controlled (right) buildings subjected to TCU063 earthquake 902

LIST OF SYMBOLS AND ABBREVIATIONS

$\ddot{\bar{x}}, \dot{\bar{x}}, \bar{x}$	Acceleration, velocity, and displacement vectors
$\emptyset_{j1}$	The j[th] floor element of the fundamental mode $\emptyset_1$
A_v	Transverse reinforcement area
$\bar{C}$	Structure damping matrix
$\bar{M}$	Mass matrix
M_1^*	The effective modal mass for the fundamental vibration mode
M_n	The nominal moment capacity of a column
S_b	The spectral displacement
V_b	The base shear forces
V_n	The nominal shear strength of a column
W_t	Total weight of structure including proportion of live load
d_c	Column core depth from centre line to centre line of ties
f_c'	The concrete strength.
f_{yh}	The yield stress of transverse reinforcement
f_{yh}	Transverse reinforcement yield strength
m_j	The lumped mass at the j[th] floor level
$\bar{r}$	The influence vector for the ground displacement
Γ_1	The modal participation factor for the fundamental mode
δ_{af}	The drift at axial failure
δ_{lf}	Drift at lateral load failure
ρ_h	The steel area ratio of transverse reinforcement
ρ_h	The transverse reinforcement ratio

C	Normalized earthquake response factor for natural period T1
D	Column width
Di	Corresponding displacement at the i^{th} story.
$F(t)$	External forces vector
Fi	Horizontal forces at the i^{th} story
K	A constant expressed as $\frac{\rho_h f_{yh}}{n f_c'}$
L	Shear span
M	The total system mass
N	The axial load ratio
S	The hoop spacing
$s(x)$	Inelastic strength matrix
S_a	The spectral acceleration
V	Maximum nominal shear stress recorded during the tests
$Vtest$	Peak shear recorded.
Wi	Floor weight of the ^{ith} story
Z	Acceleration coefficient
s	Transverse reinforcement spacing
θ	Critical crack angle from horizontal (assumed to be 65°).
ρ''	Transverse reinforcement ratio (A_{st}/bs)
ACI	The American Concrete Institute
ASCE	American Society of Civil Engineers
DPM	Damage Probability Matrices
FEMA	The Federal Emergency Management Agency
FRP	Fiber-Reinforced Polymer
HAMSYED	Hardening and Multi Stage Yielding Energy Dissipater

I	The importance factor
K	The lateral stiffness of the system
LDP	Linear Dynamic Procedure
LSP	Linear Static Procedure
N	The number of floors
NDP	Non-linear Dynamic Procedure
NSP	Non-linear Static Procedure
P	Axial load
PBSD	Performance Based Seismic Design
PH	Plastic Hinges
R	Response modification factor
RC	Reinforce Concrete
SDOF	Single Degree of Freedom
L	Column length

Chapter 1

INTRODUCTION

1.1 Overview

1.1.1 Seismic Risk

Earthquake is the most critical natural phenomena that can affect the form of the earth and also it can impose major damages to the built environment. Earthquake is the movement of Earth's crust associated with immediate release of energy that can provide seismic waves in the Earth's lithosphere. The energy can be produced by elastic strain, gravity, biochemical reactions, or indeed the movement of enormous bodies. From all mentioned cases the release of elastic strain is the most imperative source, because this form of energy is the only classification that can be accumulated in adequate volume in the Earth to produce major changes. Earthquakes associated with this type of sources are named tectonic earthquakes [1, 2].

Tectonic earthquakes are clarified by the nominal elastic rebound theory, defined by the American geologist Harry Fielding Reid after the San Andreas Fault cracked in 1906, producing the incredible San Francisco earthquake. according to the theory, a tectonic earthquake happens when strains in rock bodies have collected to a point where the resulting stresses surpass the strength of the rocks and sudden fracturing results [1][3]. When earthquake hits structures, it produces inertia forces that could be highly damaging, causing deformations, horizontal and vertical shaking. That is why a clear understanding of the seismic impact on a structure is extremely necessary, and

the influence of seismic shocks on buildings should be recognized by designers and contractors in order to set preventive measures against failures and collapses.

As shown in Figure 1 and Figure 2, high seismic risk and rapid development in many parts of the world, including TRNC and Turkey require more research and study than ever before, in seismic resistance buildings field. Unfortunately, Turkey experienced two destructive earthquakes in 1999: the Golcuk-izmit event on 17 August (Mw=7.4), and the Duzce event on 12 November (Mw=7.1); the most devastating earthquakes that this nation has suffered in recent decades. They occurred on segments of the well-known North Anatolian Fault Zone (NAFZ), the most important active fault zone in Turkey, which passes close to Istanbul and other major urban centers, and cuts across northern Turkey for about more than 1500 km, accommodating ~25 mm/yr. of right lateral motion between Anatolia and the Eurasian plate. Being located on the boundary between Eurasian and African plates, Cyprus was affected by many destructive earthquakes throughout its history. The largest earthquakes mostly occurred at the southern part of the island, causing damage in Paphos, Limassol, and Famagusta.

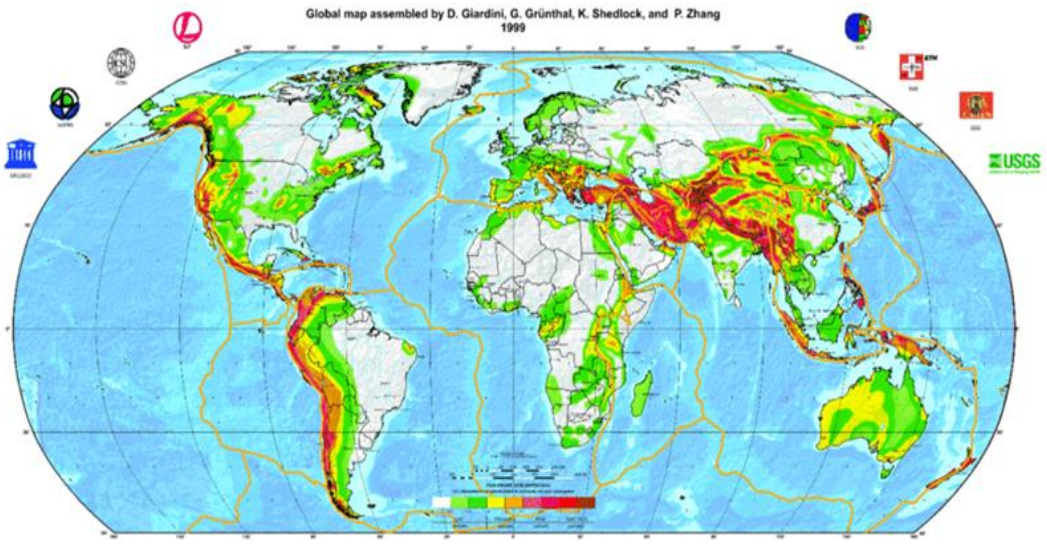

Figure 1: Global seismic hazard map [4]

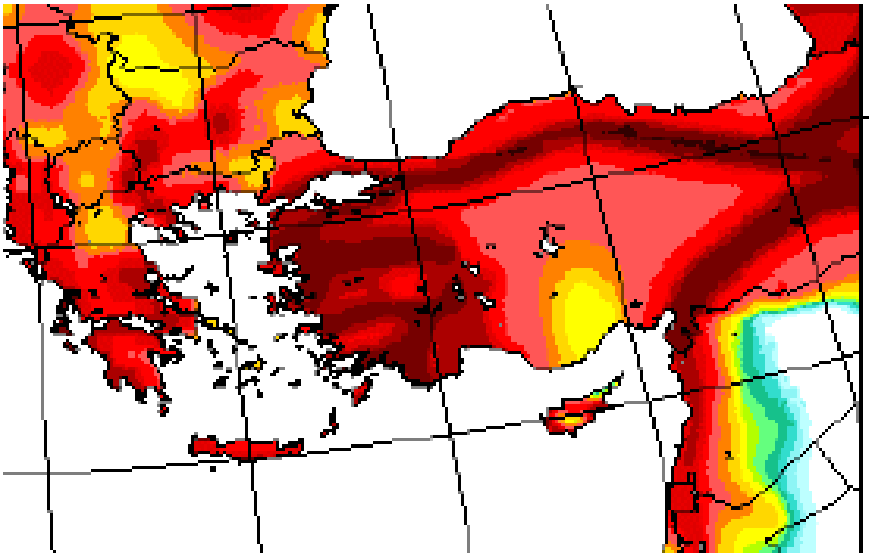

Figure 2: Seismic risk of the Mediterranean basin [5]

1.2 Building Behavior during Earthquakes

The behavior of a building during an earthquake is a vibration problem. The seismic motions of the ground do not damage a building by impact or by externally applied pressure such as wind, but by internally generated inertial forces caused by vibration of the building mass as shown in Figure 3.

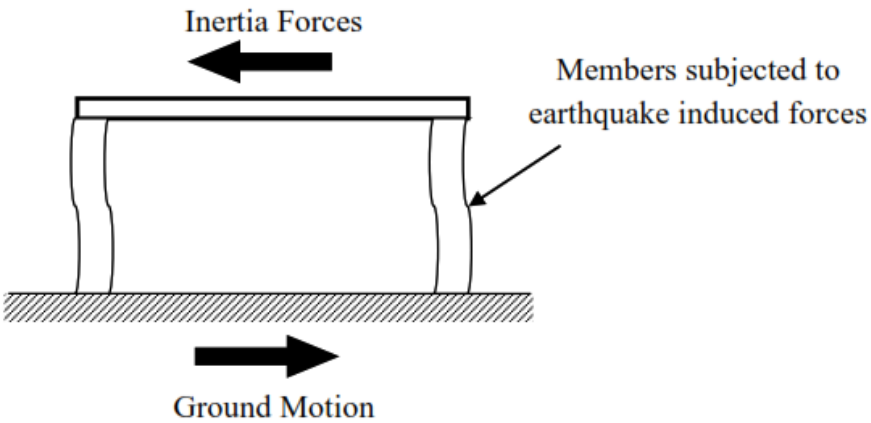

Figure 3: Earthquake effects on structures

An increase in mass has two undesirable effects on the earthquake design. First, it results in an increase in the force, and second, it can cause buckling or crushing of

columns and walls when the mass pushes down on a member bent or moved out of plumb by the lateral forces. This effect is known as the P-Δ effect and the greater the vertical forces, the greater the movement due to P-Δ. The magnitude of inertia forces induced in an earthquake depends on the building mass, ground acceleration, the nature of the foundation, and the dynamic characteristics of the structure [1].

Most popular common designs and construction mistakes or shortcomings which lead to failures in building systems include [2]:

- Soft-Story
- Short-Columns
- Inadequate Reinforcement Detailing
- Non-structural Damage
- Discontinuous Force Resisting System
- Strong Beam-Weak Column
- Inadequate Detailing
- Poor Quality Concrete
- Inferior Materials, and Densely Populated Area.

Several buildings with soft story at ground level, either existing, or new ones, mainly due to architectural preferences, can or will be seen in cities located in earthquake prone areas. Structures with a soft-story can be identified by their wide openings at the soft-story level, which are usually positioned on the lower floor for parking or shopping centers. The overall strength and stiffness of this floor in soft-story buildings is slightly lower than the upper floors according to the presence of such wide openings[3]. Although the inadequacy of masonry infill partitions at the ground floor

of structure produces immediate and unexpected discontinuities in the lateral system all along with the building. This results in severe lateral load and inelastic demand for deformation in the columns of the ground floor resulting in a soft-story failure of the building during earthquake[6, 7].

Although soft story has been looked at as a negative feature of the building, and several cases of collapse have been observed in such buildings in past earthquakes, the soft story can have an isolating role as well, if it is controlled to prevent the P- Δ effect.

Fintel and Khan discussed the soft story principle in 1969. This idea is an attempt to decrease acceleration in a frame by making the first-story column yield when an earthquake occurs and providing energy-dissipation. Unreasonable drifts in the first story, coupled with P- Δ in the columns, cause structures to fail.[8] In the US code, known as 2010-ASCE7, this issue has classified in two categories:

I. soft irregularity of soft-story
II. sharp irregularity of soft-story.

The soft-story stiffness irregularity is described as if there is a floor in the building where that floor's lateral stiffness is less than 70% of the floor's lateral stiffness or less than 80% of the three floor's average stiffness. Additionally, the strong irregularity of the soft-story stiffness arises when the lateral stiffness of the floor in the building is less than 60% of the story itself or less than 70% of the average stiffness of the three floors. When a building has either of these two anomalies, limitations may be imposed on the use of that building in seismic hazard classifications or the use of various analyzes [3].

In a structure with uniform stiffness at height, it is expected that during strong earthquakes, plastic hinges are distributed at the height of the structure and the depreciation of the earthquake can be carried out in several stations. However, the softening a floor to the upper floors totally disrupt this uniform distribution. So that all the ductility demands are concentrated only on the ground floor. In other words, the plastic hinge is formed at both ends of the column and practically the upper floors are exempt from energy dissipation. If massive earthquake energy is depreciated only in limited joints, there will be a sharp drop in stiffness and resistance of columns. For example, in 1971, San Fernando earthquake in California, an unpleasant phenomenon occurred for a hospital. A two-story hospital, which must be continual, has suffered extensive damage. In the Figure 4, it can be observed that how the lowest story of the building has been completely crushed, while interestingly, there is almost no damage to the upper stories[9].

Figure 4: Olive View Hospital, Psychiatric Unit, 1971 San Fernando Earthquake [10]

In general, where irregular inter-story drifts between adjacent stories exist during an earthquake, the lateral forces cannot be adequately spread around the building height. This condition induces focus of the lateral forces on the story (or stories) with broad displacements. Therefore, if the local ductility criteria are not fulfilled in the

construction of such a building system for that story and the inter-story drifts are not controlled, a specific collapse mechanism or, even worse, a story failure process, which can cause the device to collapse, could be created because of the strong load deformation (P-Δ) effects. The fi Figure 5 illustrates the failure process under both earthquake and gravity loads in this kind of building system, with a soft story. Known that the distribution of lateral force around the height of a building is strongly linked to the mass and stiffness of each floor. If the P-Δ range influence is assumed to be the primary explanation for the dynamic collapse of building systems during earthquakes, appropriately measured lateral displacements estimated in the elastic modeling phase may possibly give very valuable knowledge for the system's structural attitudes. Therefore, in many of the specific codes, dynamic analytical method is required for accurate distribution of the earthquake forces all over the building height, effectively determining modal effects and local ductility conditions. While some of the existing codes describe soft story irregularity by measuring the stiffness of adjacent levels, displacement-based standards for such irregularity assessment are more effective as they encompass both the principles of mass, stiffness and force distribution[11].

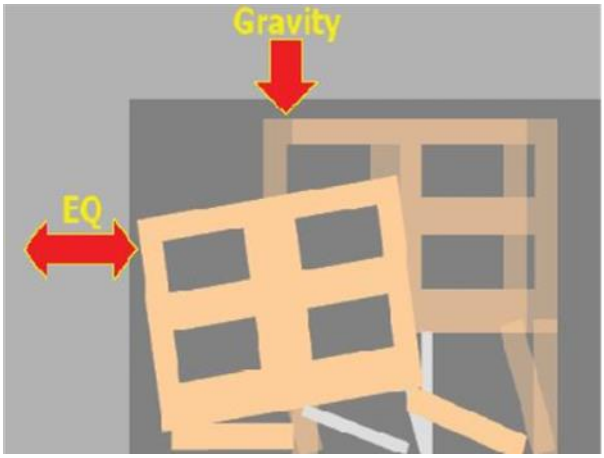

Figure 5: Collapse mechanism of a building structure having a soft soft story [12]

To reduce and resolve the effect of soft-story in buildings, several methods have been suggested; placing diagonals between the columns and shear walls; increasing the rigidity of the soft-story by increasing beam-column size of the soft-story and some other methods which regularly is costly and sometimes difficult to create or maybe it needs to ignore the architectural an economic factors or limitations. [13]

It is known that soft-story with masonry partitions endures less damages in comparison to soft-story without masonry partitions in that specific story. For that reason, the plausibility of damage will increase if there are a few masonries infills at the top story. The major decrease of infill walls in comparison with the upper story means a significant change in stiffness of the two adjacent buildings and for sure this reduction is not acceptable based on the principles of earthquake engineering. [14]

1.3 Statement of the Problem

Reinforced concrete building systems filled with or without unreinforced masonry walls are regarded as one of the world's most widely accepted forms of construction. The cost-effective, simple construction and customizable design features of the masonry walls made them a popular partition design option for architects. Nowadays, in most seismic codes of practice, masonry infill walls are tended to be non-structural elements and neglect their structural participation during excitation from the earthquake. However, as many scientists have studied, infill walls can change structural behavior by their undeniable bracing actions during the excitation of an earthquake.[14-16]

Soft story collapse was responsible for almost half of all homes that were uninhabitable in California's 1989 Loma Prieta earthquake and was expected to cause serious damage

and potential loss of 160,000 homes in the event of a more serious earthquake in the San Francisco Bay Area, California.[17]

Figure 6: Collapse and deformation of structures in the Loma Prieta earthquake [18]

Most Californians clearly recall the 1994 Northridge earthquake that killed 57 people, wounded 8,700, and displaced 22,000 from their homes. During the quake, the soft-story Northridge Meadows Apartments complex collapsed when the lower ground floor was completely crushed by the two floors above it, causing 16 deaths.[19]

Figure 7: Collapse by soft story in the Northridge earthquake 1994 [20]

Survey of the 1999 earthquake in Izmir, Turkey, reveals that soft floors caused about 85-90% of the building's debris.[21]

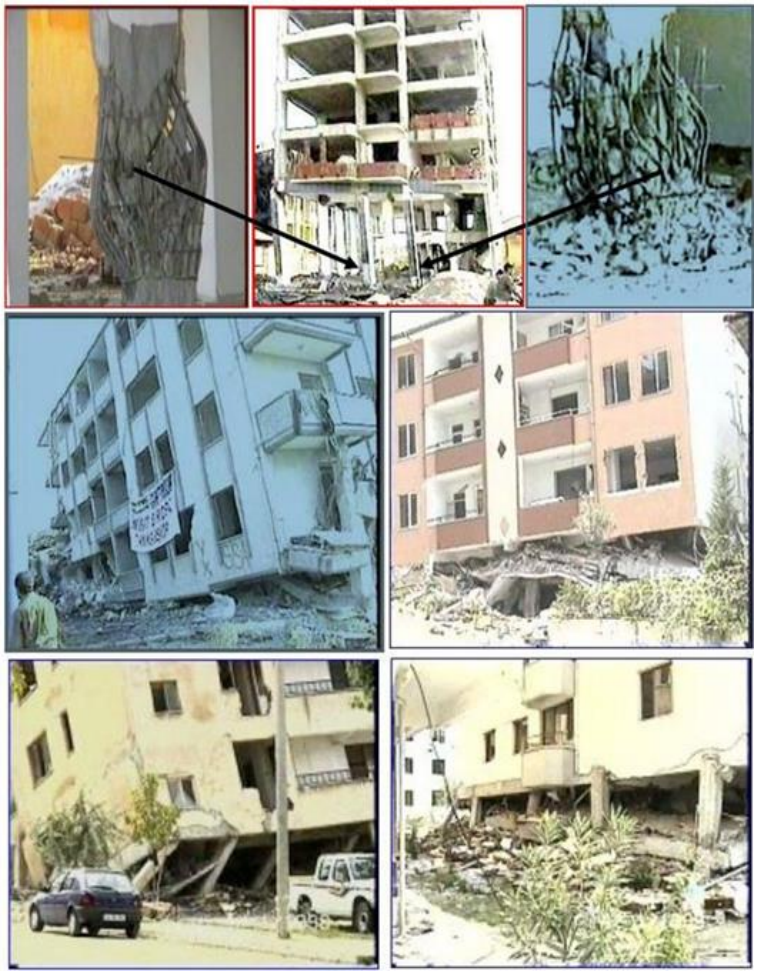

Figure 8: Soft story destruction Izmit earthquake in Turkey 1999[18]

The poor seismic performance of RC frames with infill walls, including many newly constructed structures, has been widely recorded in every single catastrophic earthquake in recent decades. The 2008 Wenchuan earthquake in China devastated hundreds of cities in the province of Sichuan and killed 69,227 people, with 374,643 injured and around 4.8 million left homeless. Various masonry infill walls with RC frame systems has experienced significant damages or failure.[22]

Figure 9: Soft story collapse 2008 Wenchuan earthquake in China[22]

Figure 9 shows collapse of a two-story infilled RC building during the 2008 Wenchuan earthquake. Van-Erciş, Turkey 2011 was another earthquake in which the soft story problem was very evident and most of the fractures in the reinforced concrete buildings of the region were caused by this mechanism and in some cases the reinforced concrete buildings were completely destroyed.[23] Figure 10 shows some of the completely destroyed buildings.

Figure 10: Occurrence of soft story in 2011 Van Turkey earthquake[18]

The Ridgecrest earthquake of 5 July 2019 and its associated foreshocks were a pressing reminder that earthquakes could occur at any time. If the next major earthquake hit Los Angeles or another populous area of SoCal, as many as 1,800 people could die and 270,000 could be displaced. In the chaos of such a great earthquake, soft-story buildings are much more likely to collapse.[24]

Despite hundreds of observations from historical earthquakes with substantial loss of human life and property, current structural design and analysis methods do not guarantee the integrity and stability of these structures during earthquake events and the intractable conflict between the theories of engineer theoretical research and the realistic experiences of seismic performance of RC frames remains unresolved.[25]

1.4 Thesis Objectives

In this study, the control device which is proposed to be used in the soft story of the building, is a hardening and multi-stage yielding energy dissipater (HAMSYED). The low initial stiffness of the device gives the building a state similar to isolation, resulting in lower seismic demands, but as the displacement at soft story increases during an earthquake, the stiffness of the fuse also increases to prevent the extensive displacements, which leads to the increases of P- Δ effect, and finally collapse of the building. Furthermore, the high energy dissipation capacity of the device reduces the amount of energy transferred to the upper stories of the building, helping them to remain basically elastic. On this basis, the main aim of this thesis is to introduce a method for keeping the structure secure from the risk of destruction of the soft-story phenomenon and followed by improving the quality of structural performance by using a HAMSYED. In order to achieve this goal, the following objectives can be considered:

- Improving/increasing structural performance and safety
- Analyzing and evaluating the real dynamic behavior of the common structure system obtained from real past earthquake data
- Applying a device to modify and upgrade the seismic behavior of buildings with soft story, either existing or new ones.
- Propose a fast and reliable technique for controlling and improving the lateral load bearing system behavior.

1.5 Content of Thesis

Chapter 1 is the introduction: It is provided an over view of the thesis and the problem statement. Brief explanations of earthquake and its impact on structures. In addition, a brief introduction and explanation of the soft floor, its mechanism and examples of its effect on history of construction.

Chapter 2 is the literature review: The literature review chapter covers similar studies that have addressed problems within the scope of the present study. It is worth mentioning that there are very few studies on controlled soft story, and therefore some researches on the adverse effect of soft story have been presented in chapter two as well.

Chapter 3 is dedicated to modeling and analysis of the considered buildings for the study: First, the conventional buildings with soft story are introduced, and then the earthquake records which have been used for seismic evaluation of the buildings by non-linear time history analyses are presented by their acceleration and pseudo velocity spectra. Also, in this chapter the performance and design of the multi-level hardening and yielding fuse are explained. Finally, in this chapter the seismic response

of controlled soft story buildings have been compared with those of their conventional counterparts.

Chapter 4 covers the results and discussion: The results obtained from the time history analyses are discussed in this chapter, and the effectiveness of the proposed technique for controlled soft story is shown.

Chapter 5 contains the conclusion and recommendations: The summary of the thesis is presented in this chapter, followed by the conclusions of the study. Finally, some recommendations are given for future studies.

Chapter 2

LITRATURE REVIEW

2.1 Introduction

In the past two centuries, buildings with a soft story condition were extensively constructed around the world. Parking, shopping areas, and lobbies on the first floor of multi-story buildings in these constructions are considered as both architectural and social advantages. Although, advantages of the first story acting as a 'soft link' have been previously studied [26-28], the weak seismic performance of these buildings, which are vulnerable to collapse, has led the earthquake engineering community to exclude this structural term from its practical usage. In addition, observational findings showed that soft story buildings are more vulnerable to collapse, because of extensive displacement concentrated in their first floor [29]. The poor performance of these buildings in past earthquakes have also led to design requirements that do not permit column side-swinging mechanisms, often correlated with a soft story action, and a number of measures have been taken to make engineers avoid from constructing similar structures [30, 31].

Recent codes resolve the soft stories issue by requiring a rise in the strength and stiffness of the columns of existing structures to minimize the probability of failure [32]. Those kinds of codes and standards are appropriate for achieving life-safety performance level, they are an efficient technique to monitor the risk of failure during severe, rare earthquakes. Nevertheless, in more frequent earthquakes, these parameters

do not necessarily mitigate the expected and loss to the entire structure and the building’s content, as the increase in rigidity and strength on the first floor leads to an increased response in the upper stories and possibly to an actual increase in structural and non-structural damage.[33] However, typical retrofitting methods including added RC walls or inclined steel braces pose many challenges to the functionality of the system.

2.2 Previous Studies on Soft Story

Elimination of the item which is resistant to lateral loads on the floors to provide entrance to the building or to install wide windows or main doors, causes soft and weak story to form. Distinguishing between the soft floor and the weak floor isn't typically easy. Stiffness is equal to the force required to create a unit displacement or is the slope of the force-displacement curve, but the resistance is equal to the maximum force, that the system can tolerate. [34]

In 1986, Moehle and Alarcon carried out the first specific research on the soft-story phenomenon and its detrimental effects in the framework. In that study a reinforced concrete structure with dual bending framework and shear wall was analytically and laboratory evaluated according to this analysis. In one of the cases, the shear wall was cut at first floor level and it was found that the member's formability at the position is 4 to 5 times the state that the shear wall is continuous.[35]

Most buildings on the ground floor are more sensitive, but this phenomenon in the upper floors may also have a significant impact on the performance of the structure. A column may be a slightly stiff but resistant, or it may be stiff but weak. Changes in the dimensions of the column can affect its stiffness and strength and should be

considered. It is also worth noting that the height adjustment generally causes a twist in the structure and leads to a decrease in strength or stiffness, resulting in a soft floor or a weak floor mechanism. The soft-story should be determined by comparing the desired floors with the adjacent floors. Some of the factors affecting the creation of a soft story are: stiffness, strength and lateral displacement of the floors and also the effect of infilled frame which are discussed below.

2.2.1 The Effect of Floors' Stiffness in Creating a Soft Story

In 1997, Valmudsson and Nau studied the effects of changes in stiffness and strength on the first floor of buildings with 5, 10 and 20 stories, and observed that by reducing the stiffness of the first floor by 20%, the drifts between floors increased by 20 to 40%. At the same time, stiffness and resistance on the first floor increased by 30%, and the demand for ductility increased by 2.22 to 3 times.[36]

Factors influencing the reduction of floor stiffness include the lack of infill walls, lateral load-resistant systems (braces, etc.) and the high floor height [37]. Soft story is usually created when the ground floor has less stiffness and resistance than the upper floors, which usually occurs in commercial and residential buildings on the ground floor and in some other buildings on the upper floors. The upper floors are usually hard and durable due to sufficient partitions, but on the ground floor between the frames, open spaces are created, which leads to a soft floor on the ground floor. In many buildings, it is noted that the filling walls or braces and shear walls on the upper floors have not been extended to the ground floor, in order to create open space for parking. In most calculations, infill walls are ignored and only the frame is included in the calculations and design.

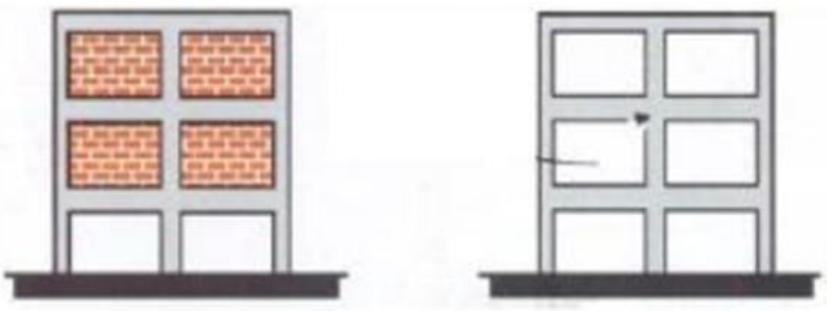

Figure 11: Buildings with open ground floor

This is especially true for concrete buildings. For these buildings, the easiest way to avoid the soft floor is to extend the brick walls on the ground floor. Some regulations, such as the Indian Code, have suggested that columns and beams be designed on the open ground floor for twice the analysis of the empty frame [38].

Ignoring the interaction between frames and infill panels in seismically prone areas is not advisable. It has been extensively reported that in every disastrous earthquake during the past few decades, severe damage and poor seismic performance of masonry infilled RC frames have been observed. The global vulnerabilities are commonly known as unexpected jeopardies or even collapse of the frame system during earthquake mainly arising from infill-frame interaction and improper arrangement of infill walls. Under lateral loading, the infill panel acts as a diagonal strut and thereby significantly increases the stiffness of the frame system, reducing the natural period of the building and magnifying the seismic force demand. On the other hand, catastrophic consequences like progressive collapse can be triggered by an irregular arrangement of infill panels horizontally and vertically. Vertical irregularity results in a severe soft story failure mechanism which has been intensively observed in past earthquake events. The horizontal irregularity of infill wall arrangement shifts the stiffness center from the mass center of a building system leading to torsional failure.[39]

The upper floors can also be soft compared to other floors. If one of the floors for some reason does not have perimeter walls and braces, etc., or is weakened or the hardness of the floor is greatly reduced, the floor is soft and should be deformed and stressed. It suffers a lot in severe earthquakes, and if this phenomenon causes problems, these changes in the hardness of the floors are not included in the design.

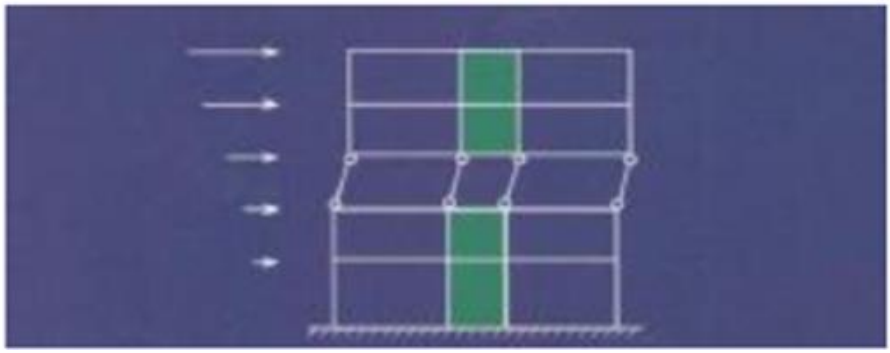

Figure 12: Create soft story in floors[39]

Another factor influencing the creation of a soft floor is the high height of one floor compared to other floors, which is often the case in ground floors due to commercial or intermediate floors with the use of community halls, and this factor reduces the hardness of the floor compared to It touches other floors and leads to a soft floor in the structure.

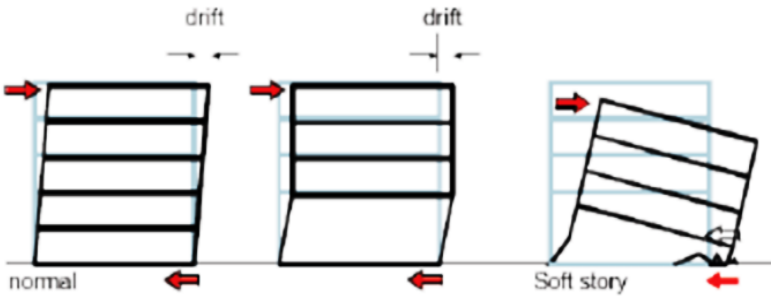

Figure 13: Creating a soft story due to the high height of the floor[39]

2.2.2 The Effect of Lateral Displacement of Floors on Soft Floor Creation

Another factor influencing the creation of a soft floor is the excessive increase in the lateral displacement of the floors, which in some codes, such as the European code, there are specific criteria for it. According to this code, the maximum relative change of position in each floor in the direction of earthquake force should not be more than 20% the relative change of other floors. If a soft story is created with this approach, by changing the significant displacement, it will create plastic hinges, which will cause permanent changes in the frame.[40]

Figure 14: Model of plastic hinges at the junction of soft story and other floors[39]

In 2004, Chopra and Chintanpakdi examined the irregular effects of stiffness and strength on drift and displacement of a 12-story building, taking into account the principle of a strong column and a weak beam in design under 20 different accelerometers. If a soft or weak floor is created, drift of that floor and the adjacent floors will be greater the original regular structure and in other floors will be less than the regular structure. Therefore, irregularity in one floor did not have much effect on the displacement created in the upper floors and was more effective in the same irregular floors.[41]

2.2.3 The Effect of Resistance of Floors in Creating a Soft Story

Reinforced concrete (RC) buildings, constructed in many countries prior to the establishment of seismic codes, have shown poor seismic efficiency in the past earthquakes [42, 43]. Soft/weak story RC buildings that caused by resistance and lateral displacement effects are the most seismically vulnerable to serious damage or complete collapse of normal buildings [44].

If the resistance of the first floor is more than 3 times the resistance of the ground floor, the creation of a soft floor is inevitable, and the Iranian earthquake Code recognizes the resistance of less than 80% of upper floors as a soft story.[37]

2.3 Seismic Design Procedures

Seismic design procedures can be classified into two types: force-based or performance-based seismic design.

2.3.1 Force-Based Seismic Design

Current seismic design in most countries in the world is carried out in accordance with force-based design methodology. The force-based design sequence is given in Figure.15

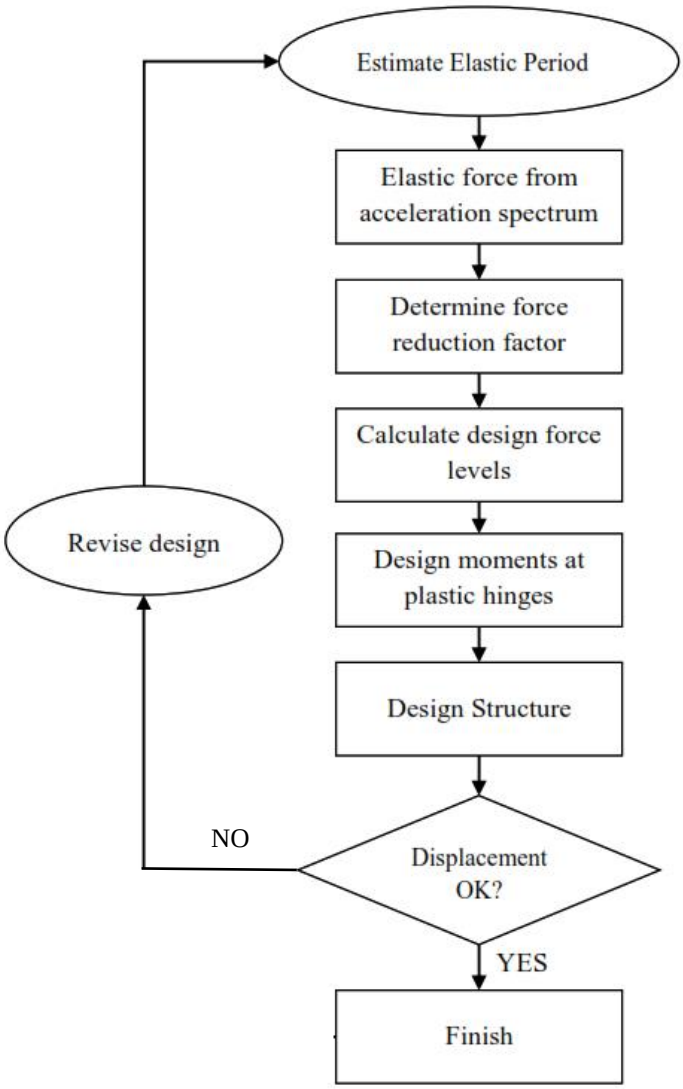

Figure 15: Design Sequence of Force-Based Design

Figure.15 briefly shows the process of determining design base shear as used in most of the current practices around the world. The force reduction factor (R) depending upon assumed ductility of the structural system, and the importance factor (I) represents occupancy factor to increase the design force for more important buildings. Lateral design forces at the floor levels (along the building height) are then determined according to the prescribed formulas to represent dynamic characteristics of the structure. Elastic analysis is performed to determine the required member strengths. After member section design for strength, a deflection amplification factor, Cd, is then used to multiply the calculated drift obtained from elastic analysis to check the

specified limits. The process is repeated in an iterative manner until the strength and drift requirements are satisfied. Proper detailing provisions are followed in order to meet the expected ductility demands.

In summary, the major weaknesses of the many current codes procedure are:

1. Assuming safety could be guaranteed by increasing the design base shear: it has been observed in many past earthquakes that collapse occurred due to local column damage.

2. Assuming design lateral force distribution along the building height based on elastic behavior: Nonlinear dynamic analyses showed that using the code distribution of lateral forces, without accounting for the fact that a structure would enter inelastic state during a major earthquake, could be the primary reason leading to numerous upper story collapses.

3. Proportioning member sizes based on initial stiffness (i.e. elastic analysis): The magnitude of individual member forces from elastic analysis is obtained based on relative elastic stiffness of structural members. However, when subjected to major earthquakes, stiffness of many members changes significantly due to concrete cracking or yielding in steel, while that of others may remain unchanged. This alters the force distribution in the structural members. Proper proportioning of member sizes cannot be achieved without using a more representative force distribution which takes into account the expected inelastic behavior.

4. Attempting to predict inelastic displacements by using approximate factors and analysis behavior: This has been shown by many prior investigations to be unrealistic, especially for structures having degrading hysteretic behavior and energy dissipation characteristics[45].

2.3.2 Performance Based Seismic Design (PBSD)

It is an iterative process that begins with the identification of performance objectives, then establishes a tentative formulation, tests how the design achieves its performance goals and eventually redesigns and reassesses it, if necessary, before the desired performance level is met. Figure.16 illustrates a process flow that shows the main stages in the design process.

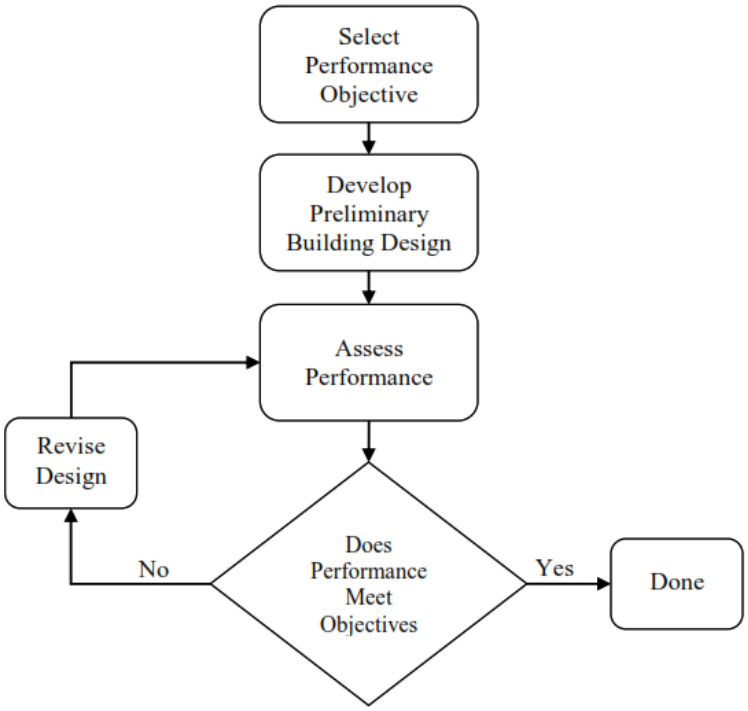

Figure 16: Performance-Based Design Flow Chart

Performance-based design starts with the selection of design criteria stated as one or more performance goals. Every performance target is a description of the reasonable risk of incurring different levels of damage at a given level of seismic hazard, and the resulting damages that result from that harm. If the performance goals have been set, a sequence of simulations (building reaction analysis to loading) are conducted to predict the building's possible performance under different construction scenario events. In the case of intense packing, as a major earthquake would give, calculations

can be rendered using nonlinear analysis methods. If the simulated performance meets the performance aims and objectives or exceeds them, the design is complete. If not, the concept should be overhauled in an iterative phase before the efficiency objectives are achieved. For certain situations, the specified purpose may not be feasible at fair expense, in which case any relaxing of the original objectives may be appropriate[46].

2.4 Seismic Evaluation Methodologies

Damages of existing buildings and loss of lives during a large number of earthquakes in different parts of the world has demonstrated the need for seismic resistance evaluation of the existing buildings especially those that are not designed to resist seismic loads. Based on that need, various organizations in various countries have introduced methodologies and guidelines for the seismic evaluation of existing buildings.

Calvi et al. (2006) classified the available seismic evaluation methodologies into two main categories: empirical (qualitative) methods and analytical (quantitative) methods. The empirical seismic evaluation methodologies are based on identifying damage patterns suffered during past seismic effects to assess the expected damage for a given building typology during future earthquakes. In another way, it tried to find damage in a building type due to a predetermined earthquake. This damage was then extrapolated to evaluate city based or region-based damage. The analytical seismic evaluation methodologies are based on a more detailed seismic evaluation with a complete numerical analysis of the building to express the relationship between seismic intensity and expected damage [47].

Rai (2003) classified the available seismic evaluation procedures into two categories: (a) configuration-related and (b) strength-related checks. The configuration-related checks involve a quick assessment of the earthquake resistance of the building by assessing the configurationally induced deficiencies known for unsatisfactory performance along with a few global level strength checks. Typical building configuration deficiencies include an irregular geometry, a weakness in a given story, a concentration of mass, or a discontinuity in the lateral force resisting system. The objective of the configuration-related checks is to screen out the significantly vulnerable structures for the detailed analysis and evaluation. The strength-related checks consist of proper force and displacement analysis to assess structural performance at both global and/or component level. Number of the available seismic evaluation methodologies are a combination of configuration-related checks and strength-related checks [48].

2.4.1 Empirical Evaluation Methodologies

According to Calvi et al. (2006), the use of empirical methods in the seismic assessment of buildings in the early 70's of the past century is came as a result of the fact that seismic hazard maps were defined in terms of a macro seismic intensity scales such as the MSK scale [49], the Modified Mercalli scale [50] and the EMS98 scale [51].

Empirical methods of seismic assessment of buildings can be classified into three main types: damage probability matrices (DPM), vulnerability index methods, and screening methods.

It should be noted that the word "vulnerability" is used to express differences in the way that buildings respond to earthquake shaking. If two groups of buildings are

subjected to the same earthquake shaking, and one group performs better than the other, then it can be said that the buildings that were less damaged had lower earthquake vulnerability than the ones that were more damaged, and vice versa.

2.4.2 Analytical Evaluation Methods

With the advancement of computational techniques, more complicated methods of seismic evaluation have been suggested. The overall objective of this type of methods are to determine the capacity of the inspected buildings to bear the seismic loads.

Analytical methods can be carried out in absence of past earthquake damage records for similar type of buildings. It also used to evaluate a specific building or type of buildings have the same structural characteristics. Based on that facts, analytical methods have been used to evaluate the seismic resistance of buildings in the undertaken research. Analytical methods can be classified into two main types: capacity spectrum-based methods and displacement-based methods.

2.5 Collapse Mechanism

There are three traditionally defined types of failure for columns under lateral load; flexure-critical, shear-critical, and flexure-shear-critical, as shown in Figure 17. A flexure-critical column is one that has enough shear strength to produce flexural yield, whereas a shear-critical column fails in shear, with the corresponding moment demand substantially lower than the moment power. A flexure-shear-critical column is one which yields in flexure at higher ductility levels before shear failure.

Calculating the Flexural-to-shear strength ratio (FSSR) and using Table will predict the failure mechanism. It should be noted that the classification scheme for columns

defined for ductility was established by the ASCE and therefore may not be directly applicable to small ductile columns:

$$FSSR = \frac{M_n}{LV_n} \quad (1)$$

Where:

- $M_{n=}$ the nominal moment capacity of a column
- $V_{n=}$ the nominal shear strength of a column
- $L =$ column length

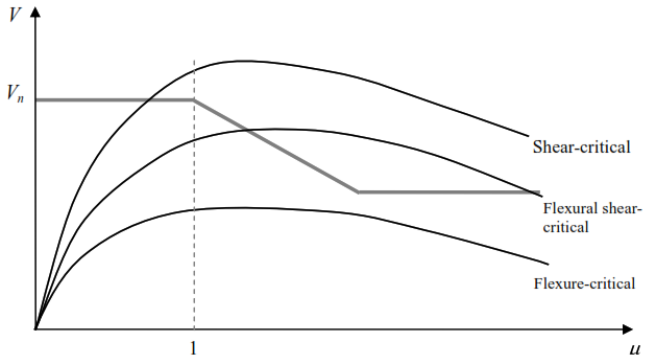

Figure 17: Shear strength degradation and displacement ductility

Table 1: Classification of Failure Mechanism (ASCE/SEI 41-06)

	Transverse Reinforcement Details		
	ACI conforming details with 135° hooks	Closed hoops with 90° hooks	Other (including lap spliced transverse reinforcement)
$FSSR \leq 0.6$	Flexure	Flexure-shear	Flexure-shear
$0.6 < FSSR \leq 1.0$	Flexure-shear	Flexure-shear	Shear
$FSSR > 1.0$	Shear	Shear	Shear

2.5.1 Drift Values at Failure Due to Lateral Load

The available models for predicting the drift ratio at lateral load failure (80% of the peak lateral load capacity) are described in the following subsections.

2.5.1.1 Sezen & Moehle Model (2002)

The model described by Sezen & Moehle in 2002 relates the shear strength of the column to the demand for displacement ductility and divides the shear force into the shear held by the concrete (V_c) and the shear held by the reinforcement through a 45° truss model (V^s)[52]:

$$V_n = k(V_c + V_s) = \left[\frac{0.5\sqrt{f_c'}}{L/d}\sqrt{1 + \frac{P}{0.5\,A_g\sqrt{f_c'}}}\right]0.8A_g + k_\mu \frac{A_v f_{yh} d}{s} \quad (2)$$

The coefficient k determines shear force degradation with increased ductility for displacement. The degradation coefficient is applied to both Vc and Vs on the assumption that the concrete component will decrease as a result of increased cracking and deterioration of the aggregate interlock system, while the steel component is expected to decrease as a result of a reduction in the bond stress capacity demanded for an effective truss.

2.5.1.2 Elwood & Moehle Model (2005)

Elwood implemented an empirical model, based on experimental database findings as shown in the Figure 18:

$$\delta_{lf} = \frac{3}{100} + 4\rho'' - \frac{1}{500}\frac{v}{\sqrt{f_c'}} - \frac{1}{40}\frac{P}{A_g f_c'} \geq \frac{1}{100} \quad (3)$$

where:

- δ_{lf} = drift at lateral load failure
- $\rho^{"}$ = transverse reinforcement ratio (A_{st}/bs)
- v = maximum nominal shear stress recorded during the tests (V_{test}/bd)
- *P* = axial load
- *Vtest* = peak shear recorded.

The model may not be valid to columns with parameters outside the ranges contained in the database, as the coefficients were chosen in Equation 3 based on a minimum square fit to the data. Further analysis is required to account for variability in demand and efficiency of the shear[53].

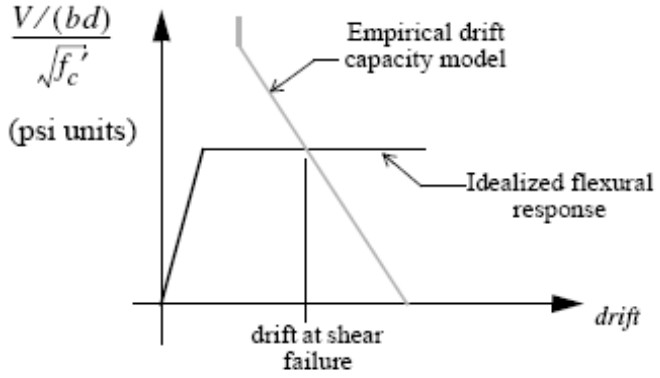

Figure 18: Evaluation of drift at lateral load failure

2.5.1.3 Zhu et al. Model (2007)

Zhu et al proposed drift as a function of the transverse reinforcement ratio, containment ratio, aspect ratio, and axial load ratio as shown in Equation 4 at lateral load failure. The proposed model suggests that lateral load failure drift increases with either an increase in the transverse reinforcement ratio and aspect ratio, or a reduction in the transverse hoop spacing ratio and axial load ratio[54]:

$$\delta_{lf} = 2.02\rho_h - 0.025\frac{s}{d} + 0.013\frac{L}{D} - 0.031\frac{P}{A_g f_c'} \quad (4)$$

Where:

- ρ_h= the transverse reinforcement ratio
- s = the hoop spacing
- D = column width
- L = shear span
- P = axial load

2.5.2 Drift Values at Failure Due to Axial Load

This section presents several models for predicting the drift ratio at axial load collapse, including: Elwood and Moehle (2003), Ousalem, Kabeyasawa and Tasai (2004) and Zhu, Elwood and Haukaas (2007).

2.5.2.1 Elwood and Moehle Model (2003)

Elwood and Moehle developed a model for predicting the drift ratio at axial load failure based on the shear friction rather than longitudinal bar strength. The model was developed for a shear-critical reinforced concrete column as a function of the transverse reinforcement and the axial load as shown in Figure 19 and the following expression:[55]

$$\delta_{af} = \frac{4}{100}\frac{1+(\tan\theta)^2}{\tan\theta+P\left[\frac{s}{A_v f_{yh} d_c \tan\theta}\right]} \quad (5)$$

where:

- d_c= column core depth from centre line to centre line of ties
- s = transverse reinforcement spacing
- A_v= transverse reinforcement area
- f_{yh}= transverse reinforcement yield strength
- P = axial load acting on the column
- θ = critical crack angle from horizontal (assumed to be 65°).

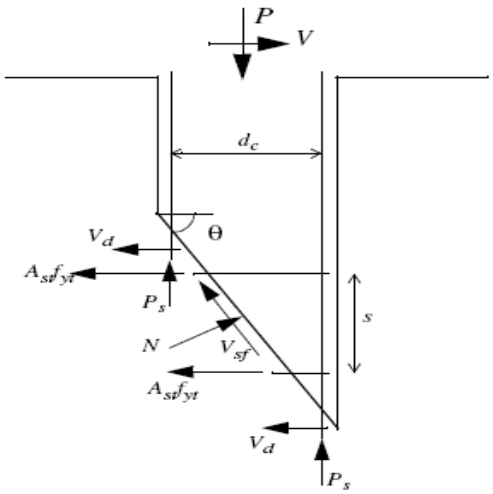

Figure 19: Free-body diagram of column after lateral load failure

2.5.2.2 Ousalem et al. Model (2004)

The formula suggested by Elwood and Moehle was modified by Ousalem et al by introducing dowel action from the transverse reinforcement and an empirical friction coefficient μ on the inclined plane as shown in Figure 20 and described in the following expression[56]:

$$\mu = 0.5(k\delta_{af})^{-0.36} \quad (6)$$

Where:

- δ_{af}= the drift at axial failure
- k = a constant expressed as $\frac{\rho_h f_{yh}}{n f_c'}$
- ρ_h= the steel area ratio of transverse reinforcement
- f_{yh} = the yield stress of transverse reinforcement
- n = the axial load ratio
- f_c'= the concrete strength.

By equating the friction expressed by Equation 6 with the friction at collapse $\left(\mu_{max} = \frac{1-k_1}{2\sqrt{k_1}}\right)$ where *k1* = 0.003+1.33*k*, the maximum drift at axial load failure is given as:

$$\delta_{af} = \frac{1}{k}\left(\frac{0.97-1.33k}{\sqrt{0.03+1.33k}}\right)^{\frac{1}{0.36}} \quad (6)$$

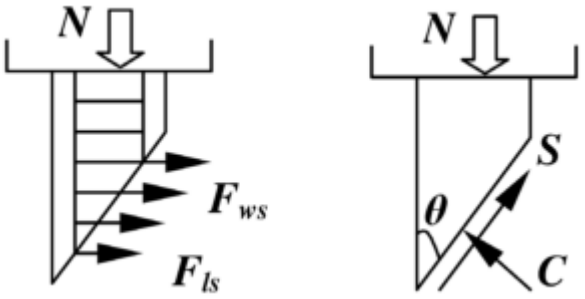

Figure 20: The equilibrium forces for shear model

2.5.2.3 Zhu et al. Model (2007)

Zhu et al. proposed an expression for drift at axial failure using the friction formula (μ) suggested by Elwood and Moehle (2003) based on 28 column specimens as follows[54]:

$$\mu=\frac{\left[\frac{P}{A_v f_{yh} d_c/s}-1\right]}{\left[\frac{P}{A_v f_{yh} d_c/s}\frac{1}{\tan\theta}+\tan\theta\right]} \quad (8a)$$

which can be simplified to the following expression:

$$\mu=\frac{\left[\frac{P}{V_s}-1\right]}{\left[\frac{P}{2.1V_s}\frac{1}{\tan\theta}+2.1\right]} \quad (8b)$$

Where:

$$V_s = \frac{A_v f_{yh}\, d}{s} \quad (9)$$

The proposed drift at axial load failure was developed experimentally by Zhu, Elwood and Haukaas and assuming $\theta = 65°$, the expression reduces to the following:

$$\delta_{af} = 0.184e^{(-1.45\mu)} \quad (10)$$

where:

- d_c = depth of the column core centreline to centreline of transverse reinforcement
- A_v = the cross-sectional area of transverse reinforcement parallel to the applied shear along one principal direction of the cross section

2.6 Seismic Performance Assessment

There are several seismic assessment methods available with varying levels of complexity; linear static procedure (LSP), linear dynamic procedure (LDP), non-linear static procedure (NSP), and non-linear dynamic procedure (NDP) as described in the following sections.

2.6.1 Linear Static Procedure (LSP)

Regular or low-rise story buildings respond primarily in the fundamental mode under earthquake excitation which allows a linear static approach to be undertaken by modelling the building as a single degree of freedom system. The elastic forces are reduced by a response modification factor to implicitly account for the inelastic response. The nominal base shear force V_b can then be calculated as follows:

$$V_b = \frac{Z\,C\,I}{R} W_t \quad (11)$$

Where:

- Z = acceleration coefficient
- *C* = normalized earthquake response factor for natural period T1
- W_t = total weight of structure including proportion of live load
- *I* = the importance factor
- *R* = response modification factor.

The fundamental natural period T1 can be estimated using the Rayleigh formula which provides an upper bound of natural frequency. This formula is derived from the law of conservation of energy by equating the potential energy with the kinetic energy of a vibrating structure.

$$T_1 = 2\pi\sqrt{\frac{M}{K}} = 2\pi\sqrt{\frac{\sum_{i=1}^{n} W_i\, d_i^2}{g\sum_{i=1}^{n} F_i d_i}} \quad (12)$$

Where:

M = the total system mass

K = the lateral stiffness of the system

Wi = floor weight of the ^{ith} story

Fi = horizontal forces at the i^{th} story

di = corresponding displacement at the i^{th} story.

These concepts of equal displacement, energy and acceleration are shown in Figure 21 and following studies by Newmark (1964, 1965, 1960), several conclusions have been reached:

- For system with a longer natural period, the equal displacement concept has been assumed since the maximum displacement for inelastic systems is similar to the elastic systems having the same period.
- For systems in the intermediate period range, the equal energy concept has been assumed since the total energy absorbed by the inelastic system is similar to the elastic system having the same period.
- For systems with short natural periods (as found in stiffer SDOF systems) the equal acceleration concept has been assumed, as the inertia force is similar for both the inelastic and elastic systems having the same natural period.

The over-strength factor R_{os} is the ratio between the actual and design strength of the structure which is dependent on detailing and material strength. For most structures, R_{os} is conservatively assumed to be in order of 1.3-1.5.

The LSP is useful tool for estimating the lateral earthquake forces imposed on a structure, although it must be noted that response modification factor (R) is a considerable simplification for estimating the effect of inelastic action and overstrength.

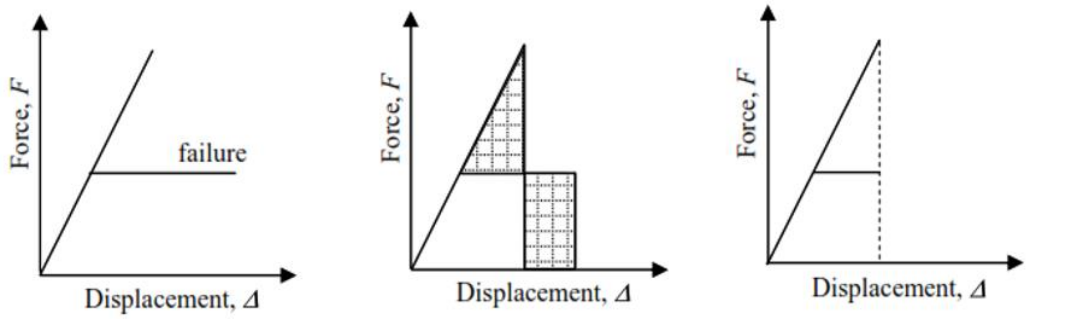

(a) Equal acceleration (b) Equal velocity (energy) (c) Equal displacement

Figure 21: Concepts of equal displacement, energy and acceleration

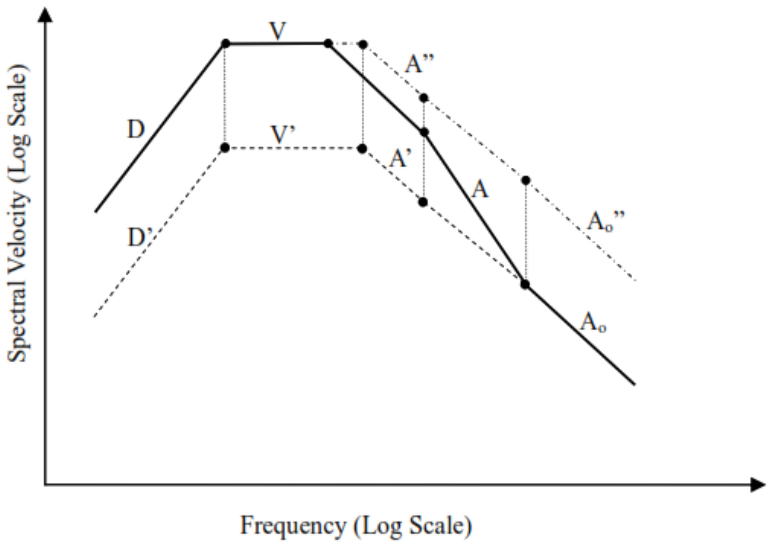

Figure 22: Inelastic response spectrum

2.6.2 Linear Dynamic Procedure (LDP)

The SDOF system model is not representative of the response of tall buildings and irregular buildings where higher modes are significant. Hence a dynamic analysis is required to accommodate the higher mode earthquake response by modelling the system as a multi degree of freedom (MDOF) system and analyzing the structure using a matrix representation of the mass, elastic stiffness and equivalent damping. The equation of motion can be written as:

$$\overline{M}.\ddot{\overline{x}} + \overline{C}.\dot{\overline{x}} + \overline{K}.\overline{x} = \overline{M}.\overline{r}.\overline{\ddot{x}_g} \quad (13)$$

where: $\overline{M}, \overline{C}, \overline{K}$ are the mass, damping, and stiffness matrices, $\ddot{\overline{x}}, \dot{\overline{x}}, \overline{x}$ are the acceleration, velocity and displacement vectors, $\overline{r}$ is the influence vector for the ground displacement, and $\overline{\ddot{x}_g}$ is the earthquake accelerogram.

The dynamic equation of motions is solved using modal analysis, whilst the earthquake ground motion is typically represented by a response spectrum. The response spectrum is typically reduced by the response modification factor (R) to implicitly account for inelastic behavior including over-strength and ductility.

The summation of modal responses is usually computed using either:

- Square Root of the Sum of Squares (SRSS) for well separated modes,
- Complete Quadratic Combination (CQC) for closely spaced modes.

Natural periods can be considered close to each other if the difference between two adjacent modes are less than 15%.

2.6.3 Non-Linear Static Procedure (NSP)

The NSP method is suitable for structures which respond primarily in their fundamental mode and has the significant advantage that inelastic behavior and over-

strength is modelled explicitly. Two common NSP methods are: a) displacement coefficient method and b) capacity spectrum method which are described in the following subsections.

2.6.3.1 Displacement Coefficient Method

The displacement coefficient is a method based on a comparison between the displacement capacity and the displacement demand of the structure which can be described as follows:

- The displacement capacity is determined using a static push-over analysis where the monotonic lateral forces are applied to the building using a distribution that is representative of the likely distribution of inertia forces in the design earthquake.
- The maximum inelastic displacement demand (Δ_t) is predicted as a product of the maximum displacement of a linear elastic system (Δ_e) with a series of displacement modification coefficients such as those described in FEMA 273, 1997:

$$\Delta_t = C_0 C_1 C_2 C_3 \Delta_e \quad (14)$$

$$\Delta_e = S_a \left(\frac{T_e}{2\pi}\right)^2 \quad (15)$$

Where, C_0 is the modal participation factor, C_1 is a coefficient modifier for the increased displacement of short period system, C_2 is a coefficient modifier for hysteretic shape, C_3 is a coefficient modifier for the second order effect, Sa is the response spectral acceleration at the effective fundamental period and damping ratio of the building, and T_e is the effective natural period of the system which can be estimated assuming a lateral stiffness equal to the secant stiffness calculated at a base shear force equal to 60% of the yield strength. According to FEMA-273, the structure

is deemed satisfactory if the displacement capacity is larger than 1.5 times the peak displacement demand at the roof level of the structure.

The reliability of this method was assessed by Whittaker et al. (1998) by comparing the estimated displacement using Equation 14 with the displacement predicted using a non-linear response-history analysis of SDOF oscillators having varying values of yield strength and post yield stiffness subjected to 20 earthquake ground motions compatible with the code spectrum. The study showed that the displacement coefficient method provided reasonable results for structures with periods greater than the predominant site period (T_g), but tended to underestimate the mean inelastic displacements for structures with shorter natural periods.

2.6.3.2 Capacity Spectrum Method

The capacity spectrum method combines the capacity curve obtained from a push-over analysis and the demand curve in the form of acceleration-displacement response spectrum to evaluate the performance point and involves the following 3 steps:

a) Capacity Curve

The push-over curve comprising base shear (V_b) and roof displacement (Δ_{top}) is converted to the corresponding capacity curve in an acceleration-displacement spectrum S_a and S_d format as follows:

$$S_a = \frac{V_b}{M_1^*} \tag{16a}$$

$$S_b = \frac{\Delta_{roof}}{\Gamma_1 \emptyset_{N1}} \tag{16b}$$

Where:

$$M_1^* = \frac{\left(\sum_{j=1}^{N} m_j \emptyset_{j1}\right)^2}{\sum_{j=1}^{N} m_j \emptyset_{ji}^2}$$

$$\Gamma_1 = \frac{\sum_{j=1}^{N} m_j \emptyset_{j1}}{\sum_{j=1}^{N} m_j \emptyset_{ji}^2}$$

- S_a = the spectral acceleration
- S_b= the spectral displacement
- V_b= the base shear forces
- M_1^* = the effective modal mass for the fundamental vibration mode
- m_j= the lumped mass at the jth floor level
- $\emptyset_{j1}$= the jth floor element of the fundamental mode $\emptyset_1$
- N= the number of floors
- Γ_1 = the modal participation factor for the fundamental mode.

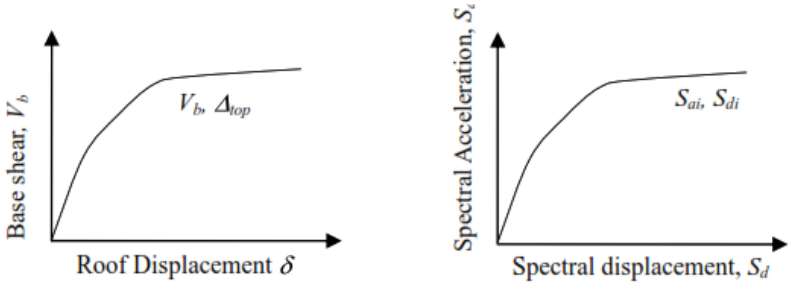

Figure 23: Conversion of capacity push-over curve to capacity curve

b) Demand Curve

The design response spectrum is converted from the standard S_a vs T format to ADRS S_a vs S_d format as follows:

$$S_d = \left(\frac{T}{2\pi}\right)^2 S_2$$

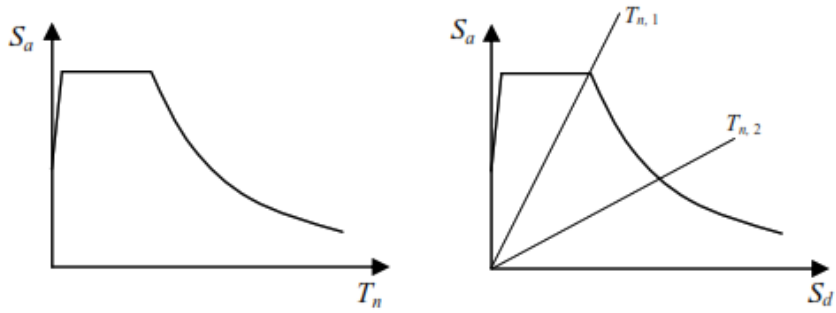

Figure 24: Conversion of elastic response spectrum from standard format to ADRS format

c) Performance Point

The capacity and demand spectrum curves are plotted together and the performance point is determined at the point where the curves intersect as shown in Figure 25 The performance point can be further optimized by adjusting the demand curve for the appropriate level of damping representative of the degree of inelastic energy absorption. The structure is deemed to have failed if the demand and capacity curves do not intersect.

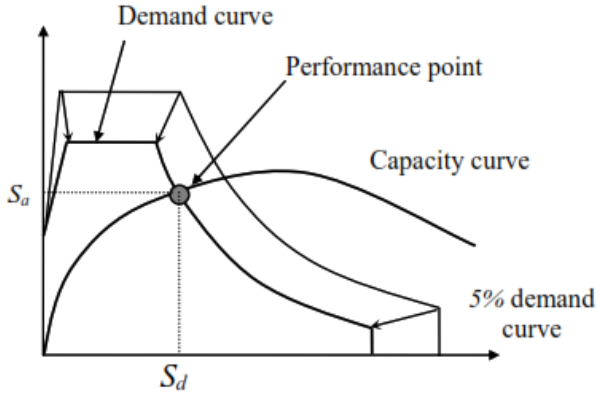

Figure 25: Seismic performance point determination

2.6.4 Non-Linear Dynamic Procedure

For irregular structures or buildings with a special purpose such as a post-disaster function, a non-linear dynamic analysis is recommended to provide a better estimate of the inelastic response. An NDP involves a nonlinear time history analysis using a

detailed structural model with nonlinear elements and a time-domain analysis solution. The equilibrium equation of motion can be expressed as:

$$\bar{M} \cdot \ddot{\bar{x}} + \bar{C} \cdot \dot{\bar{x}} + S \cdot \bar{x} = \bar{M}.\bar{r}.\ddot{\bar{x}}_g(t) \quad (17)$$

where:

- $\bar{M}$= mass matrix
- $\bar{C}$= structure damping matrix
- s(x)= inelastic strength matrix
- $\ddot{\bar{x}}, \dot{\bar{x}}, \bar{x}$= acceleration, velocity, and displacement vectors
- F(t)= external forces vector
- $\bar{r}$= the influence vector for the ground displacement
- $\ddot{\bar{x}}_g$= the earthquake accelerogram.

Equation 17 is similar to equation 13 except the stiffness matrix has been replaced by an inelastic strength term (S) which describes the hysteretic behavior of the different elements of the MDOF system. The structure damping matrix C can be determined using the Rayleigh model which is dependent on the mass (M) and stiffness (K) term as follows:

$$\bar{C} = a_0\bar{M} + a_1\bar{K} \quad (18)$$

where: *ao* and *a1* are coefficients that can be altered in order to have proportionality in the required viscous damping as shown in Figure 26.

The NDP method is time-consuming and computationally quite expensive and is also highly dependent on the characteristic of individual ground motions used in the analysis. Consequently, at least three ground motions are required to estimate the

reliable structural response. The NDP is used extensively as a research tool and for checking the performance of significant structures in regions of high seismicity.

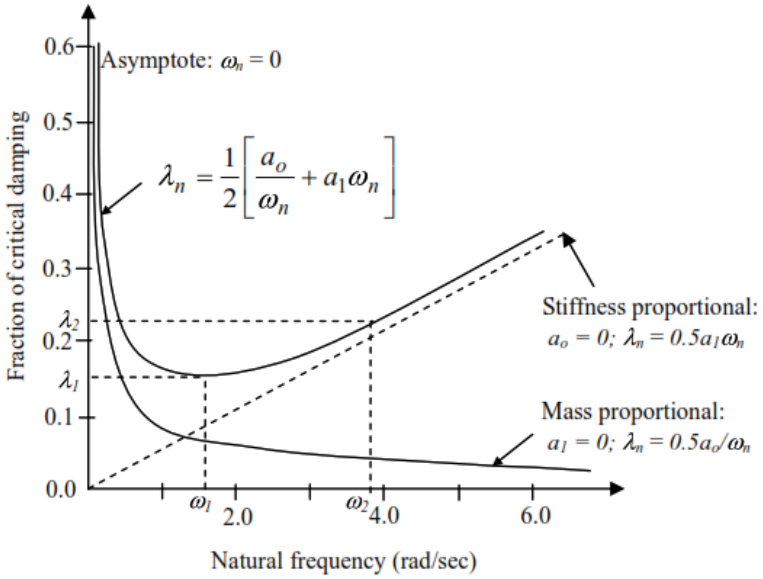

Figure 26: Rayleigh damping model

2.6.5 Comparison of Seismic Performance Evaluation Procedures

In summary, LSP and NSP are forced-based and displacement-based methods respectively which are useful for structures that responding primarily in the first mode. The LSP provides a simple method for the conceptual design and the design of elastic and regular structures, whilst the NSP provides an insight into the inelastic behavior of structures.

For structures where higher mode effects are important, such as irregular structures or buildings with a special purpose, the dynamic analysis methods such as LDP and NDP are recommended. The NDP method is the most complex and is commonly used for checking the performance of significant structures under earthquake excitation.

The NDP method will be used in this research study for assessing the seismic performance of soft story structures which can be realistically modelled the system.

2.7 Brief Review on Retrofitting Measures and Seismic Control Methods

In recent decade several methods have been proposed and applied for seismic retrofit of existing building, of which some ideas have been used for design of new buildings as well. Among the proposed methods and techniques are using hysteretic dampers, either friction or yielding types, using yielding as well as buckling restrained braces. Some of these studies are briefly reviewed in the following:

- **Sabelli and Mahin (2003):**

Traditional braced system performed poorly during earthquakes due to the failure of the connection between bracing and frame, low energy dissipation and limited ductility capacity[57]. Accordingly several retrofitting strategies are suggested in various international codes to monitor the excessive losses or total collapse of the defective RC buildings with soft/weak stories [58, 59].

Phocas and Pocanschi in 2003, adopted closed cross-bracing cable members with a yielding device as retrofitting measures for steel frames. Since the damper is separated from the frame and the cables do not affect the static behavior of the frame under dead load, the facility can be installed and replaced easily[60].

- **Khampanit, A., et al, Sahoo, D.R. and D.C. Rai (2014, 2010):**

Because the percentage of longitudinal reinforcing steel cannot be increased and/or the size of transverse stirrups at the projected plastic hinge positions of the current RC structures decreased, external intervention techniques are implemented in action. The use of passive energy dissipating devices is considered one of the efficient intervention techniques that allow seismic energy to dissipate through these devices, thereby

reducing the demand for seismic load and deformation on the existing RC frame members. Metallic yielding dampers have been shown to perform well in enhancing RC structures' seismic efficiency[61, 62].

- **Gray et al. (2014):**

The Yielding Brace Mechanism is a very ductile braking device in which the fingers of a specially built cast-steel connector dissipate seismic energy. The fingers bend when the strap is heavily filled with friction and compression, thereby offering a complete, symmetrical hysteresis. Second-order geometric impacts increase the rigidity at large displacements post-production. The device mechanics are first introduced, including several initial key equations to predict the response of a connector. These equations are then used to construct a connector of the prototype. Using the nonlinear finite element analysis is the geometry of this prototype evaluated. The findings of the total axial function concept test are evaluated after this report. This finding involves processing of tensile coupons from material directly obtained from unprocessed parts of the test specimens. The concept and research experiment revealed that the Yielding Brace Framework is a ductile connector that increases the energy efficiency of the spray brace. Strong agreement between the expected and experimental response demonstrated a good understanding of connector dynamics and a successful method for the designing of the prototype for the target production.[63]

- **Shin et al. (2016):**

Retrofitting measures which aim to improve the seismic performance of soft-story building can be divided into two types: 1.strengthening the soft story (fiber-reinforced polymer (FRP) jacketing) [64] and 2.reducing the displacement demand by adding energy dissipation elements (friction damper[65] , viscous damper[66] and metallic damper[67]) to the building. In some cases, a combination of these measures is adopted

to achieve satisfactory seismic performance of building. The use of anchoring braces is economical for controlling the lateral displacement of frames during earthquakes. Mualla and Belev investigated the seismic performance of a steel frame retrofitted with friction damper devices installed in an inverted cable V-bracing system, which can effectively reduce the displacement demand and base shear[68].

Kurata proposed a bracing system consisting of cables and a central energy dissipating device as a simple and rapid seismic retrofit strategy for steel structures.[69]

- **Guo-Qiang Li et al. (2019):**

Buckling-restricted brace (BRBs) are commonly used in the construction, in particular for braced frames as load-bearers as well. The standard BRBs are, however, elastically engineered for avoiding low-cycle fatigue under regular earthquakes and cannot lead to the dissipation of seismic energy. To address this flaw, it is proposed that traditional BRBs combine with metal tube dampers to create a new form of buckling-restricted buckling (TYBRBs) two-level braces. The TYBRB tube damper generates seismic energy during regular earthquakes. In this paper, TYBRBs are initially presented with configuration and mechanical models. Two specimens of the TYBRB are planned and cyclic load tests are conducted. It is found that: (1) low-cycle tube dampers fatigue resistance can meet TYBRB 's requirements for regular earthquake resistance; (2) TYBRB 's functions can be realized with a reasonable design; (3) BRB 's output in TYBRBs does not degrade with the combination of tube damper.[70]

- **Nobahar et al. (2020):**

Recent seismic events have shown that excessive residual drifts after the earthquake may lead to high repair cost, temporary disruption of construction functions due to necessary repair or even to complete construction destruction. As such, it is a crucial

measure to eliminate remaining drifts while the building is being rehabilitated after the seismic action. A highly resilient self-centering brace system (PT-SCYBS) after tensioning has been implemented to this purpose, which has been examined. In new or current diagonally tightened frame systems PT-SCYBS will be built to be implemented. In order to provide a hysteretic flag shaped response, the device is based on the self-centering action of the post-tension cords along with the return behavior of the steel bars. This research presents the findings of a variety of nonlinear dynamic studies and provides a comparative analysis of PTS CYBS frames, moment resistant frames (MRFs) and buckling constrained braced frames (BRBFs). The FEMA P58 methodology implemented in PACT software was then performed with a detailed comparative seismic performance evaluation of PT-STIBS buildings and the buildings MRF and BRBF references The results show that the PT-SCYBSs have lower residual drifts than the reference buildings, which lead to considerable savings in repairs and damages, and increase seismic efficiency.[71]

- **Serhat Demir and Metin Husem (2018):**

The paper introduces tests, numbers and theoretical studies of a passive energy dissipation system known as a SWESS, which is specifically designed for building safety during earthquakes, and offers high ductility and energy dissipation ability. STSED has a variety of metallic components that are uniquely formed and can dissipate energy by flexural yielding. The main feature of STSED is its configuration that makes it possible to use more metallic components than current literature schemes, while enabling a pinned connection with a framing system. The system and the related equations used in the construction of the prototype are discussed in detail. [72]

Chapter 3

METHODOLOGY

3.1 Introduction

The procedure used to conduct this study is outlined in this chapter and associated numerous steps such as: model details and modeling method, earthquake record selection, scaling and evaluation of earthquake data, building seismic assessment, performance-based earthquake engineering, and finally, proposing a method for building strengthening by using diagonal energy dissipation. Also, this chapter contains some specific details of methods and major terminologies.

3.2 Research Methodology

This research consists of three main stages. First stage is designing the three ordinary structures with soft story at lowest level, and different number of stories. The second stage is changing the designed buildings into the buildings with controlled soft story by adding the desired fuses at that level. Finally, the third stage is optimizing the fuse properties and comparing of two groups of buildings based on the results of a series of nonlinear time-history analyses.

3.3 Design Specifications

Before performing nonlinear time history analysis of structures, a structure designed based on standards or based on existing conditions and complete specifications of its structural and non-structural components is required. Here we give a complete description of the modeling method and specifications of materials and structural components and the design method and standards used in it to determine the criteria

of initial linear analysis as well as structural design criteria. EATABS software has been used for design of buildings (which employs the performance-based design according to ACI 318-11), particularly their lateral load bearing systems. The sections that have been used for columns are the square type which is the common type of section for concrete columns. The beams have designed based on gravity and lateral loads. The p-delta and eccentric effect is accordingly applied in the software.

To achieve the research objectives, a plan according to Figure 27 has been used. The number of floors of the models is 5, 7 and 9 floors with a height of 3 meters and the ground floor with a height of 4 meters.

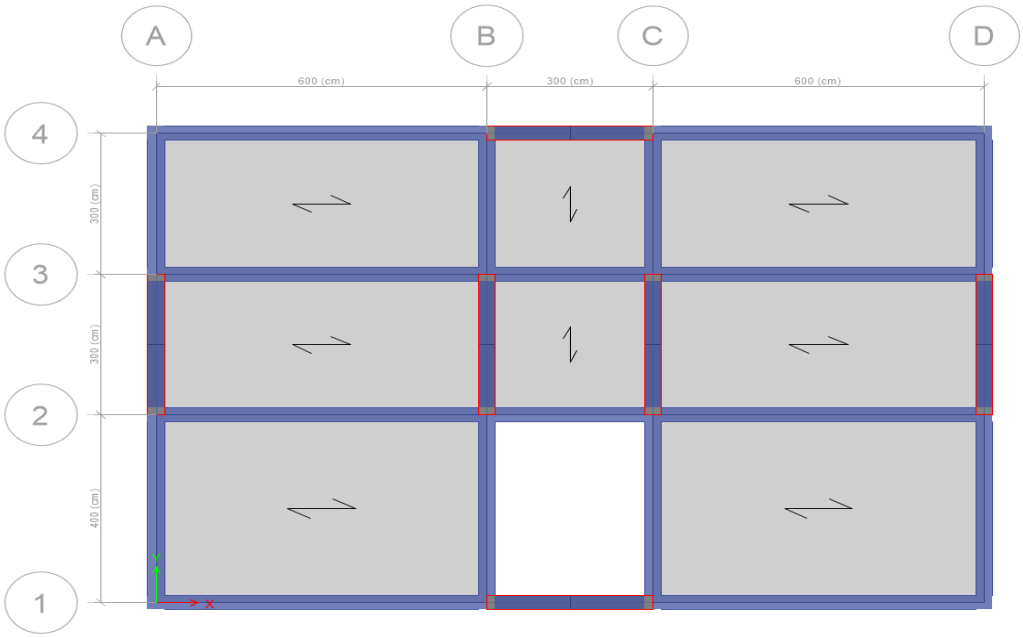

Figure 27: Ground floor plan of designed structure

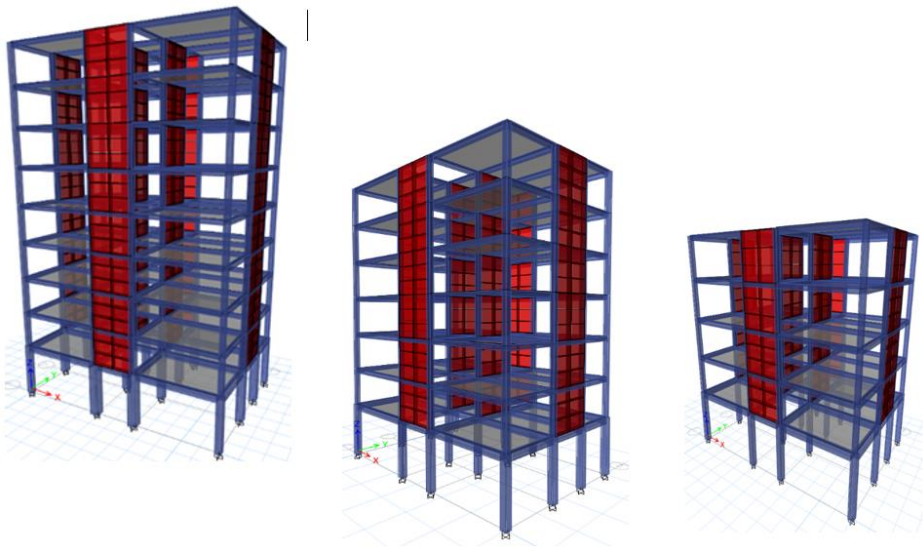

Figure 28: Three-dimensional view of designed structures

To design the considered reinforced concrete structures, ACI 318-11 and the last edition of ASCE 41-17 design code have been used and the details of all elements have been reviewed and observed in accordance with these regulations.

According to the residential use of the building, the dead and live loads of the floors and roof are as follows:

Dead load (stories): 550 $^{kgf}/_{m^2}$ Dead load (roof):500 $^{kgf}/_{m^2}$

Live load (stories):200 $^{kgf}/_{m^2}$ Live load (roof):150 $^{kgf}/_{m^2}$

For peripheral walls, a wall load of 800 kgf/m has been used. Uniform distributed loads are placed linearly according to the tributary area of each beam in two types of dead and live. Also, for marginal beams, the load of peripheral walls is applied on them, this time it is added to other dead loads.

3.3.1 Design for Earthquake Loading

To calculate the seismic lateral load the general equation of seismic evaluation has been used and the steps are briefly presented here:

$$V = \frac{1.2\ S_{DS}}{R} W \quad (19)$$

Where:

S_{DS} = the design elastic response acceleration at short period as determined in accordance with table 9.4.1.2.5.

R = the response modification factor from Table 9.5.2.2

W = the effective seismic weight of the structure as defined in Section 9.5.3

Lateral loading of the structure for seismic forces is based on American standard. To perform static and dynamic analysis of the structure, the types of soils introduced in ASCE regulations and its standard response spectra have been used for dynamic analysis. According to ASCE regulations, the amount of earthquake force is determined by the earthquake coefficient c and the weight of the structure. The earthquake coefficient entered into the structure is equal to:

$$V = C_s W \quad (20)$$

Where:

$\boldsymbol{C_s}$ = the seismic response coefficient determined in accordance with Section 9.5.5.2.1

$\boldsymbol{W}$ = the total dead load and applicable portions of other loads as indicated in Section 9.5.3.

When the fundamental period of the structure is computed, the seismic design coefficient (C_s) shall be determined in accordance with the following equation:

$$C_s = \frac{S_{DS}}{R/_I} \quad (21)$$

Where:

S_{DS} = the design spectral response acceleration in the short period range as determined from Section 9.4.1.2.5

R = the response modification factor in Table 9.5.2.2

I= the occupancy importance factor determined in accordance with Section 9.1 .4.

Based on the performed design of the considered buildings their modal periods are obtained as presented in table 2.

Table 2:´Natural periods of designed buildings

Building	First period	Second period	Third period
Nine story	1.336	1.264	1.089
Seven story	1.129	1.095	0.986
Five story	0.594	0.464	0.356

Also, optimal design of structural elements sections has been tried to be achieved for all three buildings and efforts have been made to obtain the best and closest models to the existing buildings.

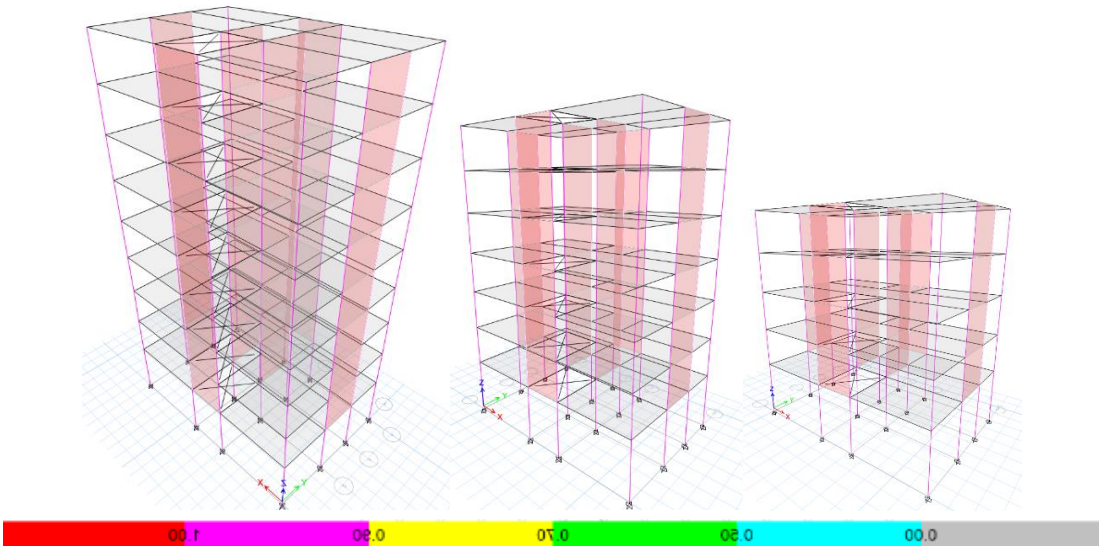

Figure 29: Colorful presentation of D/C for the designed buildings

3.4 Mechanical Properties of the Considered Materials

All the type of sections and materials are selected from the regular shape and most common materials for beams and columns and one example for each section are presented below:

ACI 318-11 Concrete Beam Design

Geometric Properties (Part 1 of 2)

Beam Label	Section Property	Length	Section Width	Section Depth	Distance to Top Rebar Center
106	BEAM 30*30	600 cm	30 cm	30 cm	6 cm

Geometric Properties (Part 2 of 2)

Distance to Bot Rebar Center
6 cm

Material Properties

Concrete Comp. Strength	Concrete Modulus	Longitudinal Rebar Yield	Shear Rebar Yield
0.281 tonf/cm²	253.456 tonf/cm²	4.218 tonf/cm²	4.218 tonf/cm²

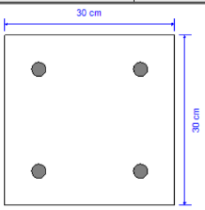

Figure 30: Beam design sample

ETABS Concrete Frame Design

ACI 318-11 Column Section Design

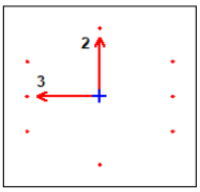

Column Element Details (Summary)

Level	Element	Unique Name	Section ID	Combo ID	Station Loc	Length (cm)	LLRF	Type
Story1	C13	65	40*40	DCon10	0	430	0.569	Sway Intermediate

Section Properties

b (cm)	h (cm)	dc (cm)	Cover (Torsion) (cm)
40	40	4.9	2.73

Material Properties

E_c (tonf/cm²)	f'_c (tonf/cm²)	Lt.Wt Factor (Unitless)	f_y (tonf/cm²)	f_{ys} (tonf/cm²)
253.456	0.281	1	4.218	4.218

Design Code Parameters

Φ_T	Φ_{CTied}	$\Phi_{CSpiral}$	Φ_{Vns}	Φ_{Vs}	Φ_{Vjoint}	Ω_0
0.9	0.65	0.75	0.75	0.6	0.85	2

Figure 31: Column design sample

3.4.1 Process of Model Analysis for Initial Design

All loads on the structure are applied to the structure according to the previous tables. For structural analysis in the design stage, static analysis has been used.

3.4.2 Loading Compounds Applied to The Structure

ACI 318 regulations have been used to design the structure. All compounds are assumed to be in accordance with US regulations and for non-linear static analysis loading compounds based on improvement instructions.

Seismic load combinations have been introduced to consider the effects of dead and live gravity loads. These compounds are:

QG = 2.2 (QD + QL) (5-5)

QG = 2.2QD (1-5)

According to the improvement instruction, QD is the dead load and QL is the live load according to this ASCE monograph. In reviewing the results, a critical load combination is considered to take into account the effects of gravity load. In the models, first the gravitational load combinations are introduced and then the nonlinear static analysis under the effect of lateral load in the continuation of these loading conditions is performed. The reason for this is that in nonlinear analysis the sum of the effects of forces is not generally valid. Therefore, for each loading combination, it is necessary to analyze the structure from the beginning and completely, so gravity loads must be applied to the structure simultaneously with the lateral loads. Gravity load compositions the improvement instruction is only to investigate the simultaneous effect of gravity loads and lateral loads caused by earthquakes and is not used to evaluate the gravity loads of the structure.

3.5 Design with Soft Story

In this section, we will discuss how to form a soft story to achieve a reasonable model for structural analysis.

As mentioned in two last chapters, the factors influencing the formation of the soft story can be divided into two main categories. The first category is the change in the height of the floor and the second is the removal of the walls between the frame or the infield walls, which all cause irregularities in the arrangement of the rigidity of the structure, which eventually creates the soft story phenomena.

After applying the effective factors in forming the soft story and performing static, dynamic analysis and general design of the structure, in the following table, it has been controlled the soft story phenomenon by using the standard codes.

According to these codes, the standard or accepted value of the floor drift in relation to the whole structure is equal to 5.66 and in relation to the higher floor is 2.356, which is not acceptable if it is more than this value.

Also, another method for controlling the soft story according to this FEMA 360 code is to check the stiffness of the floor with the upper floor or relative to the stiffness of the whole structure. The minimum value for the stiffness of the floor is 70% for the upper floor and 80% for the whole structure.

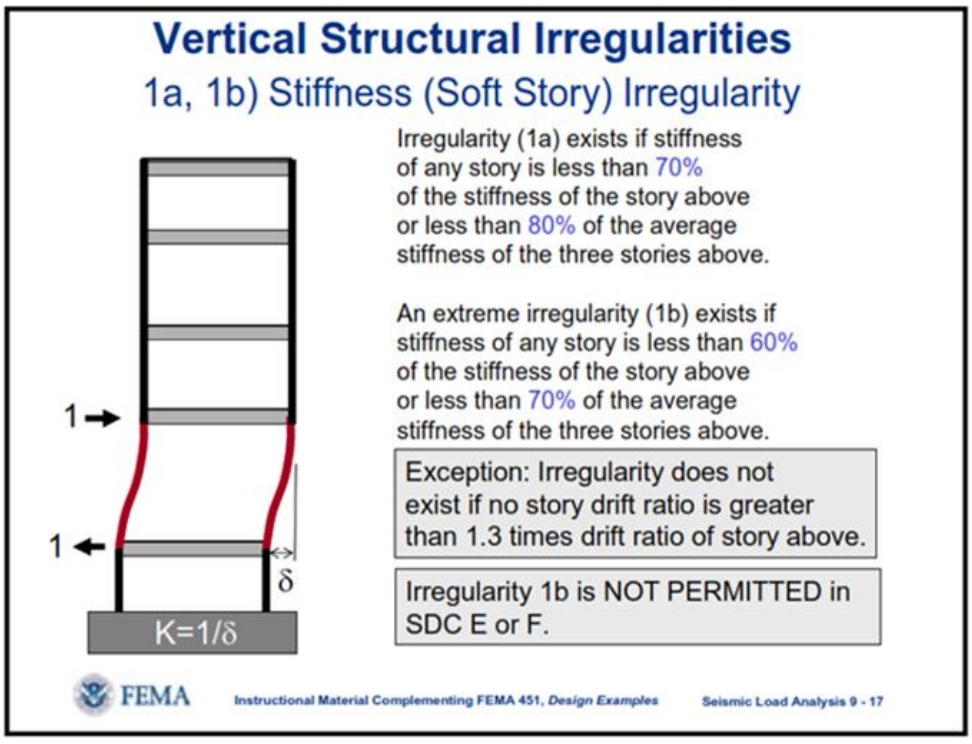

Figure 32: Soft story control regulations [71]

Table 3: Drift control of five story design building example

EARTHQUAKE 1				
Story	**Drift**	**Direction**	**Δ i+1/Δi**	**check**
			1.3	
5	0.003849	X	-	-
5	0.002143	Y	-	-
4	0.003775	X	0.980774227	ok
4	0.002121	Y	0.989734018	ok
3	0.003299	X	0.873907285	ok
3	0.001933	Y	0.911362565	ok
2	0.002582	X	0.782661413	ok
2	0.0016	Y	0.827728919	ok
1	0.033161	X	12.84314485	Soft Story
1	0.044109	Y	27.568125	Soft Story

Table 4: Drift control of seven story design building example

EARTHQUAKE 1				
Story	**Drift**	**Direction**	**Δ i+1/Δi**	**check**
			1.3	
7	0.00599	X		ok
7	0.00338	Y		ok
6	0.005959	X	0.994824708	ok
6	0.003391	Y	1.003254438	ok
5	0.005676	X	0.95250881	ok
5	0.003312	Y	1.1231E-05	ok
4	0.005137	X	0.90503876	ok
4	0.003133	Y	0.945954106	ok
3	0.004203	X	0.818181818	ok
3	0.002756	Y	0.87966805	ok
2	0.003383	X	0.804901261	ok
2	0.002306	Y	0.836719884	ok
1	0.051837	X	15.32279042	Soft Story
1	0.071921	Y	31.18863833	Soft Story

Table 5: Drift control of nine story design building example

EARTHQUAKE 1				
Story	**Drift**	**Direction**	**Δ i+1/Δi**	**check**
			1.3	
9	0.014488	X		
9	0.01043	Y		
8	0.014435	X	0.9963418	ok
8	0.010452	Y	1.0021093	ok
7	0.013765	X	0.953585036	ok
7	0.01026	Y	0.98163031	ok
6	0.012392	X	0.900254268	ok
6	0.009808	Y	0.955945419	ok
5	0.010525	X	0.849338283	ok
5	0.009026	Y	8.8527E-05	ok
4	0.008408	X	0.798859857	ok
4	0.007784	Y	0.862397518	ok
3	0.006202	X	0.737630828	ok
3	0.006139	Y	0.788669065	ok
2	0.004179	X	0.673814898	ok
2	0.00438	Y	0.713471249	ok
1	0.040701	X	9.739411342	Soft Story
1	0.053168	Y	12.13881279	Soft Story

Table 6:stiffness control of five story design building

level	**stifness**	**Direction**	**k (i)/k (i+1)** **0.7**	**check**
5	58.24	X	-	-
4	119.19	X	**2.05**	**ok**
3	181.89	X	**1.53**	**ok**
2	259.41	X	**1.43**	**ok**
1	63.30	X	**0.24**	**Soft Story**
level	**stifness**	**Direction**	**k (i)/k (i+1)** **0.7**	**check**
5	112.94	Y	-	-
4	231.61	Y	**2.05**	**ok**
3	352.12	Y	**1.52**	**ok**
2	513.10	Y	**1.46**	**ok**
1	70.27	Y	**0.14**	**Soft Story**

Table 7: stiffness control of seven story design building

level	stifness	Direction	k (i)/k (i+1) 0.7	check
7	27.12	X		
6	56.53	X	**2.08**	**ok**
5	82.06	X	**1.45**	**ok**
4	108.87	X	**1.33**	**ok**
3	146.54	X	**1.35**	**ok**
2	203.86	X	**1.39**	**ok**
1	61.65	X	**0.30**	**Soft Story**
level	**stifness**	**Direction**	**k (i)/k (i+1) 0.7**	**check**
7	52.13	Y		
6	108.78	Y	**2.09**	**ok**
5	158.03	Y	**1.45**	**ok**
4	209.99	Y	**1.33**	**ok**
3	281.48	Y	**1.34**	**ok**
2	398.86	Y	**1.42**	**ok**
1	69.29	Y	**0.17**	**Soft Story**

Table 8: stiffness control of nine story design building

level	stifness	Direction	k (i)/k (i+1) 0.7	check
9	20.04	X		
8	42.28	X	2.11	ok
7	61.65	X	1.46	ok
6	81.16	X	1.32	ok
5	104.26	X	1.28	ok
4	137.64	X	1.32	ok
3	192.39	X	1.40	ok
2	287.93	X	1.50	ok
1	138.54	X	0.48	Soft Story
level	**stifness**	**Direction**	**k (i)/k (i+1) 0.7**	**check**
9	34.73	Y		
8	73.39	Y	2.11	ok
7	106.72	Y	1.45	ok
6	139.52	Y	1.31	ok
5	176.59	Y	1.27	ok
4	226.58	Y	1.28	ok
3	313.60	Y	1.38	ok
2	466.44	Y	1.49	ok
1	148.93	Y	0.32	Soft Story

As it is seen in Tables 3 to 8, based on the drift and stiffens values in accordance to FEMA code, the lowest stories of all designed buildings are categorized as the soft story.

3.6 Introducing the Control Device and Its Modeling in ABAQUS

3.6.1 Introducing the Proposed Energy Dissipater

The proposed energy dissipating device, or structural fuse element, which is a hardening and multi stage yielding energy dissipater (HAMSYED), has been considered to be installed inside the corresponding frames at the lowest story of the building (the soft story) as shown in Figure 33.

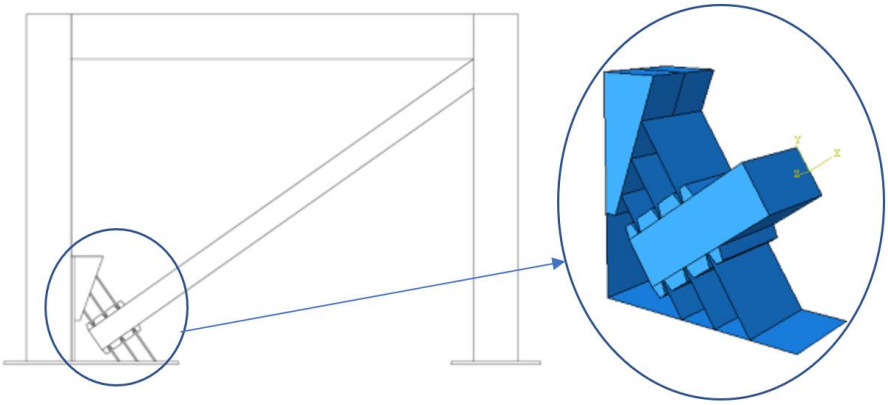

Figure 33: The installed location of the fuse in frame

The hardening stiffness and multi-stage yielding characteristics of the proposed HAMSYED device is provided by using three yielding plates with different lengths (and thicknesses if necessary) which get into action one by one successively. This successive action is because of the gaps with specific size, provided between the teeth-form elements installed at two opposite sides of the box section of the diagonal bracing element, and the two shorter (the second and the third) plates of the device, as shown in Figure 34.

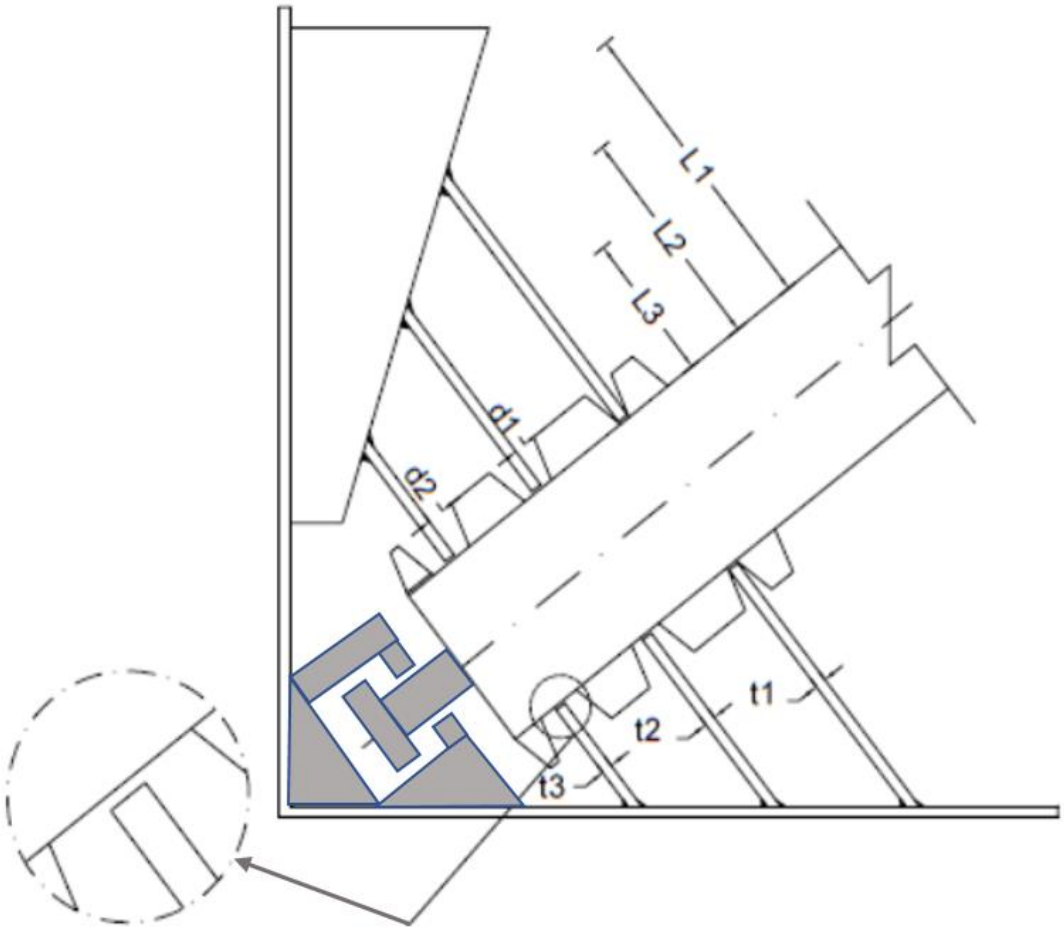

Figure 34: Details of the yielding plates, teeth-form elements and stopper (dark areas) of the HAMSYED device

It is seen in Figure 34 that plates 1, with length of L1 and thickness of t1, are fixed in the opening between the two teeth-form elements, while each one of plates 2, with length of L2 and thickness of t2, has gap of d1 (which is to be equal to the yielding displacement of plates 1) at its either sides, and each one of plates 3, with length of L3 and thickness of t3, has a gap of d2 (which is to be equal to the yielding displacement of plates 2) at its either sides. As such, when the diagonal bracing element is subjected to axial load, either compression or tension, and tends to move at its axial direction, the two plates 1 show their resistance from the beginning of the movement. At this stage the stiffness of the system is equal to the bending stiffness of the two plates 1 together in elastic range. By increase in the axial displacement of the diagonal element

and reaching the value of d1, the two plates 1 start yielding and the two plates 2 start resisting in their elastic range. In this stage the stiffness of the system is equal to the bending stiffness of plates 2 together. By more increase in the axial displacement of the diagonal element and reaching the value of gap in the stopper part of the device (say d3), the two plates 2 start yielding and the diagonal bracing element itself start resisting in its elastic range. In this last stage, the stiffness of the system is equal to the axial stiffness of the bracing element.

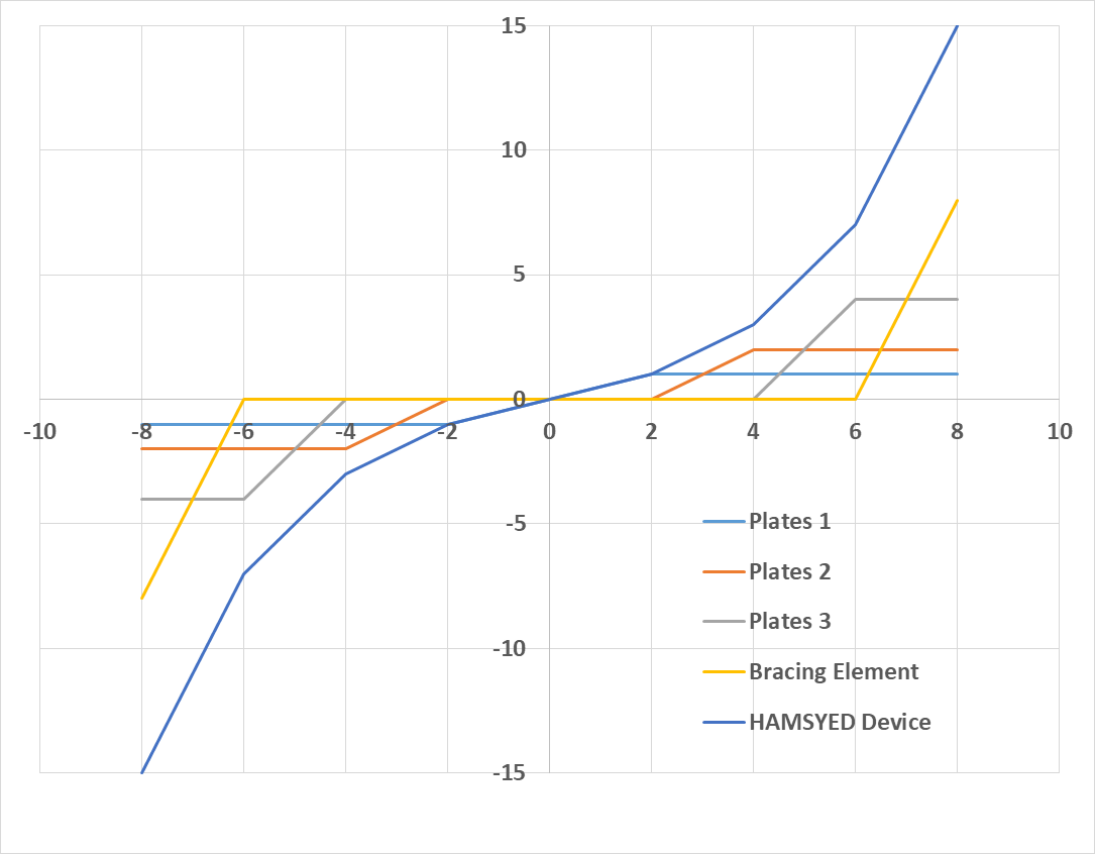

Figure 35: Schematic force – displacement curves of the HAMSYED and its yielding plates series

Based on the nonlinear behavior of the yielding plates the HAMSYED device, it has an elastic-plastic behavior, which can create a good potential for energy dissipation, as shown in the next section by modeling the device in ABAQUS software.

Its actual case, the HAMSYED is connected to the corresponding frame, either steel or RC, by using some plates, which have been previously prepared and installed in the frame corner. Considering the fact that the connection of the brace element to the structure is of pin type, by applying lateral force to the frame, only axial force is applied to the fuse element. The boundary conditions and loading of the element are as shown in Figure 36.

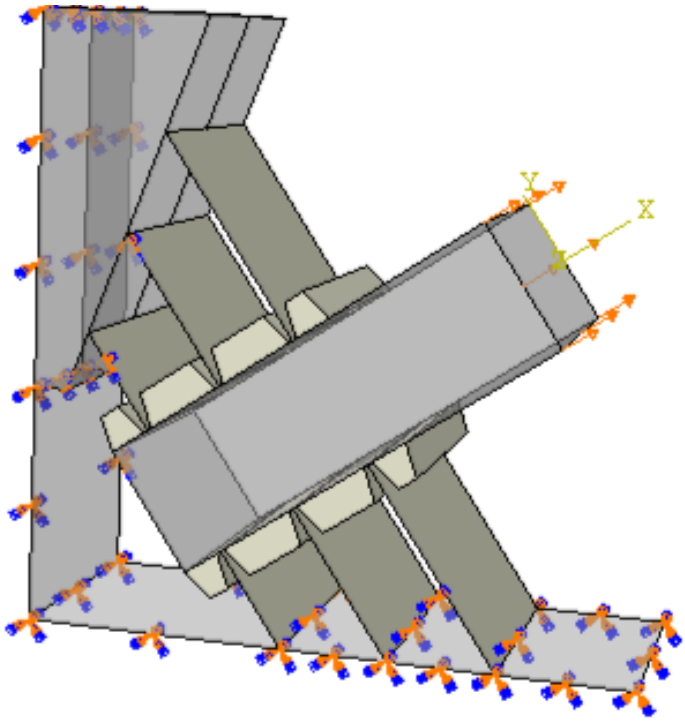

Figure 36: The boundary conditions and loading of the element in HAMSYED

In order to prevent the buckling of the plates, they are manufactured with some edge distance from the body of the bracing element. Furthermore, for proper placement of the HAMSYED device in the fame and auxiliary installation part has been considered as shown in Figure 37, which its dimensions depend on the height to span ration of the corresponding frame.

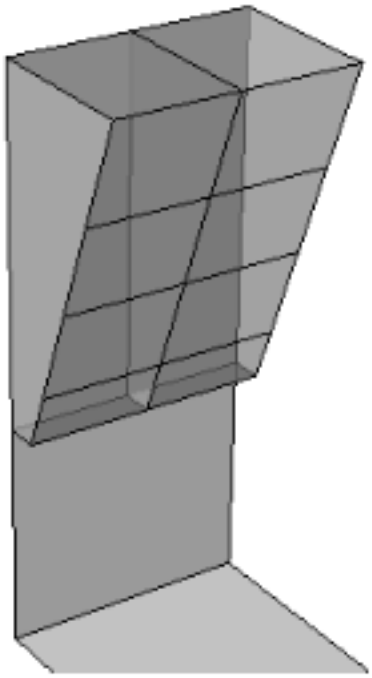

Figure 37: Installation auxiliary part of the HAMSYED device

Three set of appropriate values of the HAMSYED device geometric parameters are given in Table 9.

Table 9: Values of the HAMSYED device geometric parameters

Model	L1	L2	L3	d1	d2	t1	t2	t3
M1	27	20	13	1	1	1	1	1
M2	27	20	13	1.25	1.5	1	1.5	2
M3	27	20	13	1.75	2	1	1.5	2

In the following section, first the ABAQUS software, which has been used for finite element modeling of HAMSYED is briefly introduced, and then, a sample of numerical modeling of the HAMSYED in ABAQUS environment is presented.

3.6.2 Introducing ABAQUS Software

ABAQUS software has a large library of elements, materials and methods of analysis and with the help of finite element method has the ability to simulate the behavior of high-precision instrument systems. In this software, in order to model the behavior of

the structure in the dough range, the theory of incremental plasticity is used. The theory of mathematical relationships to express the increase in stress and strain and the behavior of materials in the dough range 1 is incremental plasticity theory. The main components of this theory include the following materials:

- Yield Criterion
- Flow Rule
- Hardening rule.

3.6.3 Yield Criterion

Under uniaxial tensile stress, the yield strength is equal to the axial stress with the yield stress of the materials. For tension Multi-axis, it is necessary to define a suitable criterion of surrender limit. Surrender by placing the amount of stress combination as equivalent stress on the submission surface of a cylinder in the direction of the axis with the principal stress equal in all directions, in a three-dimensional device or an elliptical boundary in the two-dimensional coordinates go beyond the Figure. Shows the relationship of the yield level with respect to the main stress components:

$$\frac{1}{\sqrt{2}} \times \sqrt{(\sigma 1 - \sigma 2)^2 + (\sigma 2 - \sigma 3)^2 + (\sigma 3 - \sigma 1)^2} = F_y \quad (22)$$

Hardening rule:

The yield level during plastic flow is corrected according to the law of strain hardening. If the load is applied and removed and reloaded in the original direction or loaded in the reverse direction, the law of hardening with re-submission in the material makes sense and determines the level of submission formed.

ABAQUS defines two main hardening rules to modify the level of submission:

Isotropic hardening:

The yield surface expands uniformly in all directions as the plastic flows as shown in Figure 38.

Kinematic Hardening:

The yield surface remains constant in size and expands in the direction of flow according to the Figure 38:

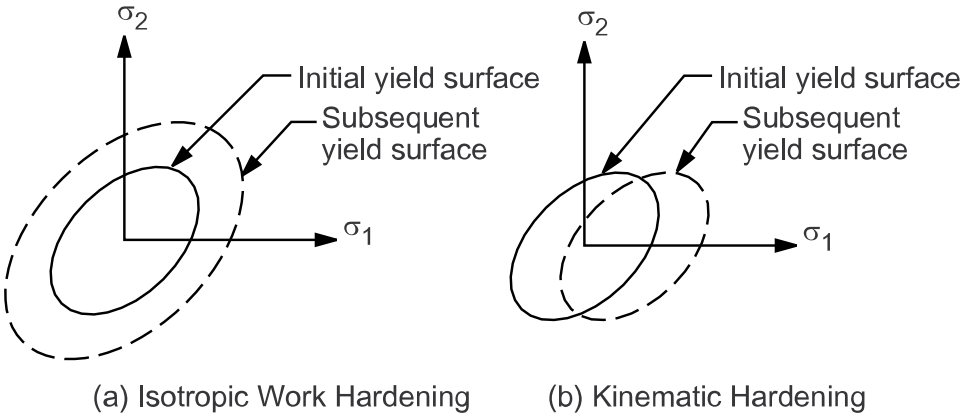

Figure 38: Hardening rule

Isotropic stiffness has been used for uniform loads and kinematic stiffness has been used for loads with varying directions of application due to the control of convergence repetitions.

In the case of isotropic stiffening behavior under the axial force of the secondary yield stress at the pressure, it reaches the extent that the yield stress under tension increases. This phenomenon is shown in Figure 39. It is shown that this decrease in resistance to the actual behavior of the steel considering the Bauschinger effect of the decontamination.

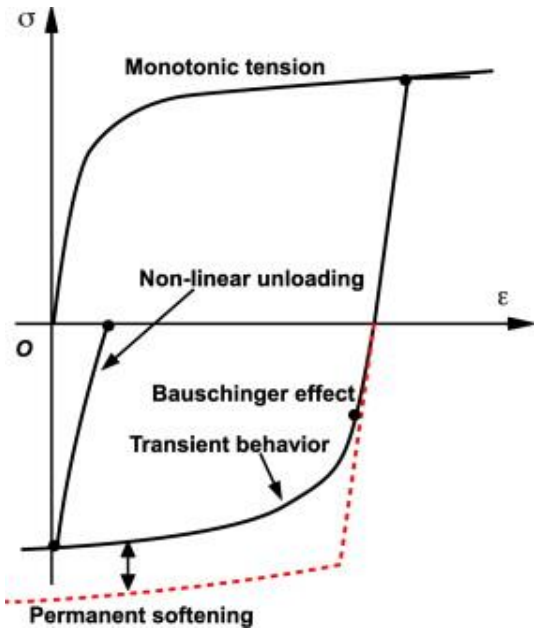

Figure 39: schematic unloading curve under reverse loading to illustrate the Bauschinger effect, transient behavior and permanent softening.

In the linear or elastic region, due to the homogeneity and linear behavior of steel materials, the state of isotropic behavior is expressed. Substances that have basic isotropic properties do not remain isotropic after yielding and experiencing kinematic hardening.

3.6.4 Modeling of the Proposed Energy Dissipater in ABAQUS Software

Examining the actual results of adding a control fuse to a soft-floor frame can only be done through laboratory work, but modeling in finite element software can also play an effective role in predicting its behavior.

By modeling the fuse element in Abaqus software and examining its nonlinear behavior under nonlinear static analysis, the behavior of the structure is evaluated in the elastic to failure range. Table 10 shows the materials used in this element. The modeling steps in Abacus software are discussed below:

Table 10: Details of materials used

Modulus of Elasticity (kgf/cm^2)	Yielding Strain	Ultimate Strain	Yielding Stress (kgf/cm^2)	Ultimate Stress (kgf/cm^2)
2.1E+6	**0.013**	**0.250**	**2400**	**3700**

The displacement-control loading of the system in the reciprocating mode was done up to 8 cm, and by performing the analysis of the distribution of von Mises stress, as shown in Figure 40.

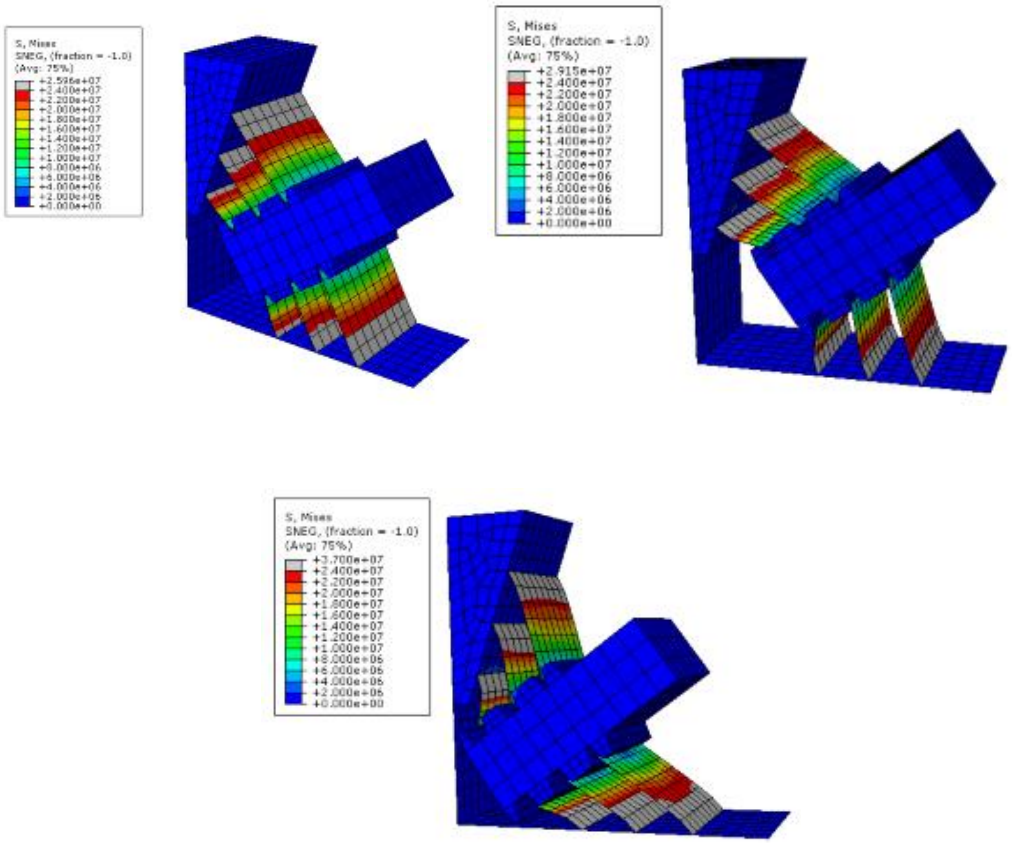

Figure 40: Check out the Von Mises stress model in ABAQUS

In order to make a full contact between the tips of the plates and the stoppers, as well as to prevent the plates' edges from sliding out, the height of the stoppers was considered as 4 cm as shown in Figure 41.

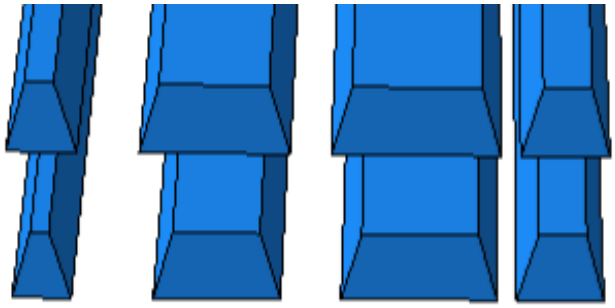

Figure 41: The close-up of the used stoppers in HAMSYED

The back-bone and the hysteretic curves of the modeled HAMSYED are shown in Figures 42 and 43.

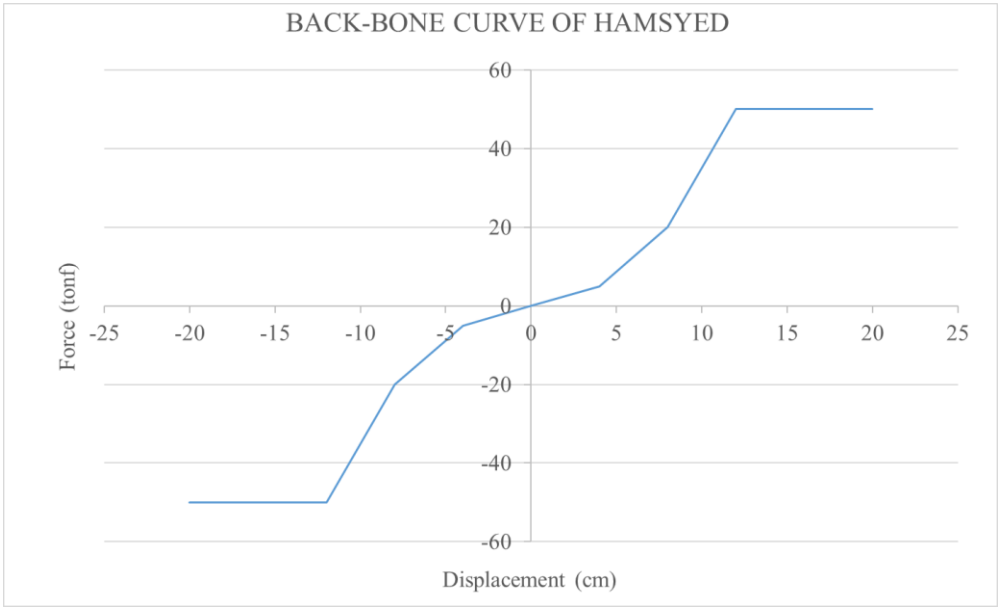

Figure 42: Back-bone curves of HAMSYED

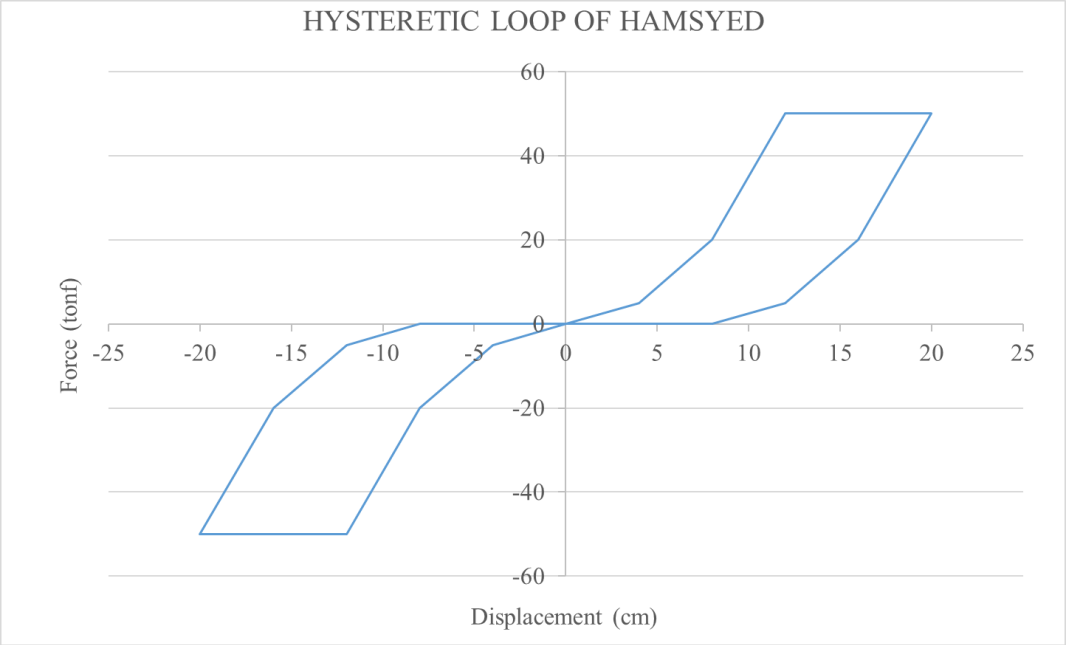

Figure 43: Hysteretic curves of HAMSYED

It is seen in Figure 43 that the hysteretic loop of the HSMSYED is wide and quite stable, and due to the appropriate distance between the connection plate and the appendage between them, the desired contact occurs. Looking at the results shown in Figure 42 it can be seen that a change of slope occurs in the curve when the connecting plates get in contact with the middle stoppers, and finally the slope of the curve decreases slightly due to the yielding of the last plate. The appropriate behavior of the element under the effect of the axial force is also seen in the Figure 43.

3.7 Finding Initial Values of HAMSYED Parameters

An important part of the study for using the appropriate HAMSYED is finding the initial values of its mechanical characteristics, including the initial, secondary and third stiffness values, as well as the first, second and third yielding strengths. For this purpose, a nonlinear SDOF system was considered in which the stiffness has the following nonlinear relationship with it displacement:

$$f_s(u) = a_1 U^1 + a_2 U^3 + a_3 U^5 \quad (23)$$

This force – displacement relationship results in the following stiffness relation:

$k = a_1 + 3a_2U^2 + 5a_3U^4$

On this basis the equation of motion of the system subjected to earthquake ground acceleration can be written as:

$$m \times \ddot{U} + c \times \dot{U} + (a_1U^1 + a_2U^3 + a_3U^5) = -m \times \ddot{U}_g(t) \quad (24)$$

From which the acceleration of the system can be stated in terms of its other response values as well as the seismic excitation, as:

$$\ddot{U} = -\ddot{U}_g - \frac{1}{m}\left(c \times \dot{U} + a_1U^1 + a_2U^3 + a_3U^5\right) \quad (25)$$

To find the appropriate values of a_1, a_2 and a_3 as well as the damping coefficient c, a computer program was developed in MATLAB platform to solve Equation 25 for a given mass of the system and a given input earthquake acceleration time history. The listing of the developed code in MATLAB is as follows:

```
clc
clear
close all
format short
a1=3;
a2=0.01;
a3=0.0001;
c=500;  %tonf.s/cm
m=700;  %tonf
acx=load('EARTH2-X_dtnew_0.00015625_.txt');
acy=load('EARTH2-Z_dtnew_0.00015625_.txt');
n1=length(acx);
A=[acx,zeros(n1,1),acy];
N=length(A);
s=ones(N,5);
sc=981;
s(:,2)=s(:,2).*sc;
s(:,5)=s(:,5).*sc;
A=A.*s;
D=A(2,1)-A(1,1);
g=981;  % cm/s^2
u(1,1)=0;  ud(1,1)=0;  udd(1,1)=0;  uddabs(1,1)=0;
t(1,1)=0;
i=1;
for n=i:N-1
k1=(D^2/2)*(-1*A(n,2)-(1/m)*(c*ud(n,1)+a1*u(n,1)+a2*u(n,1)^3+a3*u(n,1)^5));
```

```
k2=(D^2/2)*(-1*A(n,2)-
(1/m)*(c*(ud(n,1)+k1/D)+a1*(u(n,1)+((D*ud(n,1))/2+k1/4))+a2*(u(n,1)+((D*ud(n,1))
/2+k1/4))^3+a3*(u(n,1)+((D*ud(n,1))/2+k1/4))^5));
k3=(D^2/2)*(-1*A(n,2)-
(1/m)*(c*(ud(n,1)+k2/D)+a1*(u(n,1)+((D*ud(n,1))/2+k1/4))+a2*(u(n,1)+((D*ud(n,1))
/2+k1/4))^3+a3*(u(n,1)+((D*ud(n,1))/2+k1/4))^5));
k4=(D^2/2)*(-1*A(n,2)-
(1/m)*(c*(ud(n,1)+(2*k3)/D)+a1*(u(n,1)+D*ud(n,1)+k3)+a2*(u(n,1)+D*ud(n,1)+k3)^
3+a3*(u(n,1)+D*ud(n,1)+k3)^5));
u(n+1,1)=u(n,1)+D*ud(n,1)+(k1+k2+k3)/3;
ud(n+1,1)=ud(n,1)+(k1+2*k2+2*k3+k4)/(3*D);
udd(n+1,1)=(-1*A(n,2)-(1/m)*(c*ud(n,1)+a1*u(n,1)+a2*u(n,1)^3+a3*u(n,1)^5));
uddabs(n+1,1)=udd(n+1,1)+A(n,2);
t(n+1,1)=t(n,1)+D;
z=1+u(n+1,1);
end
tend=floor(max(t))+1.5;
uMax=max(abs(u(:,1)));
uddabsMax=max(abs(uddabs(:,1)));
udMax=max(abs(ud(:,1)));
Allresponse=[uMax;udMax;uddabsMax];
Allresp=fopen('Allresponse.txt','wt');
fprintf(Allresp,'%8.6f\n',Allresponse);
fclose(Allresp);
resu=fopen('u.txt','wt');
fprintf(resu,'%+15.12f\n',u);
fclose(resu);
resud=fopen('ud.txt','wt');
fprintf(resud,'%+15.12f\n',ud);
fclose(resud);
resudd=fopen('udd.txt','wt');
fprintf(resudd,'%+15.12f\n',udd);
fclose(resudd);
figure(1);
p1=plot(t,u,'k');
tmup=1.1*max(abs(u));
set(p1, 'linewidth', 1.1)
set(gca, 'FontSize', 14)
%set(p4,'color',[0.3 0 1])
grid on
xlabel('t (sec)');
ylabel('Horizontal displacement (cm)');
axis([0 tend -1*tmup tmup]);
savefig('u');
print('u','-djpeg');
figure(2);
p2=plot(t,ud,'k');
```

```
tmudp=1.1*max(abs(ud));
set(p2, 'linewidth', 1.1)
set(gca, 'FontSize', 14)
%set(p5,'color',[0.3 0 1])
grid on
xlabel('t (sec)');
ylabel('Horizontal velocity (cm/s)');
axis([0 tend -1*tmudp tmudp]);
savefig('ud');
print('ud','-djpeg');

figure(3);
p3=plot(t,udd,'k');
tmudd=1.1*max(abs(udd));
set(p3, 'linewidth', 1.1)
set(gca, 'FontSize', 14)
%set(p6,'color',[0.3 0 1])
grid on
xlabel('t (sec)');
ylabel('horizontal acceleration (cm/s^2)');
axis([0 tend+0.1 -1*tmudd tmudd]);
savefig('Udd');
print('udd','-djpeg');
figure(4);
p4=plot(t,uddabs,'k');
tmuddabs=1.1*max(abs(uddabs));
set(p4, 'linewidth', 1.1)
set(gca, 'FontSize', 14)
%set(p6,'color',[0.3 0 1])
grid on
xlabel('t (sec)');
ylabel('Absolute horizontal acceleration (cm/s^2)');
axis([0 tend+0.1 -1*tmuddabs tmuddabs]);
savefig('Uddabs');
print('uddabs','-djpeg');
%(ud(n,1)+k1/D)
% (u(n,1)+((D*ud(n,1))/2+k1/4))
%  (ud(n,1)+k2/D)
%  (u(n,1)+D*ud(n,1)+k3)
%  (ud(n,1)+(2*k3)/D).
```

The developed program starts with a given value for a_1, and zero values for other parameters, and then by a small increment, increases the values of other parameters, and calculate the maximum response of the system for each set of the considered

parameters, to find the set of parameters which minimizes the maximum response of the system. After finding the appropriate values of the parameters and drawing the third-degree curve of the nonlinear stiffness of the system, a multi-linear curve is matched to the nonlinear curve by assigning appropriate values to the initial, secondary and third stiffness values.

The appropriate values obtained by the method explained above, are used as the initial guesses for the stiffness values of the HAMSYED device in the real building model in ETABS software. By changing these parameters slightly, and repeating the seismic response, the optimal values of the parameters are finally obtained.

3.8 Evaluating the Efficiency of the Soft Story HAMSEYD

3.8.1 ETABS and Modeling the Building and Required Links

There are several nonlinear link elements in ETABS software, however none of them can be used for modeling a multi-phase hardening and yielding element, as the HAMSYED, whose hysteretic behavior has been shown in Figure 43 in the previous section. To overcome this limitation and resolve this shortcoming, a combination of multi-linear plastic spring, standing for the first set of yielding plates, combined with three gap elements, standing for other set of the yielding plates as well as the bracing element, was used. However, since the gap elements in ETABS have only linear behavior after the gap closure, they cannot show the plastic behavior of the second and third set of yielding plates, as well as the bracing element, as the main source of energy dissipation in the HAMSYED device. In order to compensate the lack of energy dissipation capability, it was decided to introduce a viscous damper to the structural system at the lowest level, parallel with the other considered links, with a specific damping coefficient, which result in the same amount of dissipated energy as the

HAMSYED device. For this purpose, the dissipated energy in once complete cycle of the HAMSYED device hysteretic curves, as the one shown in Figure 43 is calculated, then the amount of energy which can be dissipated in one cycle of the viscous damper through the relative displacement of its ends, with respect to each other, is expressed as follows:

$$\text{Damping Energy} = \int_0^{td} F_d \,.\, du = \int_0^{td} c.\dot{u}.\dot{u}.dt = c\int_0^{td} \dot{u}^2.dt \qquad (26)$$

Then, by some trial and error iterations, the appropriate damping coefficient, c, of the equivalent damper can be obtained. On this basis, the damping coefficients given in Table 11 have been found and assigned to the dampers in the lowest stories of different controlled buildings.

Table 11:Damping coefficients found based on Equation (26) and applied for different controlled buildings in their seismic response calculations

No. of Stories	5	7	9
Damping coefficient of the considered dampers (tonf.sec/cm)	4	9.8	15

3.8.2 Earthquake Record Selection

Accelerograms have been selected according to FEMA P625. This regulation divides the earthquakes into two near-field and far-field groups. This regulation, has suggested 28 far field and 22 near field earthquakes for seismic evaluation of building by time history analyses. In this study, seven far field earthquakes have been selected from those suggested earthquakes based on their dominant period to be around the fundamental periods of the considered buildings, with effective duration of at least 10 seconds. The PGA levels of earthquakes have been considered to be from low to high values so that the performance of the control devise can be evaluated for various intensities of ground motions. On this basis, no scaling has been applied to the selected

earthquakes. However, in cases of some low intensity earthquakes, no major damage was imposed to the buildings. Therefore, the intensity of those records was increased to some level to create the performance level of Collapse Prevention in the original buildings. This way, the effectiveness of the control device in reducing the level of damage in the controlled building was better indicated. Table 12 shows the list of selected earthquakes and their characteristics, including station code, station latitude, Station longitude, Epicentral distance, Effective duration and PGA.

Table 12: Specification of selected earthquakes

Station	Station latitude	Station longitude	Epicentral distance (km)	Effective duration (s)	Un-scaled PGA (g)
CHY006	23.581	120.552	39.90	14.5	0.215
CHY025	23.780	120.514	34.32	24	0.369
CHY080	23.597	120.678	31.70	29	0.727
CHY101	23.686	120.562	30.90	11	0.165
TCU053	24.194	120.669	39.20	19.5	0.123
TCU056	24.159	120.624	37.60	26	0.119
TCU063	24.108	120.616	33.20	34	0.136

Figures 44 and 45 show spectral acceleration and spectral pseudo velocity curves of the applied earthquakes.

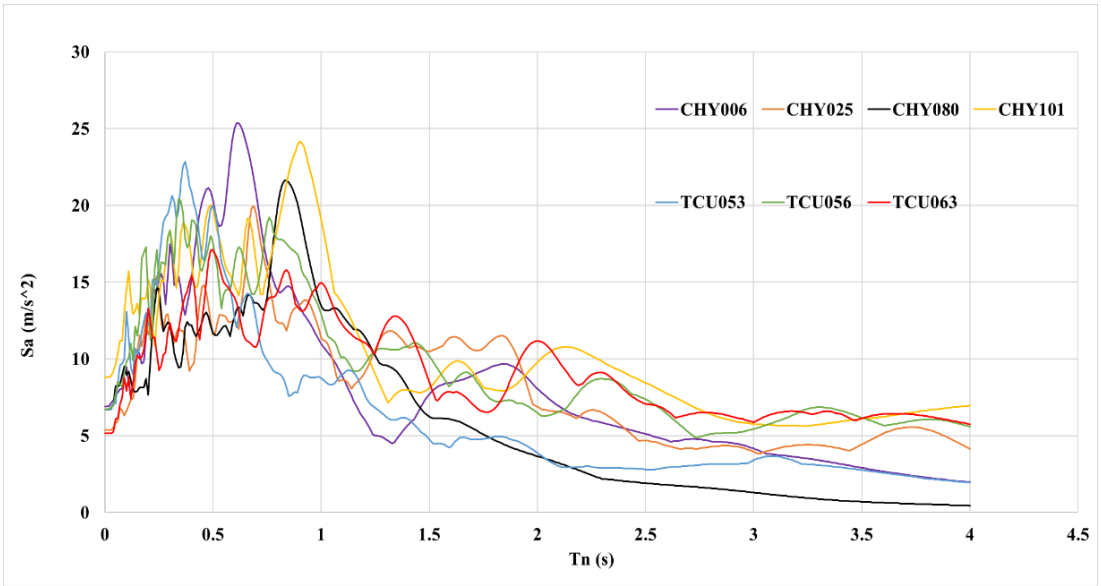

Figure 44: Spectral acceleration

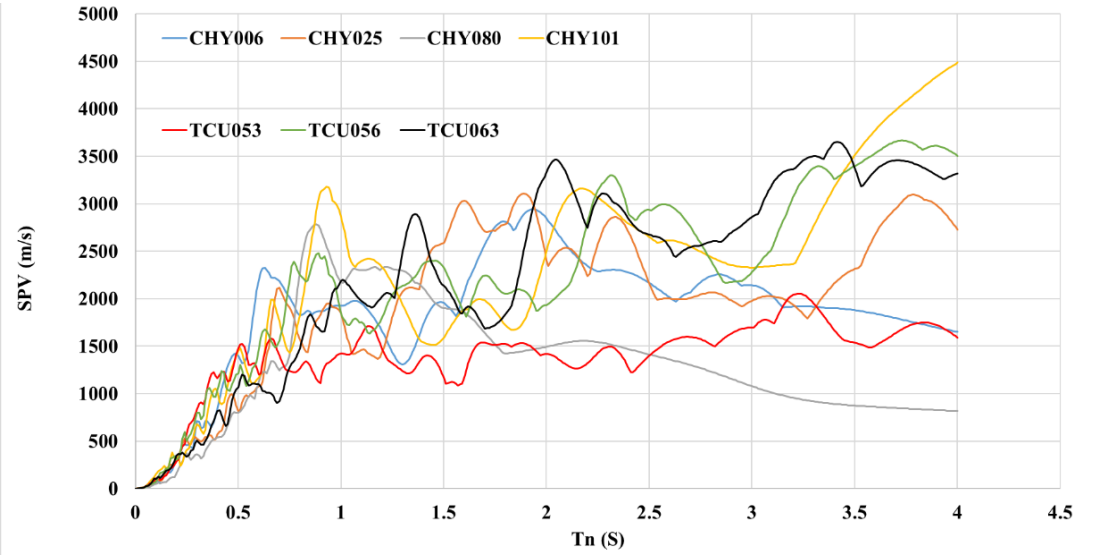

Figure 45: Spectral pseudo velocity curves

As it is seen in Figures 44 and 45 it is clear that the dominant periods for selected earthquakes are close to the fundamental periods of the designed buildings to intensify their seismic response.

Chapter 4

ANALYSIS RESULTS AND DISCUSSION

4.1 Introduction

In this chapter the results of several cases of the conducted NLTHA on the considered buildings, both original ones and those with controlled soft story, are presented and compared to show how effective is the use of the proposed HAMSYED in seismic response reduction.

4.2 Details of Modelling and Seismic Responses

The seismic responses, considered for investigation and comparison, include base shear force, roof absolute acceleration and roof relative displacement, and finally, inter-story drift. Furthermore, the formation of plastic hinges (PHs) and their performance levels have been compared in the two groups of original and controlled buildings. Before presenting the sample results of the aforementioned responses, it is useful to present a sample of the multi-linear hardening behavior of the HAMSYED device (the combination of multi-linear plastic spring and gaps, without the contribution of viscous damper), as the one shown in Figure 46.

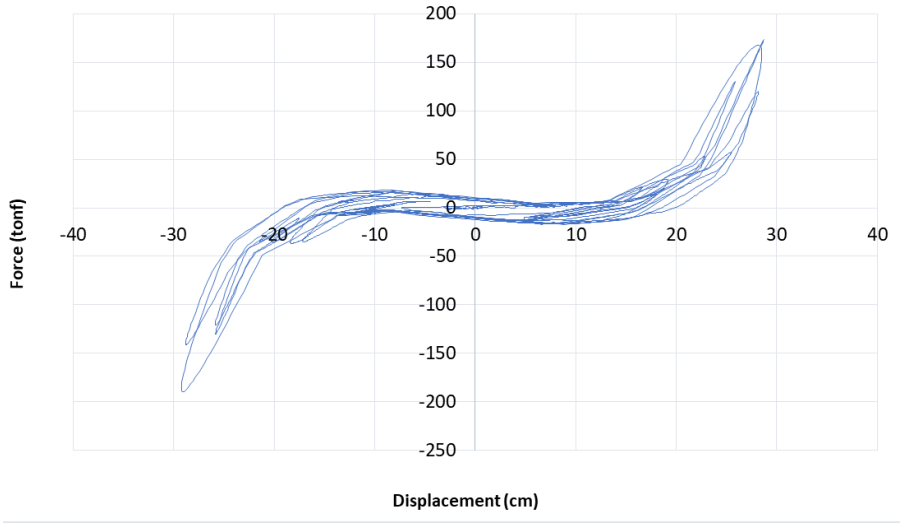

Figure 46: A sample of the multi-linear hardening behavior of the HAMSYED device

The multi-linear and hardening behavior of the HAMSYED device is clearly visible in Figure 46, however, due to the absence of damper, only a little amount of energy dissipation can be observed in the figure, as expected, which is just because of the plastic deformation of the multi-linear plastic spring.

4.3 Comparison of Time history Analysis Outputs

As samples of the numerical results of aforementioned seismic responses, Figures 47 to 70 show the time histories of the aforementioned seismic responses of 5-, 7-, and 9-story buildings subjected to CHY025 earthquake.

4.3.1 Comparing of Time History Response of 5 Stories Models

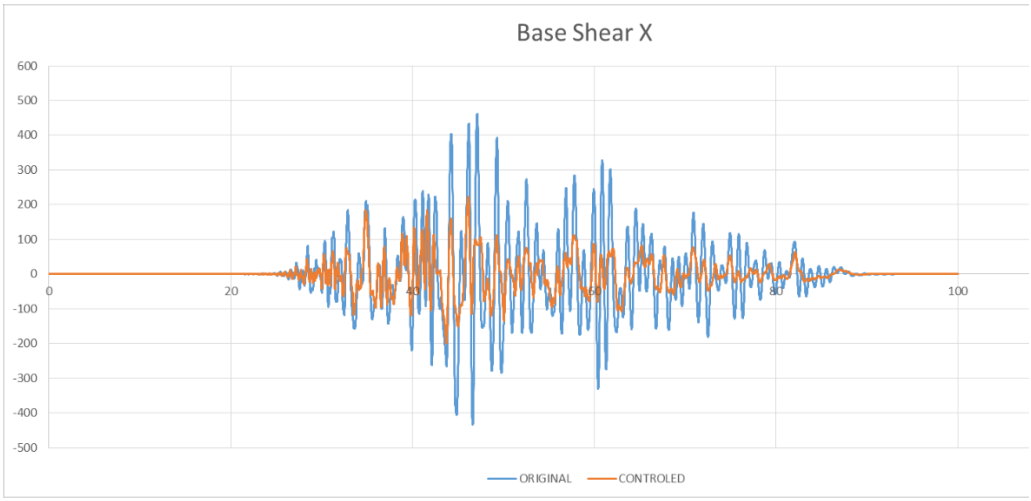

Figure 47: Shear force time histories of 5-story buildings subjected to CHY025 earthquake

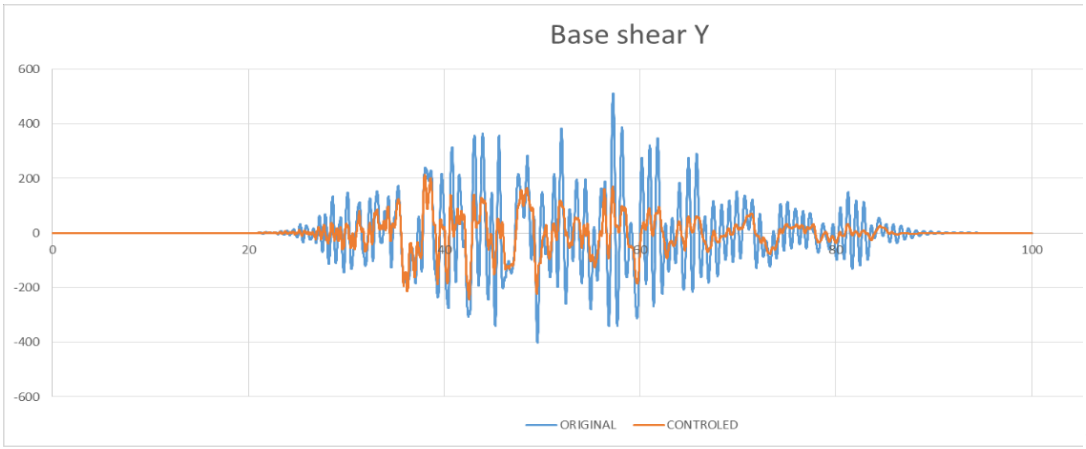

:

Figure 48: Shear force time histories of 5-story buildings subjected to CHY025 earthquake

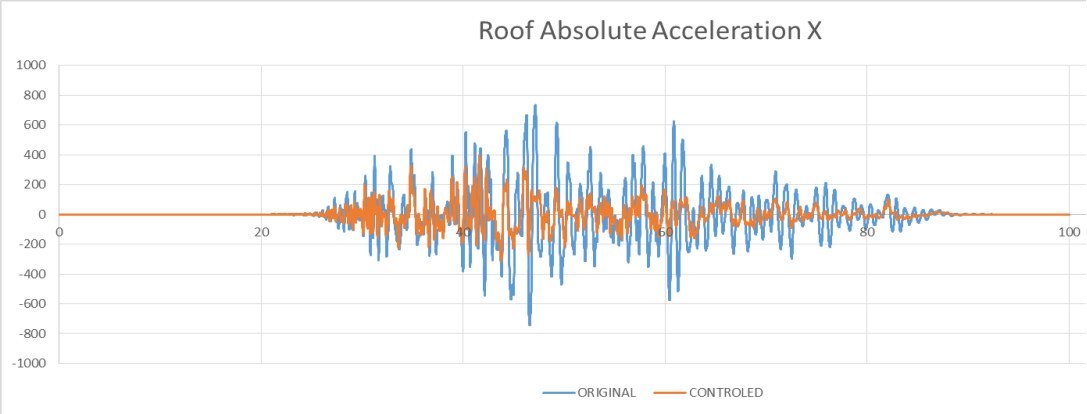

Figure 49: Absolute acceleration response history of 5-story buildings at roof level subjected to CHY025 earthquake

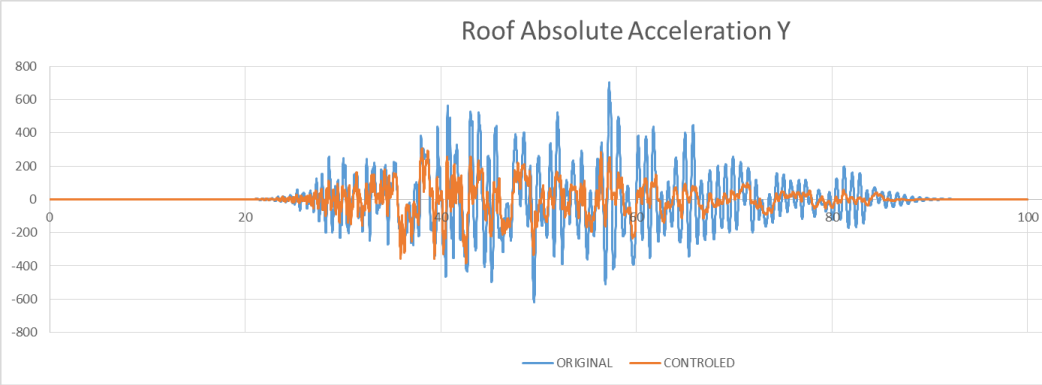

Figure 50: Absolute acceleration response history of 5-story buildings at roof level subjected to CHY025 earthquake

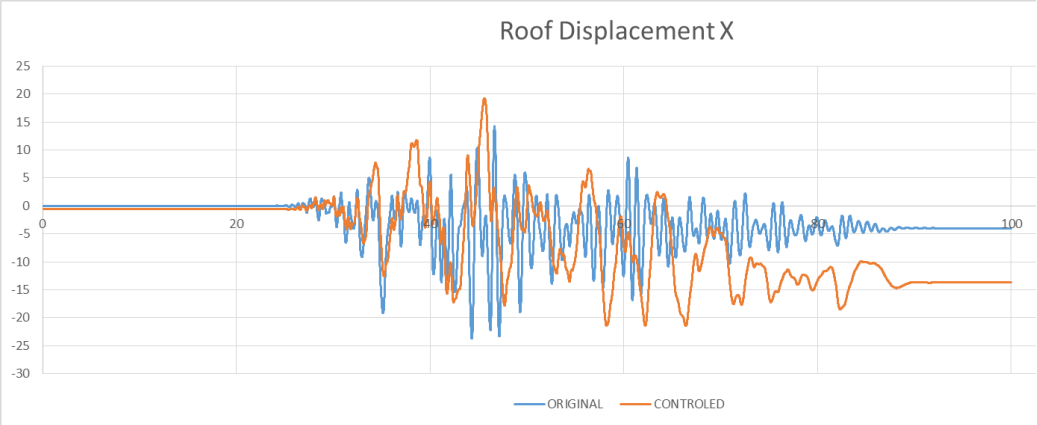

Figure 51: Displacement of 5-story buildings at roof level

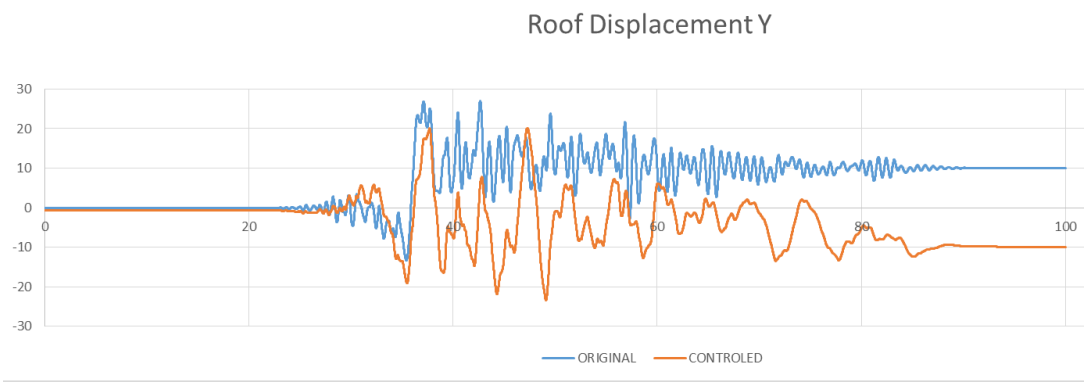

Figure 52: Displacement of 5-story buildings at roof level

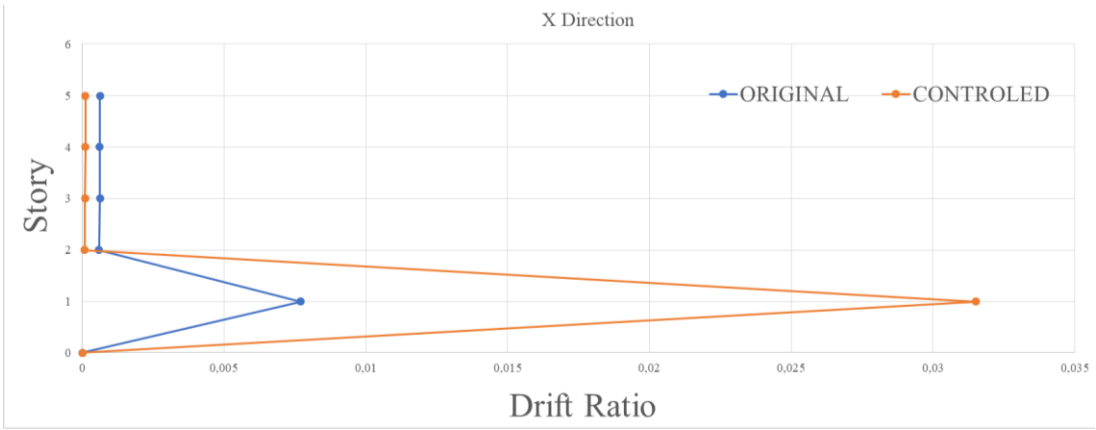

Figure 53: The peak inter-story drift of the CHY025 earthquake in 5-story buildings

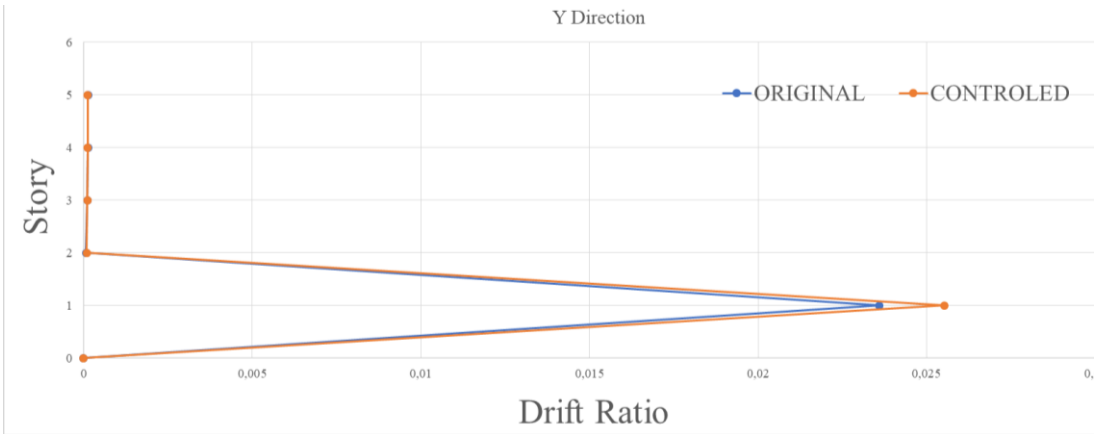

Figure 54: The peak inter-story drift of the CHY025 earthquake in 5-story buildings

It is seen in Figures 47 to 50 that the use of HAMSYED has resulted in remarkable decrease in base shear force and roof absolute acceleration in the controlled building, as well as some reduction in the roof relative displacement. As it is seen in Figure 51

in some cases residual displacement is observed both original and controlled buildings, which is due to plastic deformations. However, it should be noted that in the original building these plastic deformations have been spread all over the building body, while in the controlled building they have been basically concentrated in the lowest story in the body of HAMSYEDs, so that upper stories have remained generally elastic. In Figure 53 one can observe that although the drift ratio of the lowest story of the controlled 5-story building has increased comparing to the original building, the inter-story drift ratios in upper stories have all decreased comparing to those of the original building. The same outcomes are true in cases of 7- and 9-story buildings, whose responses are presented in Figures 55 to 62. It should be noted that although the amount of drift in the lowest story of the controlled buildings is in some cases more than the original building, those amounts of drift do not lead into collapse of the soft story. This has been assured by applying the p-delta effect consideration in the employed computer program.

4.3.2 Comparing of Time History Response of 7 Stories Models

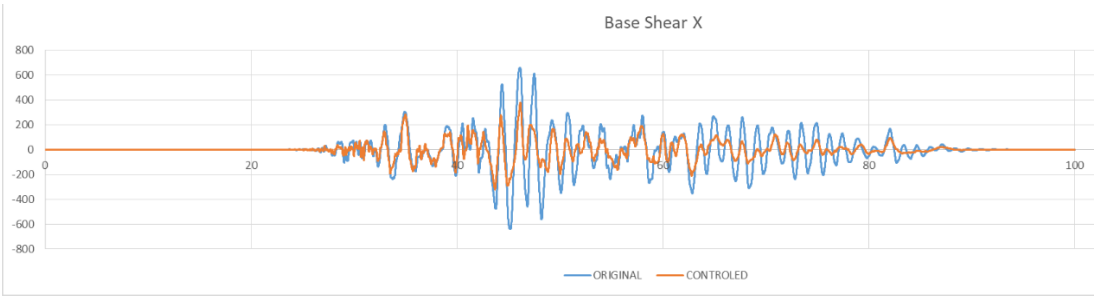

Figure 55: Shear force time histories of 7-story buildings subjected to CHY025 earthquake

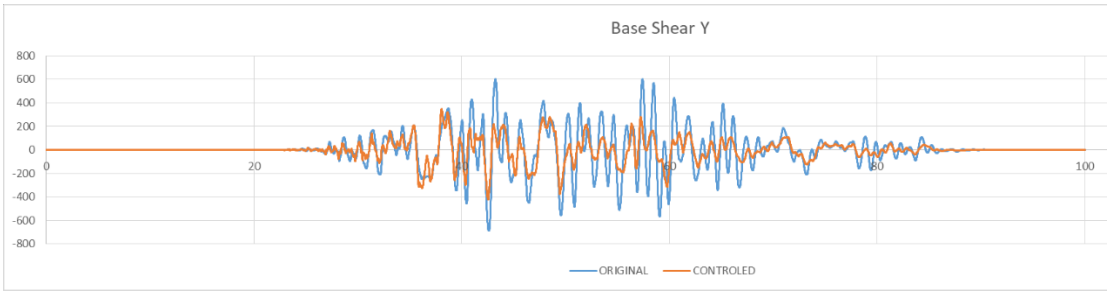

Figure 56: Shear force time histories of 7-story buildings subjected to CHY025 earthquake

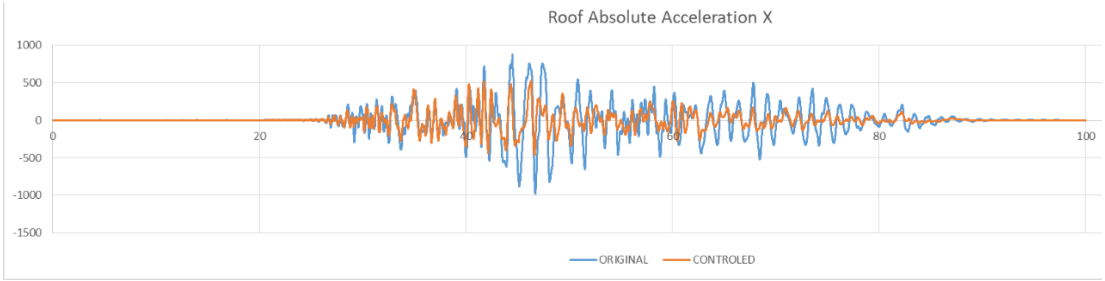

Figure 57: Absolute acceleration response history of 7-story buildings at roof level subjected to CHY025 earthquake

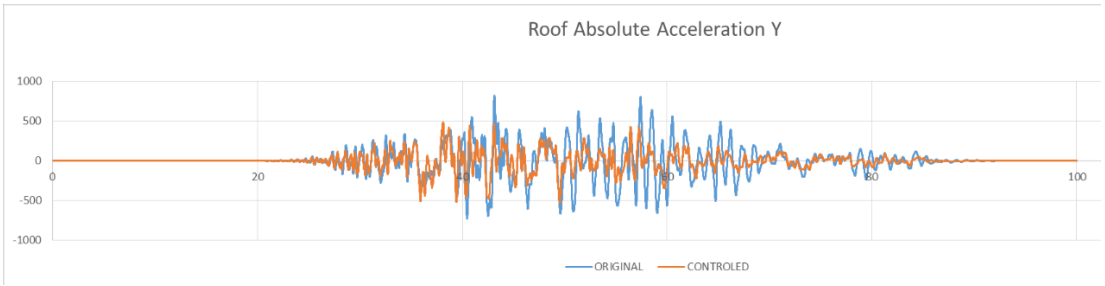

Figure 58: Absolute acceleration response history of 7-story buildings at roof level subjected to CHY025 earthquake

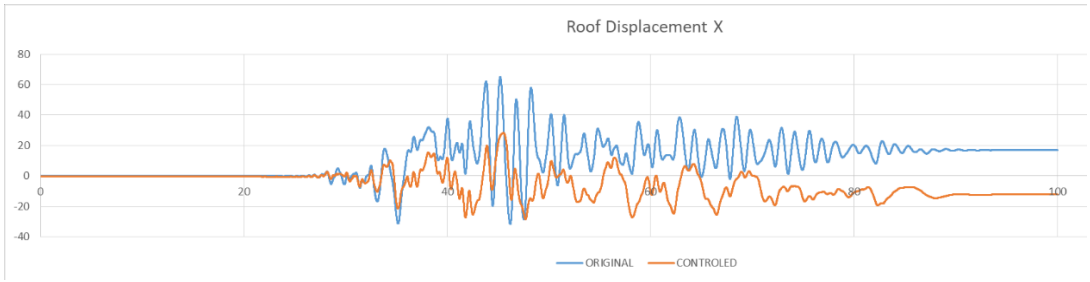

Figure 59: Displacement of 7-story buildings at roof level

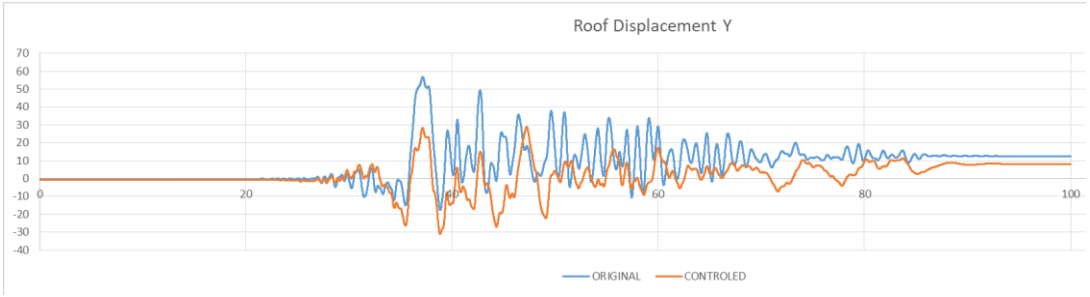

Figure 60: Displacement of 7-story buildings at roof level

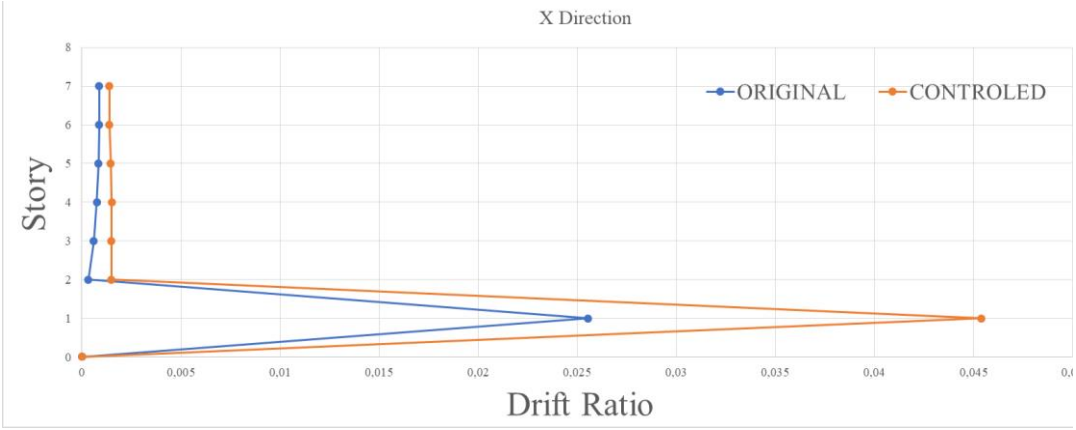

Figure 61: The peak inter-story drift of the CHY025 earthquake in 7-story buildings

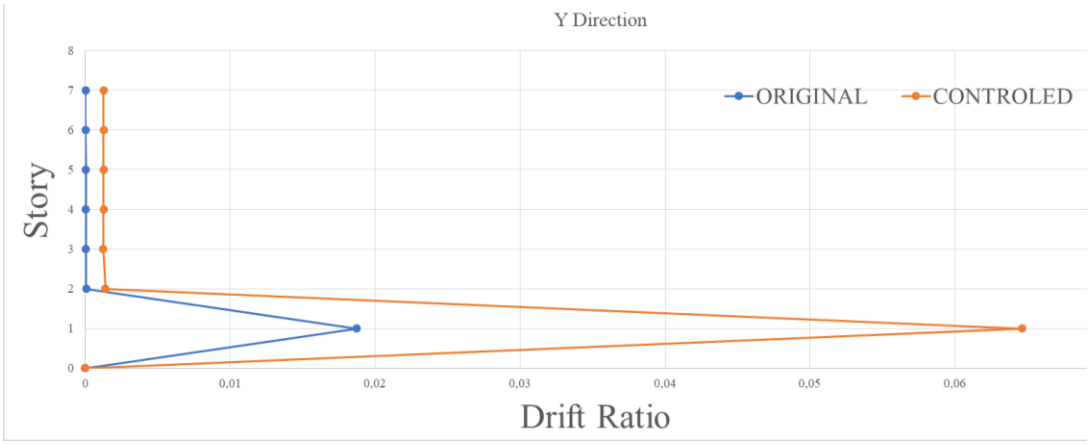

Figure 62: The peak inter-story drift of the CHY025 earthquake in 7-story buildings

4.3.3 Comparing of Time History Response of 9 Stories Buildings

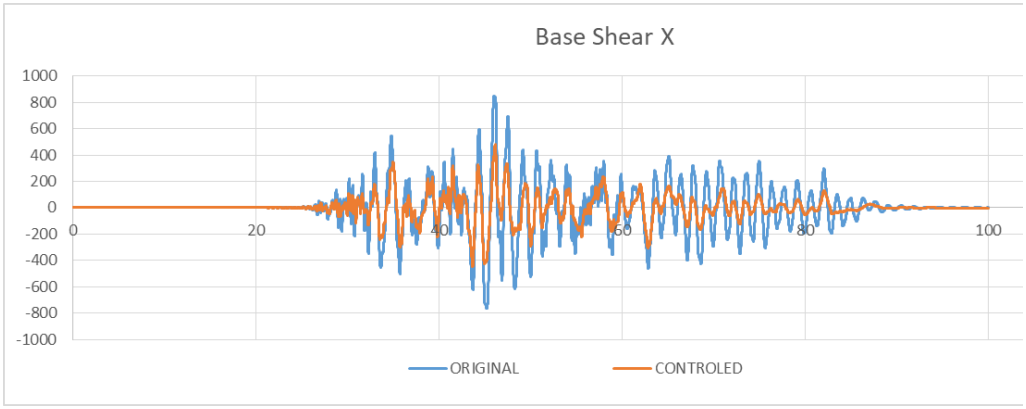

Figure 63: Shear force time histories of 9-story buildings subjected to CHY025 earthquake

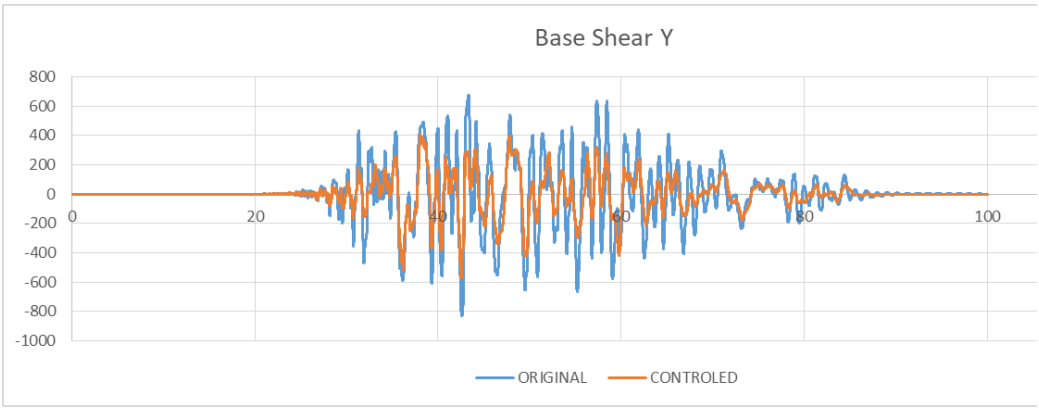

Figure 64: Shear force time histories of 9-story buildings subjected to CHY025 earthquake

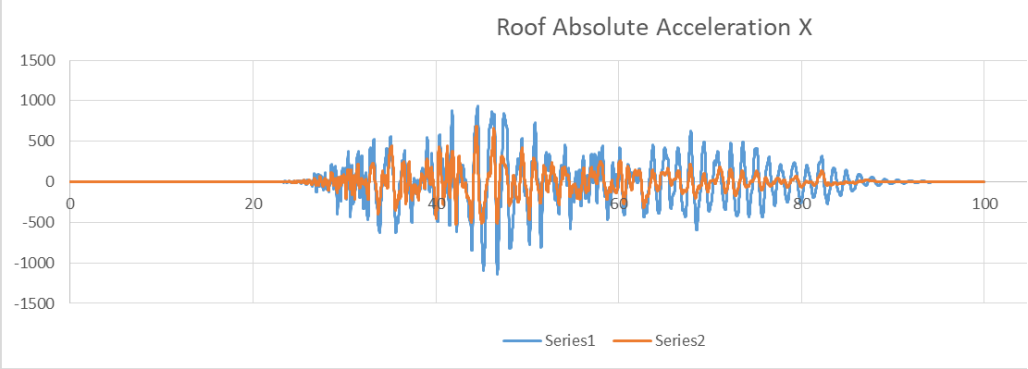

Figure 65: Absolute acceleration response history of 9-story buildings at roof level subjected to CHY025 earthquake

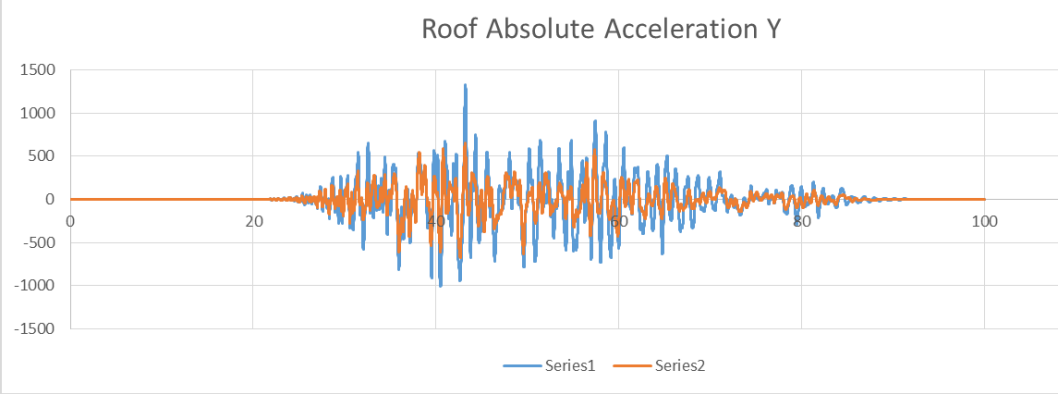

Figure 66: Absolute acceleration response history of 9-story buildings at roof level subjected to CHY025 earthquake

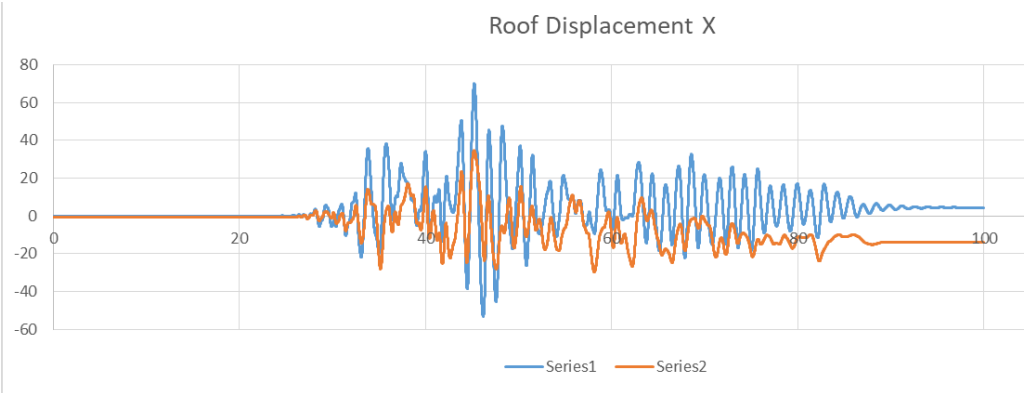

Figure 67: Displacement of 9-story buildings at roof level

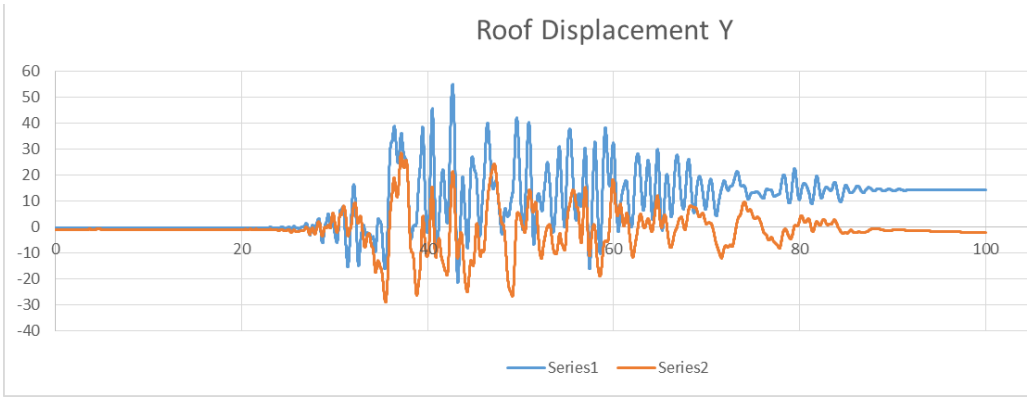

Figure 68: Displacement of 9-story buildings at roof level

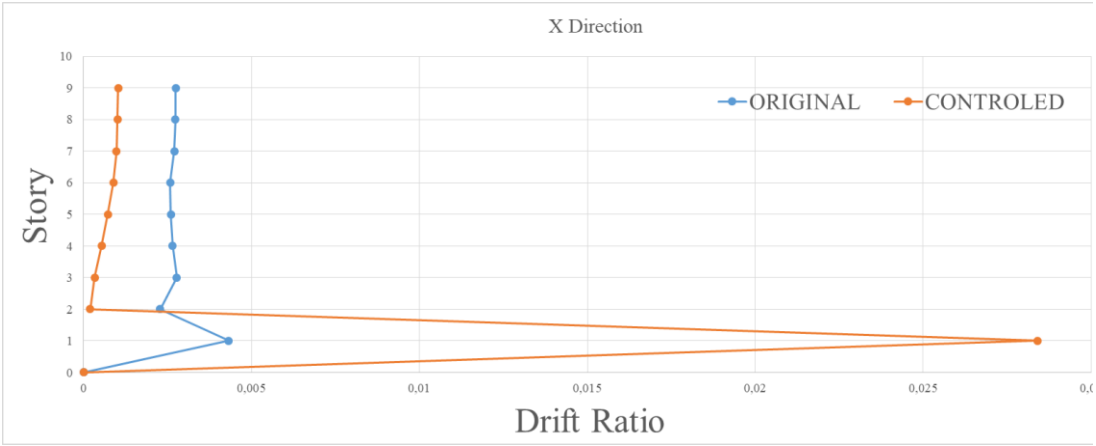

Figure 69: The peak inter-story drift of the CHY025 earthquake in 9-story buildings

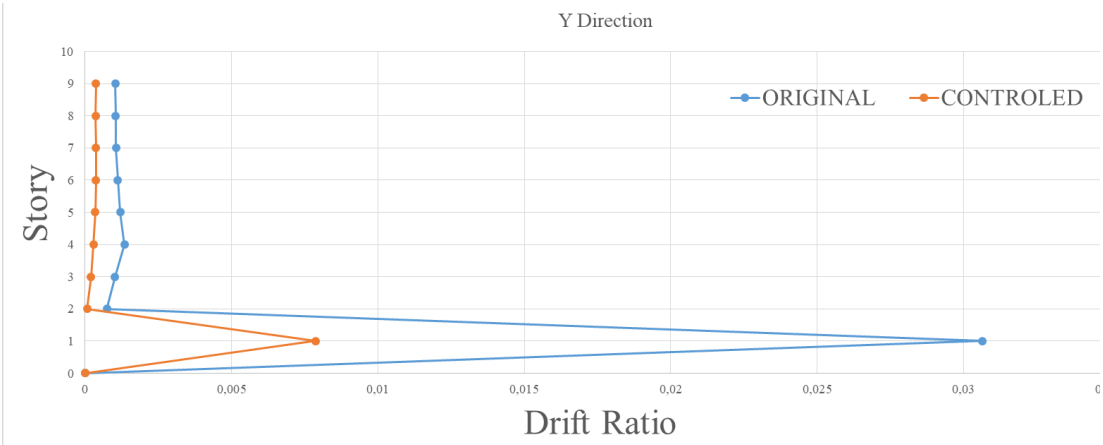

Figure 70: The peak inter-story drift of the CHY025 earthquake in 9-story buildings

By comparing Figures 51, 59 and 67 one can realize that the amount of reduction in roof relative displacement in controlled buildings increases with the number of stories of the building.

4.4 Comparing of Plastic Hinges Formation in Buildings

As samples of the last set of analyses results some cases of PHs formation in the original and controlled buildings are shown in Figures 71 to 74.

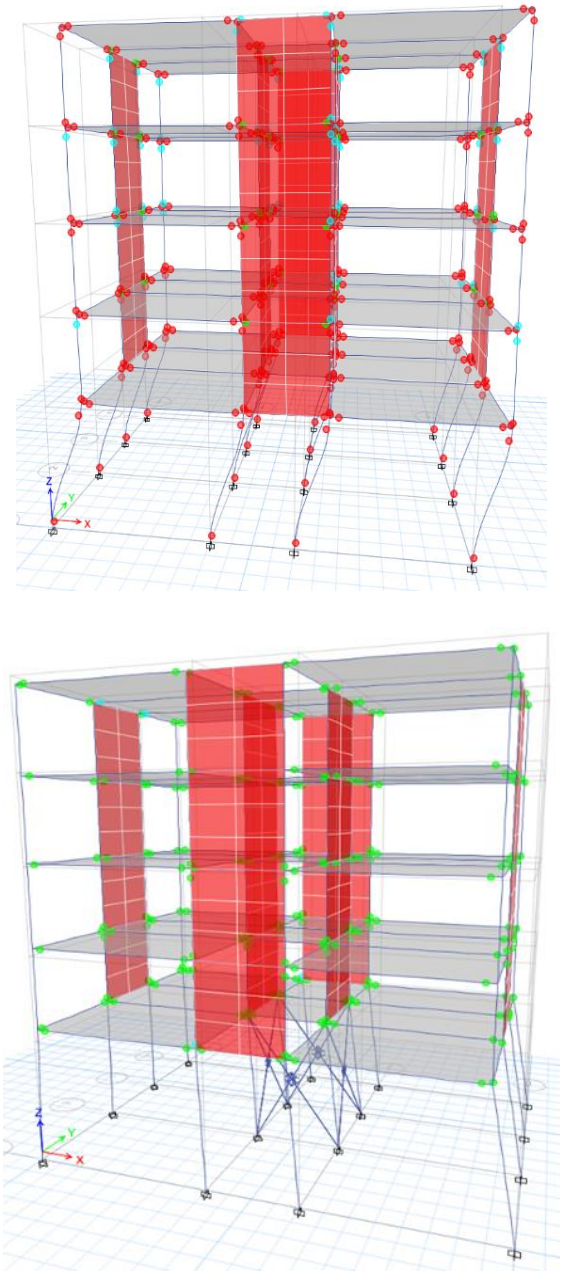

Figure 71: PHs formed in the 5-story original (up) and controlled (down) buildings subjected to TCU063 earthquake

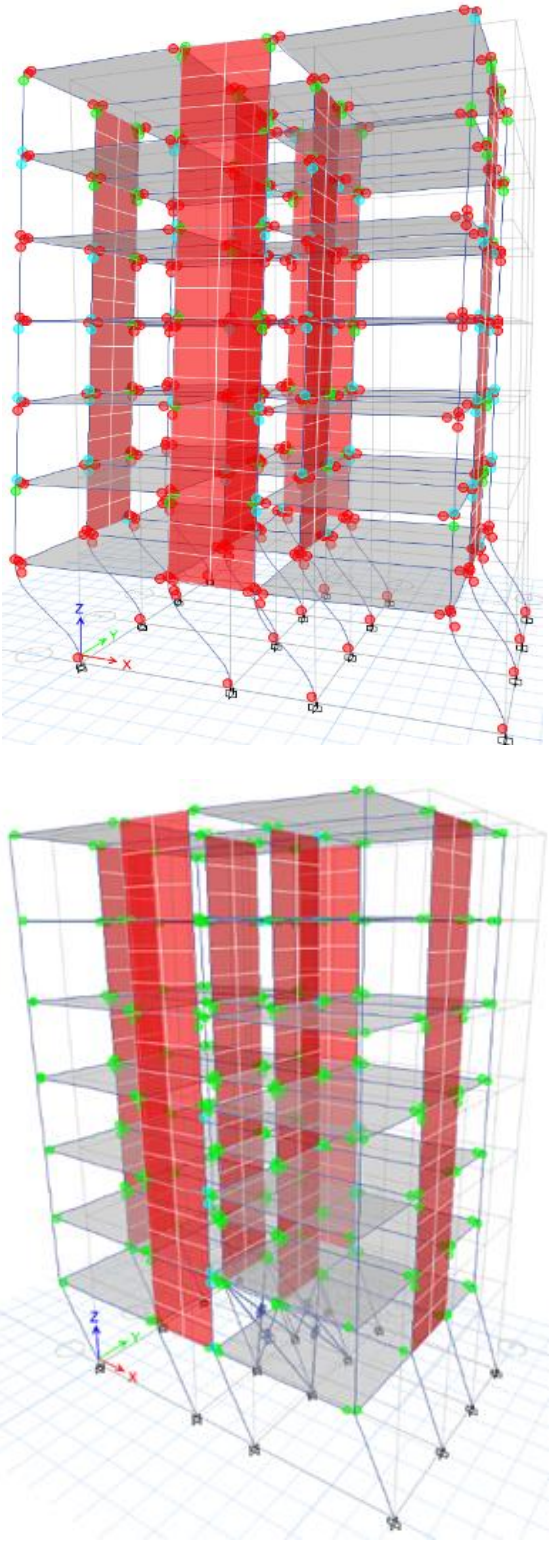

Figure 72: PHs formed in the 7-story original (up) and controlled (down) buildings subjected to TCU063 earthquake

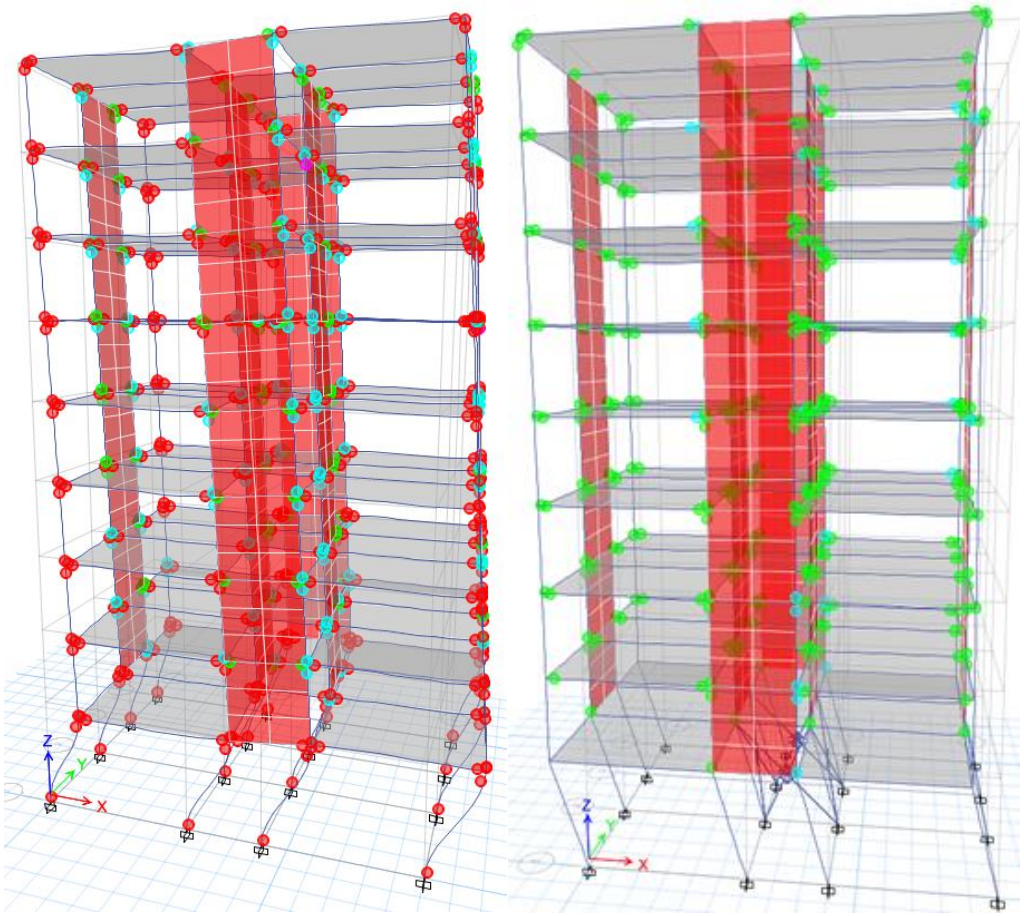

Figure 73: PHs formed in the 9-story original (left) and controlled (right) buildings subjected to TCU063 earthquake

It can be observed in Figures 71 to 73 that several PHs at collapse level has been created in the original building in beams and also columns, while in the controlled buildings the PHs are at Immediate Occupancy (IO) level, and have been created mainly in beams. This set of results again shows the high efficiency of using HAMSYED in seismic response reduction of buildings.

4.5 Maximum Response of Buildings in Both Direction

For the sake of brevity, graphical results, similar to those shown in Figures 71 to 73, are not presented for all of seven employed earthquakes, and instead, the complete set of maximum values of the aforementioned responses, in the two main directions, for all considered earthquakes are presented in Tables 13 to 18.

Table 13: Maximum responses of the 5-story buildings, in X direction, subjected to all seven considered earthquakes

Five Story X Direction								
	SAYSTEM TYPE	EAETHQUAKE 1	EAETHQUAKE 2	EAETHQUAKE 3	EAETHQUAKE 4	EAETHQUAKE 5	EAETHQUAKE 6	EAETHQUAKE 7
Base Shear X (tonf)	CONTROLLED	280	222	442	659	242	234	653
	UNCONTROLLED	235	460	475	COLLAPSE	369	441	COLLAPSE
Reduction percent (%)		-19.1	51.7	6.9		34.4	47	
Roof Displacement X (cm)	CONTROLLED	17	21	20	36	31	32	59
	UNCONTROLLED	23	24	39	COLLAPSE	28	27	COLLAPSE
Reduction percent (%)		26.1	12.5	48.7		-10.7	-19	
Absolute Accel. ROOF X (cm/sec^2)	CONTROLLED	566	396	919	1226	470	508	937
	UNCONTROLLED	685	742	1143	COLLAPSE	683	847	COLLAPSE
Reduction percent (%)		17.4	46.6	19.6		31.2	40	

Table 14: Maximum responses of the 5-story buildings, in Y direction, subjected to all seven considered earthquakes

Five Story Y Direction								
	SAYSTEM TYPE	EAETHQUAKE 1	EAETHQUAKE 2	EAETHQUAKE 3	EAETHQUAKE 4	EAETHQUAKE 5	EAETHQUAKE 6	EAETHQUAKE 7
Base Shear Y (tonf)	CONTROLLED	235	243	481	289	379	255	530
	UNCONTROLLED	230	510	379	COLLAPSE	414	463	COLLAPSE
Reduction percent (%)		-2.2	52.4	-26.9		8.5	45	
Roof Displacement Y (cm)	CONTROLLED	11	23	19	25	23	24	51
	UNCONTROLLED	16	27	41	COLLAPSE	19	29	COLLAPSE
Reduction percent (%)		31.3	14.8	53.7		-21.1	17	
Absolute Accel. ROOF Y (cm/sec^2)	CONTROLLED	464	384	857	617	717	441	719
	UNCONTROLLED	615	701	927	COLLAPSE	574	920	COLLAPSE
Reduction percent (%)		24.6	45.2	7.6		-24.9	52	

Table 15: Maximum responses of the 7-story buildings, in X direction, subjected to all seven considered earthquakes

Seven Story X Direction								
	SAYSTEM TYPE	EAETHQUAKE 1	EAETHQUAKE 2	EAETHQUAKE 3	EAETHQUAKE 4	EAETHQUAKE 5	EAETHQUAKE 6	EAETHQUAKE 7
Base shear X (tonf)	CONTROLLED	331	378	574	483	437	431	469
	UNCONTROLLED	249	660	COLLAPSE	COLLAPSE	594	COLLAPSE	COLLAPSE
Reduction percent (%)		-32,9	42,7			26,4		
Roof Displacement X (cm)	CONTROLLED	26	28	44	52	45	55	62
	UNCONTROLLED	37	65	COLLAPSE	COLLAPSE	71	COLLAPSE	COLLAPSE
Reduction percent (%)		29,7	56,9			36,6		
Absolute Accel. ROOF X (cm/sec^2)	CONTROLLED	802	524	1562	945	656	692	558
	UNCONTROLLED	588	976	COLLAPSE	COLLAPSE	851	COLLAPSE	COLLAPSE
Reduction percent (%)		-36,4	46,3			22,9		

Table 16: Maximum responses of the 7-story buildings, in Y direction, subjected to all seven considered earthquakes

Sven Story Y Direction								
	SAYSTEM TYPE	EAETHQUAKE 1	EAETHQUAKE 2	EAETHQUAKE 3	EAETHQUAKE 4	EAETHQUAKE 5	EAETHQUAKE 6	EAETHQUAKE 7
Base shear Y (tonf)	CONTROLLED	372	423	735	270	535	450	442
	UNCONTROLLED	255	686	COLLAPSE	COLLAPSE	941	COLLAPSE	COLLAPSE
Reduction percent (%)		-45,9	38,3			43,1		
Roof Displacement Y (cm)	CONTROLLED	16	30	40	26	37	38	48
	UNCONTROLLED	31	56	COLLAPSE	COLLAPSE	55	COLLAPSE	COLLAPSE
Reduction percent (%)		48,4	46,4			32,7		
Absolute Accel. ROOF Y (cm/sec^2)	CONTROLLED	653	526	1687	451	970	623	616
	UNCONTROLLED	697	823	COLLAPSE	COLLAPSE	1190	COLLAPSE	COLLAPSE
Reduction percent (%)		6,3	36,1			18,5		

Table 17: Maximum responses of the 9-story buildings, in X direction, subjected to all seven considered earthquakes

Nine Story X Direction								
	SAYSTEM TYPE	EAETHQUAKE 1	EAETHQUAKE 2	EAETHQUAKE 3	EAETHQUAKE 4	EAETHQUAKE 5	EAETHQUAKE 6	EAETHQUAKE 7
Base shear X (tonf)	CONTROLLED	466	481	637	564	650	520	666
	UNCONTROLLED	608	848	710	COLLAPSE	753	COLLAPSE	861
Reduction percent (%)		23,4	43,3	10,3		13,7		22,6
Roof Displacement X (cm)	CONTROLLED	31	34	55	54	51	54	62
	UNCONTROLLED	41	70	90	COLLAPSE	56	COLLAPSE	58
Reduction percent (%)		24,4	51,4	38,9		8,9		-6,9
Absolute Accel. ROOF X (cm/sec^2)	CONTROLLED	783	686	1393	835	707	684	618
	UNCONTROLLED	1092	1136	1281	COLLAPSE	1096	COLLAPSE	839
Reduction percent (%)		28,3	39,6	-8,7		35,5		26,3

Table 18: Maximum responses of the 9-story buildings, in Y direction, subjected to all seven considered earthquakes

Nine Story Y Direction								
	SAYSTEM TYPE	EAETHQUAKE 1	EAETHQUAKE 2	EAETHQUAKE 3	EAETHQUAKE 4	EAETHQUAKE 5	EAETHQUAKE 6	EAETHQUAKE 7
Base shear Y (tonf)	CONTROLLED	491	574	624	370	728	619	508
	UNCONTROLLED	547	832	772	COLLAPSE	1159	COLLAPSE	757
Reduction percent (%)		10,2	31,0	19,2		37,2		32,9
Roof Displacement Y (cm)	CONTROLLED	23	29	47	20	39	41	40
	UNCONTROLLED	36	54	108	COLLAPSE	54	COLLAPSE	46
Reduction percent (%)		36,1	46,3	56,5		27,8		13,0
Absolute Accel. ROOF Y (cm/sec^2)	CONTROLLED	817	672	1857	541	1102	763	615
	UNCONTROLLED	1402	1025	2129	COLLAPSE	2016	COLLAPSE	1065
Reduction percent (%)		41,7	34,4	12,8		45,3		42,3

It is seen in Tables 13 to 18 that the maximum responses of controlled buildings, including base shear force, roof relative displacement and also roof absolute acceleration, have been mostly decreased in comparison with the original buildings. This reduction is, in many cases over 40%, even in some cases over 55%, and on average it is around 30%. However, it is observed in the tables that in some cases the maximum response of the controlled building is larger than that of the original

building. Such cases, which are mostly related to long period earthquakes, are mainly because of the closeness of the elongated period of the controlled building to the dominant period of some of the considered earthquakes. Nevertheless, even in such cases, usually the controlled buildings have shown a better seismic behavior than their original counterparts.

Chapter 5

CONCLUSION AND RECOMMENDATION FOR FUTURE STUDIES

5.1 Summary and Conclusions

In this study the idea of using the controlled soft story at the lowest level of multi-story RC buildings, based on employing a set of hardening and multi-step yielding energy dissipater (HAMSYED) devices, as a technique for seismic response reduction, has been discussed and investigated. To show the efficiency of the proposed techniques, a series of nonlinear time history analyses (NLTHA) have been performed by employing a set of selected earthquake three-component accelerograms, on a set of 5-, 7- and 9-story RC building, with a simple and almost regular plan, all having a lowest soft story, once in the original state, and once more in the controlled state. The initial, secondary and third stiffness values of the HAMSYED as well as the gaps used for creation of the multi-step yielding phenomenon, are used as the controlling factors for achieving the appropriate behavior of the system against the considered earthquakes. For finding the appropriate values of the aforementioned parameters, a computer program has been developed in MATLAB platform for the initial guess of them base on a SDOF system, and then those values have been used in ETABS program to find the final appropriate values in the cases of actual buildings. The behavior of the HAMSYED has been also investigated by using ABAQUS finite element program. Based on the numerical results of the conducted NLTHA, as well as MATLAB and ABAQUS calculations, the following conclusions can be made:

- The roof absolute acceleration values of the controlled buildings are decreased between 7% and 47% in comparison with their original counterparts. This reduction is on average around 30%, 26% and 34% in 5-, 7- and 9-story buildings, respectively.
- The roof relative displacement values of the controlled buildings are decreased between 9% and 57% in comparison with their original counterparts. This reduction is on average around 29%, 42% and 34% in 5-, 7- and 9-story buildings, respectively.
- The base shear force values of the controlled buildings are decreased between 7% and 52% in comparison with their original counterparts. This reduction is on average around 35%, 37% and 24% in 5-, 7- and 9-story buildings, respectively.
- The inter-story drift values of the controlled buildings are decreased up to 70% in comparison with their original counterparts.
- In some cases, the maximum response of the controlled building has been larger than that of the original counterpart building. Such cases, which have occurred mostly for long period earthquakes, have been mainly because of the closeness of the elongated period of the controlled building to the dominant period of some of the considered earthquakes. Nevertheless, it should be noted that, even in such cases, usually the controlled buildings have shown a better seismic behavior than their original counterparts.
- The developed program in MATLAB platform for finding the appropriate values of the HAMSYED parameter results in good initial guesses, which usually are applicable in the actual buildings with only slight changes.

- The conducted finite element analyses by ABAQUS software, show the high energy dissipation capability of the proposed HAMSYED.

Base on the above conclusions, the use of the proposed HAMSYED, as a low-cost and low-tech device, as a structural fuse, with minimum maintenance cost and effort, can be strongly recommended, either for seismic upgrading of the existing buildings, or design of new ones, in earthquake prone areas around the world. It can be understood without a detailed calculation that using this technique is much cheaper than other seismic upgrading techniques for RC buildings, such as using steel jackets or FRP. Minimum disruption in the architectural setting of the existing soft story is a great advantage of the proposed technique.

Finally, it should mention that this study has been limited to only a few multi-story RC buildings, and for obtaining more extendable conclusions, more expanded study on several buildings is required. Some topics for further studies in this regard are given in the following section of this chapter.

5.2 Recommendations for Future Studies

The following studies can be conducted as the continuation of the present study for obtaining more general results:

- Studying the use of HAMSYED in RC buildings with lateral load bearing system other than the one used in the present study
- Studying the use of HAMSYED in steel buildings with various lateral load bearing systems
- Studying the use of HAMSYED in irregular building

- Considering a soil type other than the one used in the present study for the use of HAMSYED in buildings.

All of the above studies can be done in the framework of the MSc Theses. However, if the efficiency of the HAMSYED device in seismic response reduction of various types of buildings with different lateral load bearing system is shown by the above study, then a very thorough and compete study in the framework of the PhD study, for design of new building by using the HAMSYED device, in which some preliminary design rules are presented for choosing the appropriate parameters of the HAMSYED based on the type and geometry of the building.

REFERENCES

[1] Taranath, S., *Wind and Earthquake Resistant, Structural Design and Analysis. Marcel Dekker, New York, 2005*. 1: p. 22-25.

[2] Turer, A., Yakut, A., & Ugurhan, A. (2004, August). Building damage patterns in Bingol-Turkey after the May 1st, 2003 earthquake. In *13th world conference on earthquake engineering, Paper* (No. 65).

[3] ASCE Committee. (2010). Minimum Design Loads for Buildings and Other Structures (ASCE/SEI 7-10). *Structural Engineering Institute, American Society of Civil Engineering, Reston, Virginia*.

[4] Montalvo, J. G., & Reynal-Querol, M. (2019). Earthquakes and terrorism: The long lasting effect of seismic shocks. *Journal of Comparative Economics*, *47*(3), 541-561.

[5] D'Amico, A., & Currà, E. (2014). Paper 20: Urban Resilience and Urban Structure: Vulnerability assessment of historical Italian towns. *Proceedings ANDROID Residential Doctoral School*.

[6] Hall, J. F., Holmes, W. T., & Somers, P. (1994). Northridge earthquake, January 17, 1994. *Preliminary reconnaissance report*.

[7] Jain, S., et al., Preliminary observations on the origin and effects of the January 26, 2001 Bhuj (Gujarat, India) earthquake. *Earthquake Eng. Res. Inst. Spec. Earthquake Rep., EERI Newsletter, 2001: p. 1-16.*

[8] Fintel, M., & Khan, F. R. (1969, May). Shock-absorbing soft story concept for multistory earthquake structures. In *Journal Proceedings* (Vol. 66, No. 5, pp. 381-390).

[9] Faison, H., Comartin, C., & Elwood, K. (2004). Housing Report: Reinforced Concrete Moment Frame Building without Seismic Details. *Terrain*, *4*, 15.

[10] Mantawy, A. (2014). *Behavior of ductile reinforced concrete frames subjected to multiple earthquakes*. University of Southern California.

[11] Guney, D., & Aydin, E. (2012). The nonlinear effect of infill walls stiffness to prevent soft story collapse of RC structures. *The open construction and building technology journal*, *6*(1).

[12] Halde, V. V., & Deshmukh, A. H. (2015). Review on behavior of soft storey in building. *International Research Journal of Engineering and Technology (IRJET)*, *2*(8).

[13] Decanini, L. D., Liberatore, L., & Mollaioli, F. (2014). Strength and stiffness reduction factors for infilled frames with openings. *Earthquake Engineering and Engineering Vibration*, *13*(3), 437-454.

[14] Liauw, T. C., & Kwan, K. H. (1985). Unified plastic analysis for infilled frames. *Journal of Structural Engineering*, *111*(7), 1427-1448.

[15] Mehrabi, A.B. and P.B. Shing, Finite element modeling of masonry-infilled RC frames. *Journal of structural engineering, 1997. 123(5): p. 604-613*.

[16] Kakaletsis, D. J., & Karayannis, C. G. (2009). Experimental Investigation of Infilled Reinforced Concrete Frames with Openings. *ACI Structural Journal*, *106*(2).

[17] Samant, L. D., Porter, K., Cobeen, K., Tobin, L. T., Kornfield, L., Seligson, H., ... & Kidd, J. (2010). Mitigating San Francisco's Soft-Story Building Problem. In *Improving the Seismic Performance of Existing Buildings and Other Structures* (pp. 1163-1174).

[18] http://simplengi.com/2012/09/15/soft-story-buildings/

[19] Dewey, J. W., Reagor, B. G., Dengler, L., & Moley, K. (1995). Intensity distribution and isoseismal maps for the Northridge, California, earthquake of January 17, 1994. *US Geol. Surv. Open-File Rept. 95*, *92*, 35.

[20] https://newsroom.ucla.edu/stories/25-years-after-northridge-earthquake-ucla engineering-researchers-are-taking-a-data-driven-approach-to-seismic

[21] Doğan, M., Kıraç, N., & Gönen, H. (2002). Soft-Storey Behaviour in an Earthquake and Samples of İzmit-Düzce. *ECAS Uluslararasi Yapı ve Deprem Mühendisliği Sempozyumu, ODTÜ, Ankara*, *14*.

[22] Lieping, Y., Zhe, Q., Qianli, M., Xuchuan, L., Xinzheng, L., & Peng, P. (2008). Study on ensuring the strong column-weak beam mechanism for RC frames based on the damage analysis in the Wenchuan earthquake [J]. *Building Structure*, *11*.

[23] Yazgan, U., Taşkın, B., Özdemir Çağlayan, P., Erken, A., Celep, Z., Ergüven, E., ... & Mert Tuğsal, Ü. (2012). October 23rd, 2011 Van earthquake. Preliminary reconnaissance report: Structural and geotechnical aspects of the damage. In *Proc. 15th World Conference on Earthquake Engineering*.

[24] Saiyed, Z. N. (2012). *Disaster debris management and recovery of housing stock in San Francisco, CA* (Doctoral dissertation, Massachusetts Institute of Technology).

[25] Zhang, H. (2015). *Strategies of seismic damage mitigation for infilled RC frames: shake-table tests* (Doctoral dissertation).

[26] Green, N. B. (1935). Flexible first-story construction for earthquake resistance. *Transactions of the American Society of Civil Engineers*, *100*(1), 645-652.

[27] Chopra, A. K., Clough, D. P., & Clough, R. W. (1972). Earthquake resistance of buildings with a ‘soft’first storey. *Earthquake Engineering & Structural Dynamics, 1*(4), 347-355.

[28] Arnold, C. (1984). Soft first stories: truths and myths. In *8th Word Conference on Earthquake Engineering* (Vol. 5, pp. 943-950).

[29] Mahin, S. A., Bertero, V. V., Chopra, A. K., & Collins, R. G. (1976). Response of the Olive View Hospital main building during the San Fernando earthquake. *Report No. EERC*, 76-22.

[30] Vukazich, S. M., Selvaduray, G., & Tran, J. (2006). Conducting a soft first-story multifamily dwelling survey: An example using Santa Clara County, California. *Earthquake spectra*, *22*(4), 1063-1079.

[31] Naeim, F. (Ed.). (1989). *The seismic design handbook*. Springer Science & Business Media.

[32] Prestandard, F. E. M. A. (2000). commentary for the seismic rehabilitation of buildings (FEMA356). *Washington, DC: Federal Emergency Management Agency*, *7*..

[33] Agha Beigi, H., Sullivan, T. J., Calvi, G. M., & Christopoulos, C. (2013). Controlled soft storey mechanism as a seismic protection system. In *10th International Conference on Urban Earthquake Engineering*.

[34] Ebadi, P., & Maghsoudi, A. (2017). Case Study on Seismic Performance of Soft Stories in Short Steel Structures and Replacement of Braces with Equivalent Moment Resisting Frame.

[35] Moehle, J. P., & Alarcon, L. F. (1986). Seismic analysis methods for irregular buildings. *Journal of Structural Engineering*, *112*(1), 35-52.

[36] Valmundsson, E. V., & Nau, J. M. (1997). Seismic response of building frames with vertical structural irregularities. *Journal of Structural Engineering*, *123*(1), 30-41.

[37] No, S. (2005). 2800 "Iranian Code of Practice for Seismic Resistant Design of Buildings". *Third Revision, Building and Housing Research Center, Tehran*.

[38] Murty, C. V. R., & Jain, S. K. (1996). Draft IS: 1893 Provisions on Seismic Design of Buildings. *Bureau of Indian Standards, New Delhi*.

[39] Yuen, Y. P. (2012). *Seismic performance and failure mechanisms of infilled RC frames: numerical simulation and theoretical modelling* (Doctoral dissertation).

[40] Standard, B. (2005). Eurocode 8: Design of structures for earthquake resistance. *Part*, *1*, 1998-1.

[41] Chintanapakdee, C., & Chopra, A. K. (2004). Seismic response of vertically irregular frames: response history and modal pushover analyses. *Journal of Structural Engineering*, *130*(8), 1177-1185.

[42] Youd, T. L., Bardet, J. P., & Bray, J. D. (2000). Kocaeli, Turkey, earthquake of August 17, 1999 reconnaissance report. *Earthquake Spectra*, *16*.

[43] Huang, S. C., & Skokan, M. J. (2002). Collapse of the Tungshing building during the 1999 Chi-Chi earthquake in Taiwan. In *Proc., 7th US National Conf. on Earthquake Engineering*.

[44] Hengesh, J. V., Lettis, W. R., Saikia, C. K., Thio, H. K., Ichinose, G. A., Bodin, P., ... & Sinha, S. (2002). Bhuj, India earthquake of January 26, 2001-reconnaissance report.

[45] Liao, W. C. (2010). *Performance-Based Plastic Design of Earthquake Resistant Reinforced Concrete Moment Frames* (Doctoral dissertation).

[46] Agency, F.E.M., FEMA 445: Next-Generation Performance-Based Seismic Design Guidelines. 2006.

[47] Calvi, G. M., Pinho, R., Magenes, G., Bommer, J. J., Restrepo-Vélez, L. F., & Crowley, H. (2006). Development of seismic vulnerability assessment methodologies over the past 30 years. *ISET journal of Earthquake Technology*, *43*(3), 75-104.

[48] Rai, D. C. (2005). Review of documents on seismic evaluation of existing buildings. *Department of Civil Engineering, Indian Institute of Technology Kanpur India*..

[49] Calvi, G. M., Pinho, R., Magenes, G., Bommer, J. J., Restrepo-Vélez, L. F., & Crowley, H. (2006). Development of seismic vulnerability assessment methodologies over the past 30 years. *ISET journal of Earthquake Technology*, *43*(3), 75-104.

[50] Eiby, G. A. (1966). The Modified Mercalli scale of earthquake intensity and its use in New Zealand. *New Zealand journal of geology and geophysics*, *9*(1-2), 122-129.

[51] Bernardini, A., Giovinazzi, S., Lagomarsino, S., & Parodi, S. (2007). The vulnerability assessment of current buildings by a macroseismic approach derived from the EMS-98 scale.

[52] Sezen, H., & Moehle, J. P. (2002). Seismic behavior of shear-critical reinforced concrete building columns. In *Seventh US National Conference on Earthquake Engineering, Earthquake Engineering Research Institute, Boston, MA*.

[53] Elwood, K. J., & Moehle, J. P. (2005). Axial capacity model for shear-damaged columns. *ACI Structural Journal*, *102*(4), 578.

[54] Zhu, L., Elwood, K. J., & Haukaas, T. (2007). Classification and seismic safety evaluation of existing reinforced concrete columns. *Journal of Structural Engineering*, *133*(9), 1316-1330.

[55] Elwood, K. J. (2004). Shake table tests and analytical studies on the gravity load collapse of reinforced concrete frames.

[56] Ousalem, H., Kabeyasawa, T., & Tasai, A. (2004, August). Evaluation of ultimate deformation capacity at axial load collapse of reinforced concrete columns. In *Proceedings of 13th world conference on earthquake engineering*.

[57] Sabelli, R., Mahin, S., & Chang, C. (2003). Seismic demands on steel braced frame buildings with buckling-restrained braces. *Engineering Structures*, *25*(5), 655-666.

[58] American Society of Civil Engineers. (2017). Seismic Evaluation and Retrofit of Existing Buildings: ASCE/SEI, 41-17. American Society of Civil Engineers.

[59] Federal Emergency Management Agency. (2006). *Techniques for the seismic rehabilitation of existing buildings*. FEMA.

[60] Phocas, M. C., & Pocanschi, A. (2003). Steel frames with bracing mechanism and hysteretic dampers. *Earthquake engineering & structural dynamics*, *32*(5), 811-825.

[61] Khampanit, A., Leelataviwat, S., Kochanin, J., & Warnitchai, P. (2014). Energy-based seismic strengthening design of non-ductile reinforced concrete frames using buckling-restrained braces. *Engineering Structures*, *81*, 110-122.

[62] Sahoo, D. R., & Rai, D. C. (2010). Seismic strengthening of non-ductile reinforced concrete frames using aluminum shear links as energy-dissipation devices. *Engineering Structures*, *32*(11), 3548-3557.

[63] Gray, M. G., Christopoulos, C., & Packer, J. A. (2014). Cast steel yielding brace system for concentrically braced frames: concept development and experimental validations. *Journal of Structural Engineering*, *140*(4), 04013095.

[64] Shin, J., Scott, D. W., Stewart, L. K., Yang, C. S., Wright, T. R., & DesRoches, R. (2016). Dynamic response of a full-scale reinforced concrete building frame retrofitted with FRP column jackets. *Engineering Structures*, *125*, 244-253.

[65] Oyen, P. E., & Parker, J. C. (2010). Seismic rehabilitation of extreme soft-story school building with friction dampers using the ASCE 41 standard. In *Improving the Seismic Performance of Existing Buildings and Other Structures* (pp. 949-954).

[66] Abdi, H., Hejazi, F., Jaafar, M. S., & Karim, I. A. (2016). Evaluation of response modification factor for steel structures with soft story retrofitted by viscous damper device. *Advances in Structural Engineering*, *19*(8), 1275-1288..

[67] Iqbal, A. (2006, March). Soft first story with seismic isolation system. In *Memorias, NZSEE Conference, Artículo* (No. 36).

[68] Mualla, I. H., & Belev, B. (2002). Performance of steel frames with a new friction damper device under earthquake excitation. *Engineering Structures*, *24*(3), 365-371.

[69] Kurata, M., Leon, R. T., & DesRoches, R. (2012). Rapid seismic rehabilitation strategy: concept and testing of cable bracing with couples resisting damper. *Journal of structural engineering*, *138*(3), 354-362.

[70] Li, G. Q., Sun, Y. Z., Jiang, J., Sun, F. F., & Ji, C. (2019). Experimental study on two-level yielding buckling-restrained braces. *Journal of Constructional Steel Research*, *159*, 260-269.

[71] Nobahar, E., Asgarian, B., Mercan, O., & Soroushian, S. (2020). A post-tensioned self-centering yielding brace system: development and performance-based seismic analysis. *Structure and Infrastructure Engineering*, 1-21.

[72] Demir, S., & Husem, M. (2018). Saw type seismic energy dissipaters: development and cyclic loading test. *Journal of Constructional Steel Research*, *150*, 264-276.